TIME DOMAIN SCATTERING FROM SINGLE AND MULTIPLE OBJECTS

A THESIS SUBMITTED TO
THE DEPARTMENT OF ELECTRICAL AND ELECTRONICS ENGINEERING
OF
MIDDLE EAST TECHNICAL UNIVERSITY

BY

SÜHA ALP AZİZOĞLU

IN PARTIAL FULFILLMENT OF THE REQUIREMENTS
FOR
THE DEGREE OF DOCTOR OF PHILOSOPHY
IN
ELECTRICAL AND ELECTRONICS ENGINEERING

MARCH 2008

Approval of the thesis:

TIME DOMAIN SCATTERING FROM SINGLE AND MULTIPLE OBJECTS

submitted by **SÜHA ALP AZİZOĞLU** in partial fullfillment of the requirements for the degree of **Doctor of Philosophy in Electrical and Electronics Engineering Department, Middle East Technical University** by,

Prof. Dr. Canan Özgen _____
Dean, Graduate School of **Natural and Applied Sciences**

Prof. Dr. İsmet Erkmen _____
Head of Department, **Electrical and Electronics Engineering**

Assoc. Prof. Dr. S. Sencer Koç _____
Supervisor, **Electrical and Electronics Engineering Dept., METU**

Examining Committee Members:

Prof. Dr. Tuncay Birand _____
Electrical and Electronics Engineering Dept., METU

Assoc. Prof. Dr. S. Sencer Koç _____
Electrical and Electronics Engineering Dept., METU

Prof. Dr. Mustafa Kuzuoğlu _____
Electrical and Electronics Engineering Dept., METU

Prof. Dr. Gülbin Dural _____
Electrical and Electronics Engineering Dept., METU

Prof. Dr. Ayhan Altıntaş _____
Electrical and Electronics Engineering Dept., Bilkent University

Date: March 06, 2007

I hereby declare that all information in this document has been obtained and presented in accordance with academic rules and ethical conduct. I also declare that, as required by these rules and conduct, I have fully cited and referenced all material and results that are not original to this work.

Name, Last name : Süha Alp Azizoğlu

Signature :

ABSTRACT

TIME DOMAIN SCATTERING FROM SINGLE AND MULTIPLE OBJECTS

Azizoğlu, Süha Alp

Ph.D., Department of Electrical and Electronics Engineering

Supervisor : Assoc. Prof. Dr. S. Sencer Koç

March 2008, 112 pages

The importance of the T-matrix method is well-known when frequency domain scattering problems are of interest. With the relatively recent and wide-spread interest in time domain scattering problems, similar applications of the T-matrix method are expected to be useful in the time domain. In this thesis, the time domain spherical scalar wave functions are introduced, translational addition theorems for the time domain spherical scalar wave functions necessary for the solution of multiple scattering problems are given, and the formulation of time domain scattering of scalar waves by two spheres and by two scatterers of arbitrary shape is presented. The whole analysis is performed in the time domain requiring no inverse Fourier integrals to be evaluated. Scattering examples are studied in order to check the numerical accuracy, and demonstrate the utility of the expressions.

Keywords: Multiple Scattering, Spherical Wave Functions, T-Matrix Method, Time Domain Scattering, Translational Addition Theorems.

ÖZ

BİR VE BİRDEN FAZLA SAÇICILARDAN SAÇILIMIN ZAMAN UZAMINDA İNCELENMESİ

Azizoğlu, Süha Alp

Doktora, Elektrik ve Elektronik Mühendisliği Bölümü

Tez Yöneticisi : Doç. Dr. S. Sencer Koç

Mart 2008, 112 sayfa

T-matris metodunun önemi frekans uzamı saçılım problemlerinde çok iyi bilinmektedir. Zaman uzamı saçılım problemlerine olan yoğun ilgiden dolayı, T-matris metodunun benzer uygulamalarının zaman uzamında da yararlı olacağı beklenmektedir. Bu tezde, zaman uzamı skalar küresel dalga fonksiyonları tanımlanmış, birden fazla saçıcıdan saçılım problemlerinin çözümü için gerekli olan zaman uzamı küresel skalar dalga fonksiyonları için öteleme adisyon teoremleri bulunmuştur ve skalar dalgaların iki küreden ve küresel olmayan iki saçıcıdan saçılımının formulasyonu zaman uzamında yapılmıştır. Bütün analiz, ters Fourier entegrallerinin hesaplanmasına gerek duyulmaksızın zaman uzamında gerçekleştirilmiştir. Bulunan ifadeleri nümerik olarak test etmek ve ifadelerin yararını göstermek için saçılım problemleri çözülmüştür.

Anahtar Kelimeler: Birden Fazla Saçıcıdan Saçılım, Küresel Dalga Fonksiyonları, Öteleme Adisyon Teoremleri, T-Matris Metodu, Zaman Uzamında Saçılım.

To the Memory of Prof. Dr. O. Merih Büyükdura

ACKNOWLEDGMENTS

TABLE OF CONTENTS

LIST OF TABLES

TABLES

LIST OF FIGURES

FIGURES

LIST OF SYMBOLS

SYMBOLS

$\otimes$: convolution

$\oplus$: convolution sum

∇ : gradient $[\mathrm{m}^{-1}]$

x^* : complex conjugate value of x

$|x|$: absolute value of x

$\overline{\mathbf{A}}^{-1}$: inverse of $\overline{\mathbf{A}}$

$\begin{bmatrix} j_1 & j_2 & j_3 \\ m_1 & m_2 & m_3 \end{bmatrix}$: Wigner $3-j$ symbol

c : velocity of waves in free-space $[\mathrm{m\ s}^{-1}]$

f : frequency $[\mathrm{s}^{-1}]$

f_∞ : form function [-]

$\mathbf{f}^i$: column vector containing $f_{nm}^i(t)$, the coefficients of the incident field in the time domain

$\mathbf{f}^s$: column vector containing $f_{nm}^s(t)$, the coefficients of the scattered field in the time domain

$\mathbf{f}^t$: column vector containing $f_{nm}^t(t)$, the coefficients of the total field in the time domain

$\mathbf{F}^i$: column vector containing F_{nm}^i, the coefficients of the incident field in the frequency domain

$\mathbf{F}^s$: column vector containing F_{nm}^s, the coefficients of the scattered field in the frequency domain

$\mathbf{F}^t$: column vector containing F_{nm}^t, the coefficients of the total field in the frequency domain

$g_0(\mathbf{R}, \mathbf{R}';t)$: time domain free-space scalar Green's function $[\mathrm{m}^{-1}\ \mathrm{s}^{-1}]$

$G_0(\mathbf{R}, \mathbf{R}';k)$: free-space scalar Green's function $[\mathrm{m}^{-1}]$

$h_n^{(2)}$:	spherical Hankel functions of the second kind [-]
$H_n^{(2)}$:	Hankel functions of the second kind [-]
j :	$\sqrt{-1}$ [-]
j_n :	spherical Bessel functions [-]
J_n :	Bessel functions [-]
k :	free-space wavenumber [m^{-1}]
$\hat{\mathbf{n}}'$:	outward unit normal [-]
$\hat{\mathbf{n}}_e$:	inward unit normal [-]
N :	number of terms in the series expansion
O_n :	outgoing wave functions
$p(x)$:	pulse equal to unity when $-1 < x < 1$, and vanishes elsewhere [-]
$P_n(x)$:	Legendre polynomials [-]
$P_n^m(x)$:	Associated Legendre Functions of the first kind with order n and degree m [-]
$\overline{\mathbf{Q}}$:	matrix with elements $Q_{nm,\nu\mu}$, time domain or frequency domain where appropriate [-]
$\overline{\mathbf{Q}}^e$:	matrix with elements $Q_{nm,\nu\mu}^e$, time domain or frequency domain where appropriate [-]
$\mathbf{R}$:	position vector [m]
$\mathbf{R}_{o,10}$:	position vector representing the translation from origin 0 to 0_1 [m]
$\mathbf{R}_{o,12}$:	position vector representing the translation from origin 0_2 to 0_1 [m]
Re$\{x\}$:	regular part of x
S_n :	standing wave functions
t :	time [s]
$\overline{\mathbf{T}}$:	T-matrix with elements $T_{nm,\nu\mu}$, time domain or frequency domain where appropriate [-]

$u(x)$:   unit step (Heaviside) function [-]

$\mathrm{Y}_{nm}(\theta,\phi)$:   Tesseral harmonics [-]

$\alpha(m,n \mid \mu,\nu;k)$:   translation coeffiecients [-]

$\alpha(m,n \mid \mu,\nu;t)$:   translation convolving functions [s^{-2}]

$\overline{\boldsymbol{\alpha}}$:   matrix with elements $\alpha(m,n \mid \mu,\nu;k)$ or $\alpha(m,n \mid \mu,\nu;t)$ where appropriate

$\beta(m,n \mid \mu,\nu;k)$:   translation coeffiecients [-]

$\beta(m,n \mid \mu,\nu;t)$:   translation convolving functions [s^{-1}]

$\overline{\boldsymbol{\beta}}$:   matrix with elements $\beta(m,n \mid \mu,\nu;k)$ or $\beta(m,n \mid \mu,\nu;t)$ where appropriate

$\delta_{nn'}$:   Kronecker delta [-]

$\delta(x)$:   Dirac delta function [dimension is that of x^{-1}]

$\overline{\boldsymbol{\delta}}$:   diagonal matrix containing $\delta(t)$ in each diagonal entry [s^{-1}]

σ :   normalized scattering cross section [-]

σ_b :   normalized backscattering cross section [-]

τ :   half of the pulse width [s]

$\varphi_{nm}^{(1)}(k\mathbf{R})$:   incoming spherical scalar wave functions [-]

$\varphi_{nm}^{(4)}(k\mathbf{R})$:   outgoing spherical scalar wave functions [-]

$\Phi_{nm}^{(1)}(\mathbf{R},t)$:   time domain incoming spherical scalar wave functions [s^{-1}]

$\Phi_{nm}^{(4)}(\mathbf{R},t)$:   time domain outgoing spherical scalar wave functions [s^{-2}]

ψ^i :   incident field, time domain or frequency domain where appropriate

ψ^s :   scattered field, time domain or frequency domain where appropriate

ψ^t :   total field, time domain or frequency domain where appropriate

ω :   angular frequency [rad s^{-1}]

CHAPTER 1

INTRODUCTION

The time domain analysis and computation have become appealing in dealing with broadband signals since short pulses and wide bandwidths are being used increasingly in communication and radar systems. The simplicity in handling time variatians, the use of time gating, and straightforward approach in time domain modelling makes the time domain preferrable. The time domain analysis is indispensible in order to be able to model the field of moving sources and targets and to be able to assess the physical validity. The advantages and applications of the time domain electromagnetics can be found extensively in Bennett *et al.* [1]. With this motivation, the solution of multiple scattering is constructed in the time domain in this work. The time domain spherical scalar wave functions are defined, translational addition theorems for the time domain spherical scalar wave functions necessary for the solution of multiple scattering problems are presented, and the time domain solutions of the scattering of scalar waves by two spheres and by two scatterers of arbitrary shape are constructed using an equivalent of the T-matrix method formulated in the time domain. In the given solutions, the positions of the scatterers are arbitrary, i.e., no simple special case of translation is chosen for them. The present approach is that of stating, formulating, and solving the problem entirely in the time domain, i.e., requiring no inverse Fourier integrals to be evaluated.

Certain physical phenomena can be described using the scalar wave equation, for example, acoustic waves and Schrödinger waves. In certain situations, electromagnetic waves can also be described by the scalar wave equation, Chew [2]. The solution to the scalar wave equation in terms of spherical wave expansions and expansions of Green's functions in terms of orthogonal wave functions are well known to be useful in the frequency domain in the analytical solutions of scattering problems and expansions of fields radiated by general sources, Jones [3], Harrington

[4], Jackson [5], Bowman *et al.* [6], and Felsen [7]. Such expansions have also proved to be useful in the time domain, Davidon [8], Heyman *et al.* [9], Marengo *et al.* [10], Hansen [11] and [12], Buyukdura *et al.* [13], Azizoglu *et al.* [14], [15], and [16], Azizoglu [17], and Koc *et al.* [18].

The T-matrix method, Waterman [19], is a well-known and powerful method in the frequency domain provided that the shape of the scattering object is smooth, i.e., satisfying the Rayleigh condition. The T-matrix method is also known as the null-field approach, and it is an alternative to solve the surface integral equation. For a given frequency and scatterer, the T-matrix needs to be calculated once, and can be used for any illumination. Once the T-matrices for a set of scatterers are found, they can be used easily to construct the solution of multiple scattering from this set of scatterers. When more than one scatterer is present, there exists multiple scattering between the scatterers, and the translational addition theorems for the spherical wave functions should be applied for the solution, Chew [2], Twersky [20], Marnevskaya [21], Peterson *et al.* [22], and Gaunaurd *et al.* [23] and [24]; a similar approach is also possible for electromagnetic waves, Chew [2], Twersky [25], Liang *et al.* [26], Bruning *et al.* [27] and Peterson *et al.* [28].

Some of the earlier related work in the time domain is as follows, time domain scattering of scalar waves by a single soft sphere in free-space is given in Buyukdura *et al.* [13], and the application of the T-matrix method to the problem of time domain scattering of scalar waves by a single object of arbitrary shape in free-space is presented in Koc *et al.* [29]. For the T-matrix formulation in the time domain, one needs a time domain free-space Green's function in the form of an expansion in terms of wave functions which are orthogonal over spherical surfaces centered at the coordinate origin. The spherical wave expansion of the time domain scalar free-space Green's function is provided in Buyukdura *et al.* [13], and it is used in the formulation of scattering of scalar waves in the present work. For vector scattering problems, the spherical wave expansion of the time domain free-space dyadic Green's function provided in Azizoglu *et al.* [14], [15], and [16], and Azizoglu [17], and the time domain spherical vector wave functions available in Azizoglu *et al.* [14] can be used similarly.

The translational addition theorems are useful in the solution of multiple

scattering problems. They express wave functions in one coordinate system in terms of the wave functions of another coordinate system translated from the first one, Friedman *et al.* [30], Stein [31], Cruzan [32], Danos *et al.* [33], Wittmann [34], Chew [35], Chew *et al.* [36], and Varadan *et al.* [37]. The translational addition theorems for the frequency domain spherical scalar wave functions are derived in Friedman *et al.* [30], and improved and extended to vector waves in Stein [31] and Cruzan [32]. In the present work, the time domain spherical scalar wave functions and the translational addition theorems given in Azizoglu *et al.* [38] and [39] are improved, and convergence and numerical properties are discussed.

In Chapter 2, the translational addition theorems for the spherical scalar wave functions are given in the frequency domain, and then the time domain spherical scalar wave functions are defined and translational addition theorems are obtained. The convergence and numerical properties of the translational addition theorems are also discussed in this chapter. In Chapter 3, first, scattering of scalar waves by a single soft sphere in free-space is reviewed both in the frequency and in the time domain, then, the formulation and numerical results of the well-known frequency domain scattering by two soft spheres is given. As an application of the derived time domain translational addition theorems, formulation of the time domain scattering of scalar waves by two spheres in free-space is presented, and the numerical results are checked with the frequency domain solution. Chapter 5 provides the time domain scattering by an object, scatterer of arbitrary shape, in free-space using the T-matrix method. The non-spherical surface, for which the T-matrix is not diagonal, is simulated by a shifted sphere whose center is displaced from the coordinate origin and the surface integrals necessary to find the matrix entries are evaluated numerically. Time domain scattering by two scatterers of arbitrary shape is presented in the second part of Chapter 5 using the time domain isolated-scatterer T-matrix of the single object and the time domain multiple scattering formulation. Chapter 5 gives the concluding remarks. Appendix A and B include the time domain T-matrix formulation and direct matrix deconvolution algorithm, respectively, and the formulation necessary for the numerical evaluation of the surface integrals in the T-matrix method for the shifted sphere , whose center is displaced from the coordinate origin, is given in Appendix C.

Throughout the thesis, $e^{j\omega t}$ time convention is used in the frequency domain expressions and suppressed. The velocity of waves in free space is represented by c. (R,θ,ϕ) are the familiar spherical coordinates of the point of observation with reference to the first coordinate system with origin 0, and (R',θ',ϕ') are the spherical coordinates of the same point with reference to the second coordinate system with origin $0'$, where $0'$ has the coordinates (R_0,θ_0,ϕ_0) with respect to 0.

CHAPTER 2

TRANSLATIONAL ADDITION THEOREMS FOR

THE TIME DOMAIN SPHERICAL SCALAR WAVE FUNCTIONS

This chapter deals with the addition theorems for the spherical scalar wave functions under coordinate translation. In Section 2.1, the translational addition theorems for the spherical scalar wave functions are described in the frequency domain. In Section 2.2, first the time domain spherical scalar wave functions are defined, and then, a time domain representation of a plane wave propagating in an arbitrary direction is found in terms of elementary spherical waves about a fixed center. This representation is, then, used in the derivation of the translational addition theorems for the time domain spherical scalar wave functions. The derived expressions are checked numerically in Section 2.3.

2.1 Translational Addition Theorems for the Spherical Scalar Wave Functions in the Frequency Domain

The spherical scalar wave functions $\varphi_{nm}(k\mathbf{R})$ are defined as

$$\varphi_{nm}^{(1)}(k\mathbf{R}) = z_n^{(1)}(kR)P_n^m(\cos\theta)e^{jm\phi} \ , \tag{2.1}$$

$$\varphi_{nm}^{(4)}(k\mathbf{R}) = z_n^{(4)}(kR)P_n^m(\cos\theta)e^{jm\phi} \ , \tag{2.2}$$

for $-n \leq m \leq n$, and $0 \leq n \leq \infty$, where $\varphi_{nm}^{(1)}(k\mathbf{R})$ and $\varphi_{nm}^{(4)}(k\mathbf{R})$ represent the incoming and outgoing wave functions, respectively. $\mathbf{R}$ stands for the position vector from the origin 0, denoting the observation point, and k is the free-space

wavenumber, $k = \omega/c$ where ω is the angular frequency and c is the velocity of waves in free-space. $z_n^{(1)}(kR)$ and $z_n^{(4)}(kR)$ denotes the spherical Bessel functions of order n and the spherical Hankel functions of the second kind of order n, respectively, Abramowitz *et al.* [40], i.e.,

$$z_n^{(1)}(kR) = j_n(kR) \ , \tag{2.3}$$

$$z_n^{(4)}(kR) = h_n^{(2)}(kR) \ . \tag{2.4}$$

The spherical Bessel functions are related to the half-integer order Bessel functions through

$$j_n(kR) = \sqrt{\frac{\pi}{2kR}} \quad J_{n+\frac{1}{2}}(kR) \ , \tag{2.5}$$

and they are finite at $R = 0$. The spherical Hankel functions of the second kind are related to the half-integer order Hankel functions of the second kind through

$$h_n^{(2)}(kR) = \sqrt{\frac{\pi}{2kR}} \quad H_{n+\frac{1}{2}}^{(2)}(kR) \ , \tag{2.6}$$

and they satisfy the radiation condition. $P_n^m(x)$ are the Associated Legendre Functions of the first kind with order n and degree m, Abramowitz *et al.* [40], and they are defined for nonnegative integer values of n and m as,

$$P_n^m(x) = (-1)^m (1-x^2)^{m/2} \frac{d^m}{dx^m} P_n(x) \ , \tag{2.7}$$

where $P_n(x)$ are the Legendre polynomials, which can be obtained using Rodrigues' formula,

6

$$P_n(x) = \frac{1}{2^n n!} \frac{d^n}{dx^n} (x^2 - 1)^n \ . \tag{2.8}$$

For $m < 0$, $P_n^m(x)$ is defined as

$$P_n^m(x) = (-1)^m \frac{(n+m)!}{(n-m)!} P_n^{-m}(x) \ . \tag{2.9}$$

The set of functions $\varphi_{nm}^{(1),(4)}(k\mathbf{R})$ are orthogonal over a spherical surface and they satisfy the scalar Helmholtz equation,

$$(\nabla^2 + k^2) \, \varphi_{nm}(k\mathbf{R}) = 0 \ . \tag{2.10}$$

The spherical scalar wave functions, $\varphi_{nm}^{(1),(4)}(k\mathbf{R})$ defined in Eqs. (2.1) and (2.2), can also be expressed in terms of the Tesseral harmonics as

$$\varphi_{nm}^{(1),(4)}(k\mathbf{R}) = z_n^{(1),(4)}(kR) \mathrm{Y}_{nm}(\theta, \phi) \ , \tag{2.11}$$

where the Tesseral harmonics are defined as

$$\mathrm{Y}_{nm}(\theta, \phi) = P_n^m(\cos\theta) e^{jm\phi} \ , \tag{2.12}$$

and they are well known to be orthogonal over a spherical surface, i.e.,

$$\int_{\theta=0}^{\pi} \int_{\phi=0}^{2\pi} \mathrm{Y}_{nm}(\theta, \phi) \mathrm{Y}_{n'm'}^*(\theta, \phi) \sin\theta \, d\theta \, d\phi = \frac{4\pi(n+m)!}{(2n+1)(n-m)!} \delta_{nn'} \delta_{mm'} \ , \tag{2.13}$$

where $\mathrm{Y}_{nm}^*(\theta, \phi)$ is the complex conjugate of $\mathrm{Y}_{nm}(\theta, \phi)$, and $\delta_{nn'}$ is the Kronecker delta, i.e.,

$$\delta_{nn'} = 1, \quad n = n$$
$$= 0, \quad n \neq n'.$$

(2.14)

Translational addition theorems express $\varphi_{nm}^{(1),(4)}(k\mathbf{R})$, with reference to the origin 0, in terms of the spherical scalar wave functions with reference to the origin $0'$, where $0'$ has the coordinates (R_0, θ_0, ϕ_0) with respect to 0. The set of spherical coordinates (R', θ', ϕ') is introduced with respect to $0'$, such that the polar axis, $\theta' = 0$, and the azimuth axis, $\phi' = 0$, are, respectively, parallel to the corresponding axes, $\theta = 0$ and $\phi = 0$. This is a rigid translation of the coordinate system, i.e.,

$$\mathbf{R} = \mathbf{R}_0 + \mathbf{R}' ,$$

(2.15)

which is illustrated in Figure 2.1.
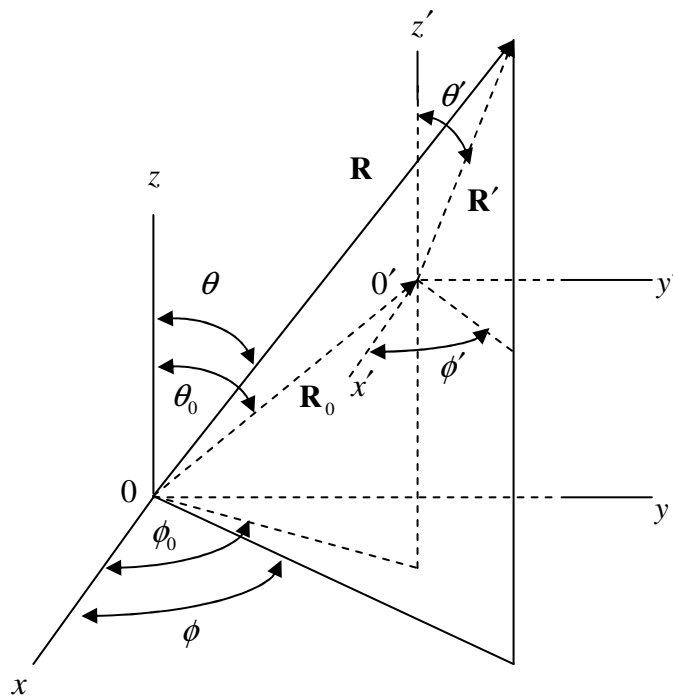
Figure 2.1 Coordinate translation.

The spherical scalar wave functions φ_{nm} defined in Eqs. (2.1) and (2.2) can be expressed with respect to this new coordinate system using the addition theorems, given in Friedman *et al.* [30], Stein [31], and Cruzan [32], as

$$
z_n^{(1),(4)}(kR)P_n^m(\cos\theta)e^{jm\phi} = \sum_{\nu=0}^{\infty}\sum_{\mu=-\nu}^{\nu}\sum_{\rho}\left\{(-1)^{\mu}(j)^{\nu+\rho-n}(2\nu+1)\,a\!\left(m,n\mid-\mu,\nu\mid\rho\right)\right.
$$

$$
\times\,j_{\nu}(kR_<)\,z_{\rho}^{(1),(4)}(kR_>)\,P_{\nu}^{\mu}(\cos\theta_<)\,P_{\rho}^{m-\mu}(\cos\theta_>)
$$

$$
\left.\times\,e^{j\mu\phi_<}e^{j(m-\mu)\phi_>}\right\},
$$

$$(2.16)$$

where

$$
\left.\begin{cases}
R_> = R', & R_< = R_0 \\
\theta_> = \theta', & \theta_< = \theta_0 \\
\phi_> = \phi', & \phi_< = \phi_0
\end{cases}\right\} \quad \text{when} \quad R' > R_0 ,
$$

$$(2.17)$$

and

$$
\left.\begin{cases}
R_> = R_0 , & R_< = R' \\
\theta_> = \theta_0 , & \theta_< = \theta' \\
\phi_> = \phi_0 , & \phi_< = \phi'
\end{cases}\right\} \quad \text{when} \quad R' < R_0 .
$$

$$(2.18)$$

It can be shown that either Eq. (2.17) or Eq. (2.18) may be used for the incoming wave function, $\varphi_{nm}^{(1)}(k\mathbf{R})$, without restriction on the relative size of R' and R_0, Cruzan [32]. Eq. (2.16) is valid for $n \geq 0$, $-n \leq m \leq n$, and the summation over ρ is finite covering the range $|n-\nu|, |n-\nu|+2, \ldots, (n+\nu)$. The coefficients $a\!\left(m,n\mid\mu,\nu\mid\rho\right)$ are defined by the linearization expansion,

$$
P_n^m(x)\,P_{\nu}^{\mu}(x) = \sum_{\rho}a\!\left(m,n\mid\mu,\nu\mid\rho\right)P_{\rho}^{m+\mu}(x) ,
$$

$$(2.19)$$

and may be identified with a product of two Wigner $3-j$ symbols, Wigner [41], as

$$a(m,n \mid \mu,\nu \mid \rho) = (-1)^{m+\mu} (2\rho+1) \left[\frac{(n+m)!\,(\nu+\mu)!\,(\rho-m-\mu)!}{(n-m)!\,(\nu-\mu)!\,(\rho+m+\mu)!} \right]^{1/2}$$

$$\times \begin{bmatrix} n & \nu & \rho \\ 0 & 0 & 0 \end{bmatrix} \begin{bmatrix} n & \nu & \rho \\ m & \mu & -m-\mu \end{bmatrix},$$

(2.20)

where $\begin{bmatrix} j_1 & j_2 & j_3 \\ m_1 & m_2 & m_3 \end{bmatrix}$ is the Wigner $3-j$ symbol which is related to the Clebsch-

Gordan Coefficients as, Abramowitz *et al.* [40],

$$\begin{bmatrix} j_1 & j_2 & j_3 \\ m_1 & m_2 & m_3 \end{bmatrix} = \frac{(-1)^{j_1-j_2-m_3}}{\sqrt{2j_3+1}} \left(j_1 m_1 j_2 m_2 \mid j_1 j_2 j_3, -m_3 \right).$$

(2.21)

The Wigner 3-j symbol is expressed explicitly by the Racah formula, Messiah [42],

$$\begin{bmatrix} j_1 & j_2 & j_3 \\ m_1 & m_2 & m_3 \end{bmatrix} = (-1)^{j_1-j_2-m_3} (\delta_{m_1+m_2+m_3,0})$$

$$\times \sqrt{\frac{(j_1+j_2-j_3)!\,(j_1-j_2+j_3)!\,(-j_1+j_2+j_3)!}{(j_1+j_2+j_3+1)!}}$$

$$\times \sqrt{(j_1+m_1)!(j_1-m_1)!(j_2+m_2)!(j_2-m_2)!(j_3+m_3)!(j_3-m_3)!}$$

$$\times \sum_x \left\{ (-1)^x \frac{1}{x!\,(j_1+j_2-j_3-x)!\,(j_1-m_1-x)!} \right.$$

$$\left. \times \frac{1}{(j_2+m_2-x)!(j_3-j_2+m_1+x)!(j_3-j_1-m_2+x)!} \right\},$$

(2.22)

and is nonzero only if $m_3 = -m_1 - m_2$, $|j_1 - j_2| \leq j_3 \leq j_1 + j_2$, and if $|m_1| \leq j_1, |m_2| \leq j_2, |m_3| \leq j_3$. The summation in Eq. (2.22) is over all integers x, such that the factorials all have non-negative arguments. As seen, Wigner $3-j$ symbol involves summations of multitudes of factorials. Therefore, straightforward calculation using Eq. (2.22) is very inefficient. A recursion relation for the coefficients $a(m,n \mid \mu, \nu \mid \rho)$, in which only the index ρ cycles, is highly desirable, especially for machine computation. Such relations exist and can be found in Peterson *et al.* [22], Bruning *et al.* [27], Cruzan [32], Danos *et al.* [33], and Wittman [34].

Eq. (2.16) can be written in a compact form as

$$\varphi_{nm}^{(1),(4)}(k\mathbf{R}) = \sum_{\nu=0}^{\infty} \sum_{\mu=-\nu}^{\nu} \sum_{\rho} \left\{ (-1)^{\mu} (j)^{\nu+\rho-n} (2\nu+1) \, a(m,n \mid -\mu, \nu \mid \rho) \right.$$

$$\left. \times \varphi_{\nu\mu}^{(1)}(k\mathbf{R}') \, \varphi_{\rho,(m-\mu)}^{(1),(4)}(k\mathbf{R}_0) \right\}, \qquad R' < R_0$$

$$= \sum_{\nu=0}^{\infty} \sum_{\mu=-\nu}^{\nu} \sum_{\rho} \left\{ (-1)^{\mu} (j)^{\nu+\rho-n} (2\nu+1) \, a(m,n \mid -\mu, \nu \mid \rho) \right.$$

$$\left. \times \varphi_{\nu\mu}^{(1)}(k\mathbf{R}_0) \, \varphi_{\rho,(m-\mu)}^{(1),(4)}(k\mathbf{R}') \right\}, \qquad R' > R_0 \; .$$

(2.23)

The translational addition theorems can also be written in the form similar to Chew [2] as

$$\varphi_{nm}^{(1)}(k\mathbf{R}) = \sum_{\nu=0}^{\infty} \sum_{\mu=-\nu}^{\nu} \beta(m,n \mid \mu, \nu; k) \, \varphi_{\nu\mu}^{(1)}(k\mathbf{R}') \; , \tag{2.24}$$

$$\varphi_{nm}^{(4)}(k\mathbf{R}) = \sum_{v=0}^{\infty} \sum_{\mu=-v}^{v} \alpha\big(m,n \,\big|\, \mu,v;k\big) \varphi_{v\mu}^{(1)}(k\mathbf{R}'), \qquad R' < R_0$$

$$= \sum_{v=0}^{\infty} \sum_{\mu=-v}^{v} \beta\big(m,n \,\big|\, \mu,v;k\big) \varphi_{v\mu}^{(4)}(k\mathbf{R}'), \qquad R' > R_0,$$

(2.25)

where the translation coefficients are given by

$$\beta\big(m,n \,\big|\, \mu,v;k\big) = (-1)^{\mu}(j)^{v-n}(2v+1) \sum_{\rho} \Big\{ (j)^{\rho} \; a\big(m,n \,\big| -\mu,v \,\big| \,\rho\big) \varphi_{\rho,(m-\mu)}^{(1)}(k\mathbf{R}_0) \Big\},$$

(2.26)

$$\alpha\big(m,n \,\big|\, \mu,v;k\big) = (-1)^{\mu}(j)^{v-n}(2v+1) \sum_{\rho} \Big\{ (j)^{\rho} \; a\big(m,n \,\big| -\mu,v \,\big| \,\rho\big) \varphi_{\rho,(m-\mu)}^{(4)}(k\mathbf{R}_0) \Big\}.$$

(2.27)

Eq. (2.24) and Eq. (2.25) for $R' < R_0$ follow directly from Eq. (2.16), and Eq. (2.25) for $R' > R_0$ can be obtained from Eq. (2.15) by interchanging the orders of summation, substituting new indices, and using the properties of the Wigner coefficients and Associated Legendre functions, Stein [31].

The interpretation of the addition theorems is as follows; Eq. (2.24) expands the incoming wave functions with reference to the origin 0 in terms of the incoming wave functions with reference to the origin $0'$. Eq. (2.25) for $R' < R_0$ (inside the circle $R' = R_0$ in Figure 2.2) expresses the outgoing wave functions with reference to the origin 0 in terms of the incoming wave functions with reference to the origin $0'$; and in the region $R' > R_0$ (outside the circle $R' = R_0$ in Figure 2.2), the outgoing wave functions with reference to the origin 0 are expressed in terms of the outgoing wave functions with reference to the origin $0'$. On the boundary $R' = R_0$, the outgoing wave functions are singular.

The spherical scalar wave functions in Eqs. (2.1) and (2.2) could also have been chosen in terms of $\begin{pmatrix} \cos m\phi \\ \sin m\phi \end{pmatrix}$ harmonics instead of $e^{jm\phi}$, however, such a choice

would result in more complicated expressions for the addition theorems, Varadan *et al.* [37].

For the efficient computation of the addition theorems, recurrence relations for the translation coefficients $\beta(m,n\,|\,\mu,\nu;k)$ and $\alpha(m,n\,|\,\mu,\nu;k)$, Chew [35] and Chew *et al.* [36], can be used as an alternative to the recurrence relations for the coefficients $a(m,n\,|\,\mu,\nu\,|\,\rho)$.
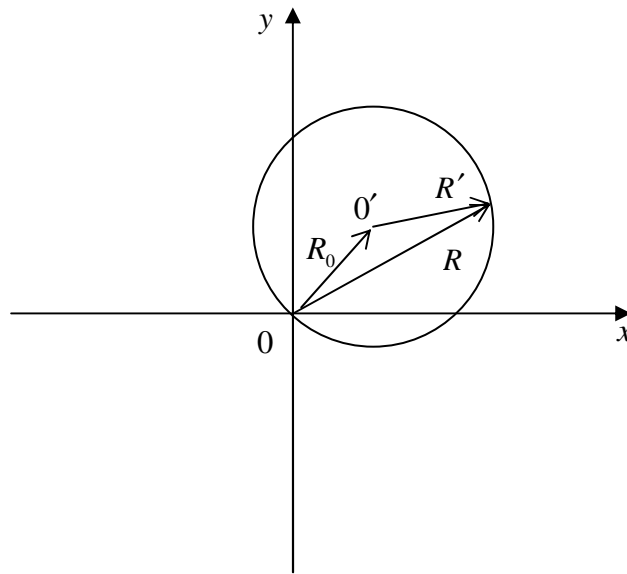
Figure 2.2 $R' = R_0$ circle on the transverse xy plane.

2.2 Formulation of the Translational Addition Theorems for the Time Domain Spherical Scalar Wave Functions

In this section, first the time domain spherical scalar wave functions are defined; next an impulsive plane wave coming in along an arbitrary direction is expressed in terms of spherical waves with center at the origin in the time domain. Along with this expansion, following similar steps and using the time domain equivalents of the

identities in Friedman *et al.* [30], but now entirely in the time domain, the translational addition theorems are obtained.

The time domain spherical scalar wave functions $\Phi_{nm}(\mathbf{R}, t)$ are defined as

$$\Phi_{nm}^{(1)}(\mathbf{R}, t) = S_n\left(\frac{R}{c}, t\right) P_n^m(\cos\theta) e^{jm\phi} \ , \tag{2.28}$$

$$\Phi_{nm}^{(4)}(\mathbf{R}, t) = O_n\left(\frac{R}{c}, t\right) P_n^m(\cos\theta) e^{jm\phi} \ , \tag{2.29}$$

for $-n \leq m \leq n$, and $0 \leq n \leq \infty$, where $\Phi_{nm}^{(1)}(\mathbf{R}, t)$ and $\Phi_{nm}^{(4)}(\mathbf{R}, t)$ represent the incoming and outgoing wave functions, respectively. The set of functions $\Phi_{nm}^{(1),(4)}(\mathbf{R}, t)$ are orthogonal over a spherical surface and they satisfy the scalar wave equation,

$$\left[\nabla^2 - \frac{1}{c^2}\frac{\partial^2}{\partial t^2}\right]\Phi_{nm}(\mathbf{R}, t) = 0 \ . \tag{2.30}$$

$\Phi_{nm}^{(1),(4)}(\mathbf{R}, t)$ are obtained using the inverse Fourier transforms given in Buyukdura *et al.* [13], and related to the well known spherical scalar wave functions as,

$$S_n\left(\frac{R}{c}, t\right) P_n^m(\cos\theta) e^{jm\phi} = 2 j^{-n} F^{-1}\left\{j_n(kR) P_n^m(\cos\theta) e^{jm\phi}\right\}, \tag{2.31}$$

$$O_n\left(\frac{R}{c}, t\right) P_n^m(\cos\theta) e^{jm\phi} = -j^{-n} F^{-1}\left\{j\omega h_n^{(2)}(kR) P_n^m(\cos\theta) e^{jm\phi}\right\}. \tag{2.32}$$

It is worth noting that the inverse transform of the Bessel functions are found easily, Abramowitz *et al.* [40], however the inverse transform of the Hankel functions exist

in the sense that for any function $G(\omega)$ whose inverse Fourier transform is $g(t)$, if $\omega^{-n+1}G(\omega)$ remains bounded as $\omega \to 0$, then the inverse Fourier transform of the product $(-j\omega)h_n^{(2)}(\omega)G(\omega)$ is given by the convolution of $g(t)$ and $j^n O_n(1,t)$, Buyukdura *et al.* [13], Azizoglu *et al.* [14], and Azizoglu [17].

The standing wave functions, S_n, are defined as,

$$S_n(R,t) = \frac{1}{R}P_n\left(\frac{t}{R}\right)p\left(\frac{t}{R}\right), \tag{2.33}$$

where $p(\cdot)$ is a pulse equal to unity when its argument is between -1 and 1, and vanishes elsewhere; and O_n represents the outgoing wave functions, Azizoglu *et al.* [14], i.e.,

$$O_0(R,t) = \frac{1}{R}\delta(t-R),$$

$$O_1(R,t) = \frac{1}{R}\delta(t-R) + \frac{1}{R^2}u(t-R),$$

$$O_2(R,t) = \frac{1}{R}\delta(t-R) + \frac{3}{R^2}u(t-R) + \frac{3}{R^3}(t-R)u(t-R),$$

$$\vdots$$

$$O_n(R,t) = \frac{\delta(t-R)}{R} + \sum_{i=1}^{n}\frac{(n+i)!}{2^i i!(i-1)!(n-i)!}\frac{(t-R)^{i-1}}{R^{i+1}}u(t-R),$$

$$\tag{2.34}$$

where $\delta(\cdot)$ is the Dirac delta function, and $u(\cdot)$ stands for the unit step (Heaviside) function. In general, $O_n(R/c,t)$ consists of a delta function striking at $t = R/c$ and an $(n-1)$th order polynomial in $(t - R/c)$ for $t > R/c$. It is possible to express O_n as,

$$O_n(R,t) = \frac{1}{R}\frac{d}{dt}\left[P_n\left(\frac{t}{R}\right)u(t-R)\right] , \tag{2.35}$$

and it is related to U_n of Buyukdura *et al.* [13] as

$$O_n(R,t) = \frac{U_n(R,t)}{R} . \tag{2.36}$$

It is also shown in Buyukdura *et al.* [13] that

$$\frac{1}{RR'}\left[P_n\left(\frac{R^2 + R'^2 - t^2}{2RR'}\right)p\left(\frac{t-R}{R'}\right)\right] = (-1)^n S_n(R',t) \otimes O_n(R,t) , \tag{2.37}$$

where $\otimes$ stands for the convolution operation.

In order to derive the translational addition theorems for the time domain spherical scalar wave functions, first an impulsive plane wave coming in along an arbitrary direction should be expanded in terms of spherical waves with center at the origin in the time domain. Consider the impulsive plane wave, i.e., $\psi^i(\mathbf{R},t) = \delta(t + R\cos\gamma/c)$ coming along the direction $\theta = \alpha$ and $\phi = \beta$. Here γ is the angle between the directions (α,β) and (θ,ϕ) so that $\cos\gamma = \cos\theta\cos\alpha + \sin\theta\sin\alpha\cos(\phi - \beta)$. The incident field can be written in terms of spherical waves with center at the origin 0 as

$$\psi^i(\mathbf{R},t) = \sum_{n=0}^{\infty}\sum_{m=-n}^{n} f_{nm}^i(t) \otimes \Phi_{nm}^{(1)}(\mathbf{R},t) . \tag{2.38}$$

In order to find the convolving function $f_{nm}^i(t)$ (we would call it coefficient if we were in the frequency domain), consider a point source, $b(t)\delta(\mathbf{R} - \mathbf{R}')$; the incident field due to this point source located at $\mathbf{R}'$ can be written as

$$\psi_{ps}(\mathbf{R},t) = -\int_V \int_{\tau=-\infty}^{\infty} g_0(\mathbf{R},\mathbf{R}'';t-\tau)b(\tau)\delta(\mathbf{R}''-\mathbf{R}')\,d\tau\,dv'' , \qquad (2.39)$$

where V is the region occupied by the source and g_0 is simply the inverse Fourier transform of the well known expression for the closed form Green's function in the frequency domain, Chew [2], i.e.,

$$G_0(\mathbf{R},\mathbf{R}';k) = \frac{e^{-jk|\mathbf{R}-\mathbf{R}'|}}{4\pi|\mathbf{R}-\mathbf{R}'|} , \qquad (2.40)$$

and

$$g_0(\mathbf{R},\mathbf{R}';t) = \frac{\delta(t-|\mathbf{R}-\mathbf{R}'|/c)}{4\pi|\mathbf{R}-\mathbf{R}'|} . \qquad (2.41)$$

Eq. (2.39) can be written as

$$\psi_{ps}(\mathbf{R},t) = -b(t) \otimes g_0(\mathbf{R},\mathbf{R}';t) . \qquad (2.42)$$

In order to obtain a plane wave we let $R' \to \infty$, and approximate the field at the origin due to the point source as,

$$\psi_{ps}(R=0,t) \approx -b(t) \otimes \frac{\delta(t-R'/c)}{4\pi R'} . \qquad (2.43)$$

Now adjust the amplitude and delay (or rather, advance) such that the field at the origin is,

$$\psi_{ps}(R=0,t) = \delta(t) . \qquad (2.44)$$

Thus we have,

$$b(t) = -4\pi R' \delta(t + R'/c) .$$
(2.45)

Now, in Eq. (2.42) use the eigenfunction expansion for g_0 given in Buyukdura *et al.* [13], also given in Eq. (A.3),

$$\psi_{ps}(\mathbf{R},t) = -b(t) \otimes \frac{1}{8\pi c} \sum_{n=0}^{\infty} \sum_{m=-n}^{n} \left\{ (-1)^n (2n+1) \frac{(n-m)!}{(n+m)!} S_n\left(\frac{R}{c},t\right) \otimes O_n\left(\frac{R'}{c},t\right) \right.$$

$$\left. \times P_n^m(\cos\theta) e^{jm\phi} P_n^m(\cos\theta') e^{-jm\phi'} \right\} .$$
(2.46)

Using the large argument form of $h_n^{(2)}(kR)$, one can obtain

$$\lim_{R'\to\infty} O_n\left(\frac{R'}{c},t\right) = \frac{\delta(t - R'/c)}{R'/c} .$$
(2.47)

Upon substituting Eqs. (2.45) and (2.47) in Eq. (2.46), expansion of the impulsive plane wave coming in along an arbitrary direction can be written in terms of the time domain spherical wave functions as,

$$\delta(t + R\cos\gamma/c) = \frac{1}{2} \sum_{n=0}^{\infty} \sum_{m=-n}^{n} \left\{ (-1)^n (2n+1) \frac{(n-m)!}{(n+m)!} S_n\left(\frac{R}{c},t\right) \right.$$

$$\left. \times P_n^m(\cos\alpha) P_n^m(\cos\theta) e^{-jm(\beta-\phi)} \right\} .$$
(2.48)

These results agree with the result obtained using inverse Fourier transformation of the well known frequency domain expression, i.e.,

$$e^{jkR\cos\gamma} = \sum_{n=0}^{\infty}\sum_{m=-n}^{n}(j)^n(2n+1)\frac{(n-m)!}{(n+m)!}j_n(kR)P_n^m(\cos\alpha)P_n^m(\cos\theta)e^{-jm(\beta-\phi)} \ .$$

(2.49)

Now, we first obtain the translational addition theorem for $\Phi_{nm}^{(1)}(\mathbf{R},t)$. Consider a point P which has the spherical coordinates (R,θ,ϕ) with respect to the origin 0. From the expansion of Eq. (2.48), an integral representation of elementary spherical wave functions can be obtained. Multiplying both sides of the equation by $P_n^m(\cos\alpha)e^{jm\beta}$, and using the orthogonality property of the Tesseral Harmonics over a spherical surface, Eq. (2.13),

$$S_n\left(\frac{R}{c},t\right)P_n^m(\cos\theta)e^{jm\phi} = \frac{(-1)^{-n}}{2\pi}$$

$$\times\int_{\beta=0}^{2\pi}\int_{\alpha=0}^{\pi}\delta(t+R\cos\gamma/c)P_n^m(\cos\alpha)e^{jm\beta}\sin\alpha\,d\alpha\,d\beta \ .$$

(2.50)

is obtained. Introduce a new origin $0'$, where $0'$ has the coordinates (R_0,θ_0,ϕ_0) with respect to 0 (Figure 2.1), and let (R',θ',ϕ') be the spherical coordinates of the point P with respect to $0'$. We shall now obtain an expansion for a standing spherical wave around 0 such as $S_n(R/c,t)P_n^m(\cos\theta)e^{jm\phi}$ in terms of standing spherical waves around $0'$ such as $S_n(R'/c,t)P_n^m(\cos\theta')e^{jm\phi'}$. It can be shown that, Friedman *et al.* [30],

$$R\cos\gamma = R'\cos\gamma' + R_0\cos\gamma_0 \ .$$

(2.51)

Here γ' is the angle between the directions (α,β) and (θ',ϕ'), while γ_0 is the angle between the directions (α,β) and (θ_0,ϕ_0).

Using Eq. (2.51) in Eq. (2.50) we have

$$S_n\left(\frac{R}{c}, t\right) P_n^m(\cos\theta) e^{jm\phi} = \frac{(-1)^{-n}}{2\pi}$$

$$\times \int_{\beta=0}^{2\pi} \int_{\alpha=0}^{\pi} \left\{ \delta\left(t + R'\cos\gamma'/c + R_0\cos\gamma_0/c\right) \right.$$

$$\left. \times P_n^m(\cos\alpha) e^{jm\beta} \sin\alpha \, d\alpha \, d\beta \right\}.$$

(2.52)

For the term $\delta\left(t + R'\cos\gamma'/c\right)$, the expansion corresponding to Eq. (2.48) can be used, i.e.,

$$\delta\left(t + R'\cos\gamma'/c\right) = \frac{1}{2} \sum_{\nu=0}^{\infty} \sum_{\mu=-\nu}^{\nu} \left\{ (-1)^\nu (2\nu+1) \frac{(\nu-\mu)!}{(\nu+\mu)!} S_\nu\left(\frac{R'}{c}, t\right) \right.$$

$$\left. \times P_\nu^\mu(\cos\alpha) P_\nu^\mu(\cos\theta') e^{-j\mu(\phi'-\beta)} \right\}.$$

(2.53)

It is assumed that when the above expansion is substituted into Eq. (2.52), the order of summation and integration may be interchanged, Friedman *et al.* [30]. Therefore,

$$S_n\left(\frac{R}{c}, t\right) P_n^m(\cos\theta) e^{jm\phi} = \frac{(-1)^{-n}}{4\pi} \sum_{\nu=0}^{\infty} \sum_{\mu=-\nu}^{\nu} \left\{ (-1)^\nu (2\nu+1) \frac{(\nu-\mu)!}{(\nu+\mu)!} \right.$$

$$\times S_\nu\left(\frac{R'}{c}, t\right) P_\nu^\mu(\cos\theta') e^{-j\mu\phi'}$$

$$\otimes \int_{\beta=0}^{2\pi} \int_{\alpha=0}^{\pi} \delta\left(t + R_0\cos\gamma_0/c\right) P_n^m(\cos\alpha) P_\nu^\mu(\cos\alpha)$$

$$\left. \times e^{j(m+\mu)\beta} \sin\alpha \, d\alpha \, d\beta \right\}.$$

(2.54)

In writing Eq. (2.54), the following relation is used,

$$\delta(t + R\cos\gamma/c) = \delta(t + R_0\cos\gamma_0/c) \otimes \delta(t + R'\cos\gamma'/c) \ . \tag{2.55}$$

Using Eq. (2.19) in Eq. (2.54) results in

$$S_n(R,t)P_n^m(\cos\theta)e^{jm\phi} = \frac{(-1)^{-n}}{4\pi}$$

$$\times \sum_{\nu=0}^{\infty}\sum_{\mu=-\nu}^{\nu}\sum_{\rho} \left\{ (-1)^\nu(2\nu+1)\frac{(\nu-\mu)!}{(\nu+\mu)!}a(m,n\mid\mu,\nu\mid\rho) \right.$$

$$\left. \times S_\nu\left(\frac{R'}{c},t\right)P_\nu^\mu(\cos\theta')e^{-j\mu\phi'} \otimes I_\rho^{\mu,m} \right\},$$

$$\tag{2.56}$$

where $I_\rho^{\mu,m}$ are integrals of the form

$$I_\rho^{\mu,m} = \int_{\beta=0}^{2\pi}\int_{\alpha=0}^{\pi} \delta(t + R_0\cos\gamma_0/c)\, P_\rho^{m+\mu}(\cos\alpha)\, e^{j(m+\mu)\beta}\, \sin\alpha\, d\alpha\, d\beta \ . \tag{2.57}$$

It is possible to evaluate these integrals directly using Eq. (2.50), Stratton [43],

$$I_\rho^{\mu,m} = 2\pi(-1)^\rho S_\rho\left(\frac{R_0}{c},t\right)P_\rho^{m+\mu}(\cos\theta_0)e^{j(m+\mu)\phi_o} \ . \tag{2.58}$$

By substituting Eq.(2.58) into Eq.(2.56), the expansion of a spherical wave with respect to one origin, in terms of the spherical waves with respect another origin is obtained as,

$$S_n\left(\frac{R}{c},t\right)P_n^m(\cos\theta)e^{jm\phi} = \frac{1}{2}\sum_{v=0}^{\infty}\sum_{\mu=-v}^{v}\sum_{\rho}\left\{(-1)^{v+\rho-n}(2v+1)\frac{(v-\mu)!}{(v+\mu)!}a\big(m,n\mid\mu,v\mid\rho\big)\right.$$

$$\times S_\rho\left(\frac{R_0}{c},t\right)\otimes S_v\left(\frac{R'}{c},t\right)$$

$$\left.\times P_\rho^{m+\mu}(\cos\theta_0)P_v^\mu(\cos\theta')e^{-jm\phi'}e^{j(m+\mu)\phi_0}\right\},$$

(2.59)

which can equivalently be written as

$$S_n\left(\frac{R}{c},t\right)P_n^m(\cos\theta)e^{jm\phi} = \frac{1}{2}\sum_{v=0}^{\infty}\sum_{\mu=-v}^{v}\sum_{\rho}\left\{(-1)^{v+\rho-n+\mu}(2v+1)a\big(m,n\mid-\mu,v\mid\rho\big)\right.$$

$$\times S_\rho\left(\frac{R_0}{c},t\right)\otimes S_v\left(\frac{R'}{c},t\right)$$

$$\left.\times P_\rho^{m-\mu}(\cos\theta_0)P_v^\mu(\cos\theta')e^{jm\phi'}e^{j(m-\mu)\phi_0}\right\},$$

(2.60)

using Eq.(2.9).

In order to obtain the addition theorems for the outgoing spherical functions $\Phi_{nm}^{(4)}(\mathbf{R},t)$, the integral representation for this function must first be obtained. The representation of the spherical wave functions in terms of plane waves, Stratton [43], in the time domain is,

$$\frac{c}{R_1}\delta(t+R_1/c) = \frac{1}{2\pi}\int_{\beta=0}^{2\pi}\int_{\alpha=0}^{\pi/2-j\infty}\delta'(t+R_1\cos\gamma_1/c)\sin\alpha\,d\alpha\,d\beta,$$

(2.61)

where δ' is the derivative of the Dirac delta function, i.e. the unit doublet and (R_1,θ_1,ϕ_1) are the spherical coordinates of a point P_1 with respect to the origin 0_1.

Now let the point P_1 have spherical coordinates (R, θ, ϕ) with respect to the origin 0, and let 0_1 have coordinates (R^0, θ^0, ϕ^0) with respect to 0. Similar to Eq. (2.51),

$$R \cos \gamma = R^0 \cos \gamma^0 + R_1 \cos \gamma_1 \ , \tag{2.62}$$

and similar to Eq. (2.48), $\delta\left(t - R^0 \cos \gamma^0 / c\right)$ can be expanded as

$$\delta\left(t - R^0 \cos \gamma^0 / c\right) = \frac{1}{2} \sum_{n=0}^{\infty} \sum_{m=-n}^{n} \left\{ (2n+1) \frac{(n-m)!}{(n+m)!} S_n\left(\frac{R^0}{c}, t\right) \right.$$

$$\left. P_n^m(\cos \alpha) P_n^m(\cos \theta^0) e^{jm(\beta - \phi_0)} \right\}. \tag{2.63}$$

We also have the formula, Stratton [43], for $R^0 < R$ as,

$$\frac{c \delta\left(t + R_1 / c\right)}{R_1} = -\frac{1}{2} \sum_{n=0}^{\infty} \sum_{m=-n}^{n} \left\{ (-1)^n (2n+1) \frac{(n-m)!}{(n+m)!} S_n\left(\frac{R^0}{c}, t\right) \otimes O_n\left(\frac{R}{c}, t\right) \right.$$

$$\left. P_n^m(\cos \theta^0) P_n^m(\cos \theta) e^{jm(\phi - \phi^0)} \right\}. \tag{2.64}$$

Using Eq.(2.62) and Eq.(2.63) in Eq.(2.61) and comparing with Eq.(2.64), the integral representation can be found as

$$O_n\left(\frac{R}{c}, t\right) P_n^m(\cos \theta) e^{jm\phi} = -\frac{(-1)^{-n}}{2\pi} \int_{\beta=0}^{2\pi} \int_{\alpha=0}^{\pi/2 - j\infty} \left\{ \delta'\left(t + R \cos \gamma / c\right) \right.$$

$$\left. \times P_n^m(\cos \alpha) e^{jm\beta} \sin \alpha \, d\alpha \, d\beta \right\}. \tag{2.65}$$

Now let the point P have spherical coordinates (R', θ', ϕ') with reference to another origin $0'$, where $0'$ has coordinates (R_0, θ_0, ϕ_0) with respect to 0, Figure 2.1. Using Eq. (2.51) and Eq. (2.53) in Eq.(2.65) along with

$$\delta'(t + R\cos\gamma/c) = \delta'(t + R_0\cos\gamma_0/c) \otimes \delta(t + R'\cos\gamma'/c) \,, \tag{2.66}$$

it can be shown that it is possible to interchange the order of summation and integration provided that $R' < R_0$, Friedman *et al.* [30]. Therefore we have

$$O_n\left(\frac{R}{c}, t\right) P_n^m(\cos\theta) e^{jm\phi} = -\frac{(-1)^{-n}}{4\pi} \sum_{\nu=0}^{\infty} \sum_{\mu=-\nu}^{\nu} \left\{ (-1)^\nu (2\nu+1) \frac{(\nu-\mu)!}{(\nu+\mu)!} \right.$$

$$\times S_\nu\left(\frac{R'}{c}, t\right) P_\nu^\mu(\cos\theta') e^{-j\mu\phi'}$$

$$\otimes \int_{\beta=0}^{2\pi} \int_{\alpha=0}^{\pi/2-j\infty} \delta'(t + R_0\cos\gamma_0/c) P_n^m(\cos\alpha) P_\nu^\mu(\cos\alpha)$$

$$\left. \times e^{j(m+\mu)\beta} \sin\alpha \, d\alpha \, d\beta \right\}, \qquad R' < R_0 \,. \tag{2.67}$$

Using Eq. (2.19) in Eq.(2.67) results in

$$O_n\left(\frac{R}{c}, t\right) P_n^m(\cos\theta) e^{jm\phi} = -\frac{(-1)^{-n}}{4\pi} \sum_{\nu=0}^{\infty} \sum_{\mu=-\nu}^{\nu} \sum_{\rho} \left\{ (-1)^\nu (2\nu+1) \frac{(\nu-\mu)!}{(\nu+\mu)!} \right.$$

$$\times a(m,n \mid \mu,\nu \mid \rho) S_\nu\left(\frac{R'}{c}, t\right) P_\nu^\mu(\cos\theta') e^{-j\mu\phi'}$$

$$\left. \otimes K_\rho^{\mu,m} \right\}, \qquad R' < R_0 \,, \tag{2.68}$$

where $K_\rho^{\mu,m}$ are integrals of the form

$$K_\rho^{\mu,m} = \int_{\beta=0}^{2\pi} \int_{\alpha=0}^{\pi/2-j\infty} \delta'\left(t + R_0 \cos\gamma_0 / c\right) P_\rho^{m+\mu}(\cos\alpha) \, e^{j(m+\mu)\beta} \sin\alpha \, d\alpha \, d\beta.$$

(2.69)

These integrals can be evaluated directly, using Eq.(2.65), as

$$K_\rho^{\mu,m} = -2\pi(-1)^\rho O_\rho\left(\frac{R_0}{c}, t\right) P_\rho^{m+\mu}(\cos\theta_0) \, e^{j(m+\mu)\phi_0} \ .$$

(2.70)

Substituting Eq. (2.70) into Eq. (2.68) leads to

$$O_n\left(\frac{R}{c}, t\right) P_n^m(\cos\theta) e^{jm\phi} = \frac{1}{2} \sum_{\nu=0}^{\infty} \sum_{\mu=-\nu}^{\nu} \sum_\rho \left\{ (-1)^{\nu+\rho-n}(2\nu+1)\frac{(\nu-\mu)!}{(\nu+\mu)!} a(m,n \mid \mu,\nu \mid \rho) \right.$$

$$\times S_\nu\left(\frac{R'}{c}, t\right) \otimes O_\rho\left(\frac{R_0}{c}, t\right) P_\nu^\mu(\cos\theta') P_\rho^{m+\mu}(\cos\theta_0)$$

$$\left. \times e^{-jm\phi'} e^{j(m+\mu)\phi_0} \right\}, \qquad R' < R_0 \ .$$

(2.71)

When $R_0 < R'$, the resulting expansion would be the above equation with (R', θ', ϕ') interchanged with (R_0, θ_0, ϕ_0). Using the relation in Eq.(2.9) and using the notation defined in Eqs. (2.17) and (2.18), the expansion for the spherical wave $\Phi_{nm}^{(4)}(\mathbf{R}, t)$ about one origin can be written in terms of spherical waves around another origin as,

$$O_n\left(\frac{R}{c},t\right)P_n^m(\cos\theta)e^{jm\phi} = \frac{1}{2}\sum_{v=0}^{\infty}\sum_{\mu=-v}^{v}\sum_{\rho}\left\{(-1)^{v+\rho-n+\mu}(2v+1)\,a(m,n\mid-\mu,v\mid\rho)\right.$$

$$S_v\left(\frac{R_<}{c},t\right)\otimes O_\rho\left(\frac{R_>}{c},t\right)P_v^\mu(\cos\theta_<)P_\rho^{m-\mu}(\cos\theta_>)$$

$$\left.e^{j\mu\phi_<}e^{j(m-\mu)\phi_>}\right\},$$

$$(2.72)$$

Finally, the translational addition theorems for both the incoming and the outgoing wave functions can be written as

$$\Phi_{nm}^{(1),(4)}(\mathbf{R},t) = \frac{1}{2}\sum_{v=0}^{\infty}\sum_{\mu=-v}^{v}\sum_{\rho}\left\{(-1)^{v+\rho-n+\mu}(2v+1)\,a(m,n\mid-\mu,v\mid\rho)\right.$$

$$\left.\Phi_{v\mu}^{(1)}(\mathbf{R}',t)\otimes\Phi_{\rho,(m-\mu)}^{(1),(4)}(\mathbf{R}_0,t)\right\},\qquad R'<R_0$$

$$= \frac{1}{2}\sum_{v=0}^{\infty}\sum_{\mu=-v}^{v}\sum_{\rho}\left\{(-1)^{v+\rho-n+\mu}(2v+1)\,a(m,n\mid-\mu,v\mid\rho)\right.$$

$$\left.\Phi_{v\mu}^{(1)}(\mathbf{R}_0,t)\otimes\Phi_{\rho,(m-\mu)}^{(1),(4)}(\mathbf{R}',t)\right\},\qquad R'>R_0\,,$$

$$(2.73)$$

in which wave functions with $\mathbf{R}$ dependence is expressed in terms of wave functions with $\mathbf{R}_0$ dependence convolved with wave functions with $\mathbf{R}'$ dependence. Similar to the frequency domain expression, Eq. (2.23), either the first or the second line may be used with $\Phi_{nm}^{(1)}(\mathbf{R},t)$, without restriction on the relative size of R' and R_0, and $\Phi_{nm}^{(4)}(\mathbf{R},t)$ is singular across the boundary $R'=R_0$, Figure 2.2. Eq. (2.73) can be written in the form similar to Eqs. (2.24) – (2.27) as

$$\Phi_{nm}^{(1)}(\mathbf{R},t) = \sum_{v=0}^{\infty}\sum_{\mu=-v}^{v}\beta(m,n\mid\mu,v;t)\otimes\Phi_{v\mu}^{(1)}(\mathbf{R}',t)\,,\qquad(2.74)$$

$$\Phi_{nm}^{(4)}(\mathbf{R},t) = \sum_{\nu=0}^{\infty} \sum_{\mu=-\nu}^{\nu} \alpha\!\left(m,n\,|\,\mu,\nu;t\right) \otimes \Phi_{\nu\mu}^{(1)}(\mathbf{R}',t), \qquad R' < R_0$$

$$= \sum_{\nu=0}^{\infty} \sum_{\mu=-\nu}^{\nu} \beta\!\left(m,n\,|\,\mu,\nu;t\right) \otimes \Phi_{\nu\mu}^{(4)}(\mathbf{R}',t), \qquad R' > R_0,$$

(2.75)

where the time domain translation convolving functions are

$$\beta\!\left(m,n\,|\,\mu,\nu;t\right) = \frac{1}{2}(-1)^{\nu-n+\mu}(2\nu+1)\sum_{\rho}\;(-1)^{\rho}\,a\!\left(m,n\,|\,-\mu,\nu\,|\,\rho\right)\Phi_{\rho,(m-\mu)}^{(1)}(\mathbf{R}_o,t),$$

(2.76)

$$\alpha\!\left(m,n\,|\,\mu,\nu;t\right) = \frac{1}{2}(-1)^{\nu-n+\mu}(2\nu+1)\sum_{\rho}\;(-1)^{\rho}\,a\!\left(m,n\,|\,-\mu,\nu\,|\,\rho\right)\Phi_{\rho,(m-\mu)}^{(4)}(\mathbf{R}_o,t).$$

(2.77)

The expressions derived in this section for the time domain translational addition theorems are in agreement with the results obtained using inverse Fourier transformation of the frequency domain expressions given in the previous section. Also, note that the interpretation of the addition theorems given in the previous section for the frequency domain expansions is still valid for the time domain expansions.

2.3 Numerical Properties of the Translational Addition Theorems for the Time Domain Spherical Scalar Wave Functions

The wave functions, $\Phi_{nm}^{(1),(4)}(\mathbf{R},t)$, are discontinuous in time, so for numerical check, both sides of Eq. (2.73) are convolved by a smooth function, which is chosen to be the Gaussian waveform in this study; and then each side is evaluated for various n, m, $\mathbf{R}$ and $\mathbf{R}_0$ for comparison. The logarithmic error, expressed in dB, and the percent error are defined as

27

$$\text{error} = 10\log\left\{\frac{\|g(t) - g_a(t)\|}{\|g(t)\|}\right\} , \tag{2.78}$$

$$\text{percent error} = \frac{\|g(t) - g_a(t)\|}{\|g(t)\|} \times 100 , \tag{2.79}$$

where

$$\|g(t)\| = \int_u \left|g(t)\right|^2 dt . \tag{2.80}$$

In these equations, $g(t)$ is the left hand side of Eq. (2.73), and $g_a(t)$ represents the approximating function which is defined by the expansion on the right hand side and truncated to include N terms depending on the required accuracy .

In the numerical computations, the Gaussian waveform is chosen to be $e^{-5.65t^2/\tau^2}$, which is roughly of duration $2\tau \cong 17$ ns provided the wave velocity is that of light in vacuum, and the convolution operations encountered are all achieved by using Gaussian integration, Abramowitz *et al.* [40], in order to obtain accurate results. In order to accelerate the computations, the Associated Legendre functions are computed using their tabulated coefficients, the functions obtained by this method are checked to be accurate up to the order $n = 16$.

Consider first the expression for the incoming wave functions, $\Phi_{nm}^{(1)}(\mathbf{R}, t)$. Although frequency domain expansion has no singularities; $R = 0$, $R_0 = 0$, and $R' = 0$ are singularities for the time domain expansion.

In order to check the expansion in Eq. (2.73), specific values of n and m, and a specific translation is taken. Both sides are convolved with the waveform, and the real and the imaginary parts are compared for the desired observation point. Figures 2.3 and 2.4 depict the excellent agreement for $n = 4$, $m = 2$, when the specific observation point is $(R = 5, \theta = \pi/2, \phi = \pi/6)$, and the specific translation is

$(R_0 = 4, \theta_0 = \pi/2, \phi_0 = \pi/4)$. The error is -45 dB, which corresponds to percent error less than 0.01 %, when 6 terms are included in the series expansion.

Figure 2.3 Real parts of the incoming wave function $\Phi_{nm}^{(1)}(\mathbf{R}, t)$, left hand side and its expansion, right hand side, in Eq. (2.73) for $n = 4$, $m = 2$, $(R = 5, \theta = \pi/2, \phi = \pi/6)$, and $(R_0 = 4, \theta_0 = \pi/2, \phi_0 = \pi/4)$, 6 terms are included in the series expansion.
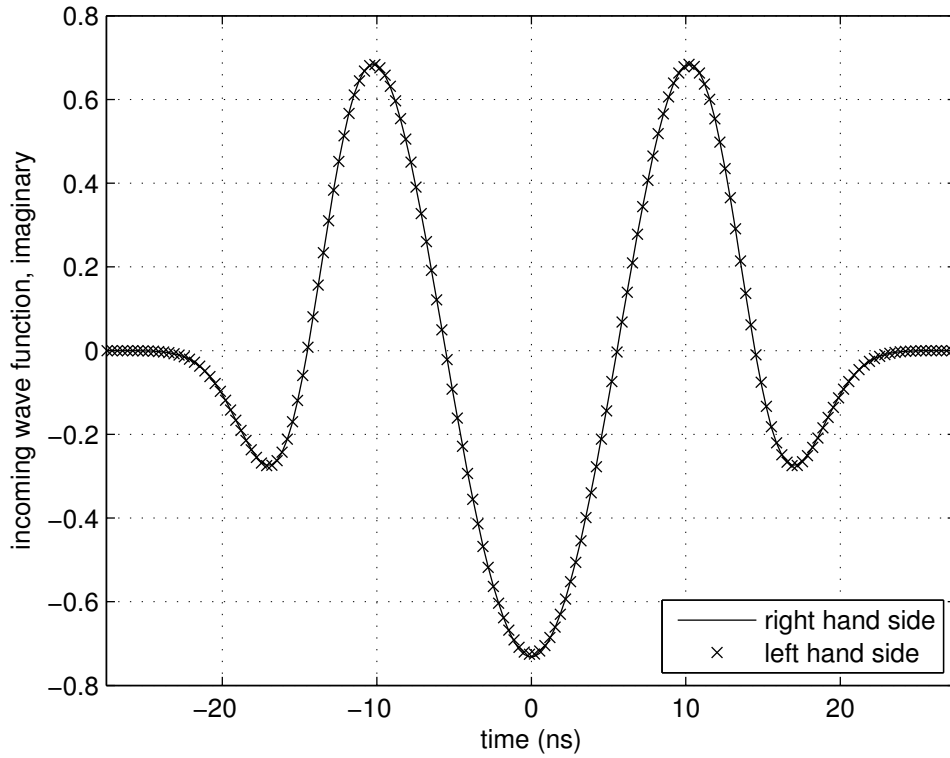
Figure 2.4 Imaginary parts of the incoming wave function $\Phi_{nm}^{(1)}(\mathbf{R},t)$, left hand side and its expansion, right hand side, in Eq. (2.73) for $n = 4$, $m = 2$, $(R = 5$, $\theta = \pi/2$, $\phi = \pi/6)$, and $(R_0 = 4$, $\theta_0 = \pi/2$, $\phi_0 = \pi/4)$, 6 terms are included in the series expansion.

In order to picture the error with the variation of the observation point, $n = 4$, $m = 2$, $(R_0 = 4$, $\theta_0 = \pi/2$, $\phi_0 = \pi/4)$ is chosen, and $\mathbf{R}$ is varied on the transverse xy plane, error in dB is plotted by including at most 7 terms in the expansion, Figure 2.5. Except at the singularities and the points in the vicinity of the origin 0, i.e., $R = 0$, error of -20 dB, corresponding to 1 % percent error, can be achieved. In Figure 2.5, it is clearly seen that error is very small in the vicinity of the origin $0'$ which has the coordinates $(R_0 = 4$, $\theta_0 = \pi/2$, $\phi_0 = \pi/4)$ with reference to 0, where R' is very small. The error can be reduced, which means the light colored region in Figure 2.5 can be shrunk approaching the origin 0, in most cases by including more terms in the series expansion, so one can conclude that reducing R,

i.e. narrowing the pulse on the left hand side of Eq. (2.73), increase the number of terms that should be included in the expansion for a particular numerical accuracy. The contour plot of Figure 2.5 does not show perfect circular symmetry around the origins 0 and $0'$, which is theoretically expected, due to the numerical errors depending on the direction and magnitude of the translation.

Figure 2.5 Contour plot of error in dB for the expansion of the incoming wave function, $\Phi_{nm}^{(1)}(\mathbf{R},t)$, in Eq. (2.73), on the transverse xy plane for $n=4$, $m=2$, and $(R_0 = 4$, $\theta_0 = \pi/2$, $\phi_0 = \pi/4)$, at most 7 terms are included in the series expansion.

The observations made after the study of many cases are given in the following discussion. In the tabulated results, the error criterion is chosen to be 1 % percent error. Table 2.1 is an example which shows that increasing the order and degree of

the wave functions, n, m, respectively, while keeping R' and R_0 constant increase the number of terms that should be included in the wave function expansion.

Table 2.1 Number of terms retained in the wave function expansion of $\Phi_{nm}^{(1)}(\mathbf{R}, t)$, N, with respect to n and m for 1 % percent error, for the case $(R = 3, \theta = \pi/8, \phi = \pi/2)$ and $(R_0 = 2.5, \theta_0 = 0, \phi_0 = \pi/2)$.

n	m	N
0	0	2
1	0	2
1	1	3
2	0	2
2	1	3
2	2	4
3	0	3
3	3	5
5	0	4
5	5	7

It is also observed that one has to include more terms in the series expansion, as $\min\{R', R_o\}$ gets larger for fixed n, m, R, and numerical accuracy, Table 2.2.

Table 2.2 Number of terms retained in the wave function expansion of $\Phi_{nm}^{(1)}(\mathbf{R},t)$, N, with respect to $\min\{R',R_o\}$ for 1 % percent error, for the case $n=2$, $m=2$, $(R=5$, $\theta=\pi/2$, $\phi=0)$, and $(\theta_0=\pi/2$, $\phi_0=0)$.

$\min\{R',R_o\}$, m	N
0.1	1
0.5	2
1	3
2	4
2.5	4

The effect of the pulse width of the waveform used in smoothing, 2τ, on N can be seen in Table 2.3. The pulse width, 2τ, corresponds to the duration of the Gaussian waveform, $e^{-5.65t^2/\tau^2}$, provided the wave velocity is that of light in vacuum. As τ is decreased, N should be increased in order to obtain the same accuracy.

Table 2.3 Number of terms retained in the wave function expansion of $\Phi_{nm}^{(1)}(\mathbf{R},t)$, N, with respect to τ for 1 % percent error, for the case $n=2$, $m=2$, $(R=5$, $\theta=\pi/2$, $\phi=0)$, and $(R_0=1$, $\theta_0=\pi/2$, $\phi_0=0)$.

τ, ns	N
17	2
8.5	3
4.25	4

For the incoming wave function, $\Phi_{nm}^{(1)}(\mathbf{R},t)$, both lines in Eq. (2.73) are valid without restriction on the relative size of R' and R_0, however with different numerical behavior. Using the first line when $R'\le R_0$ and the second when $R'\ge R_0$

decreases the number of terms that should be included in the series expansion as compared to doing vice versa.

In the same manner, one can check the expansion for the outgoing wave functions, $\Phi_{nm}^{(4)}(\mathbf{R},t)$. Figures 2.6 and 2.7 depict the agreement of both sides of Eq. (2.73) for $n=4$, $m=2$, when the specific observation point is $(R=25$, $\theta=\pi/2$, $\phi=\pi/6)$, and the specific translation is $(R_0=2$, $\theta_0=\pi/2$, $\phi_0=\pi/4)$. The error in dB is -31.4, which corresponds to percent error less than 0.1 %, when 5 terms are included in the series expansion. One can get even better results, in which the waveforms show excellent agreement, than Figures 2.6 and 2.7, for smaller translations, i.e., $R_0<2$.
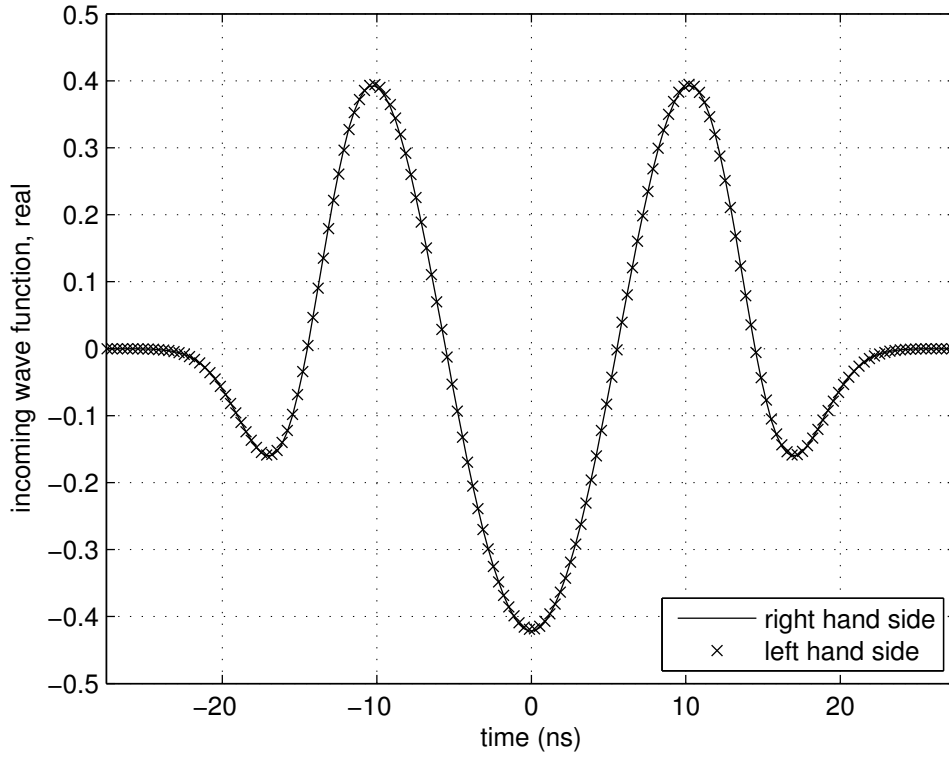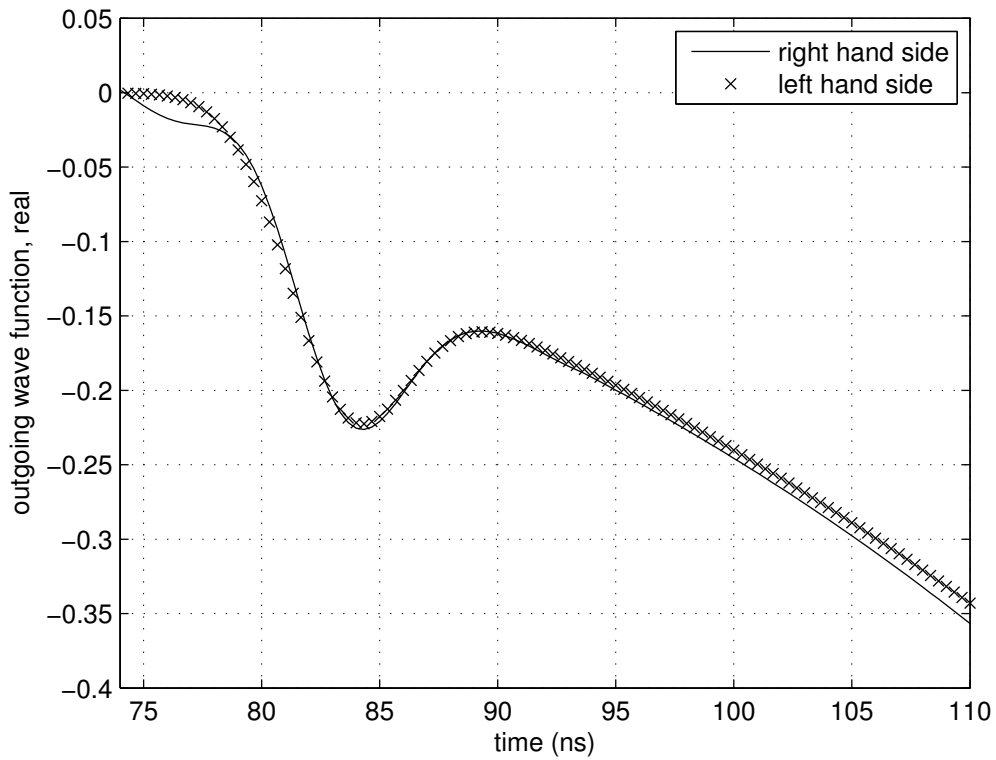

Figure 2.6 Real parts of the outgoing wave function $\Phi_{nm}^{(4)}(\mathbf{R},t)$, left hand side and its expansion, right hand side, in Eq. (2.73) for $n=4$, $m=2$, $(R=25$, $\theta=\pi/2$, $\phi=\pi/6)$, and $(R_0=2$, $\theta_0=\pi/2$, $\phi_0=\pi/4)$, 5 terms are included in the series expansion.
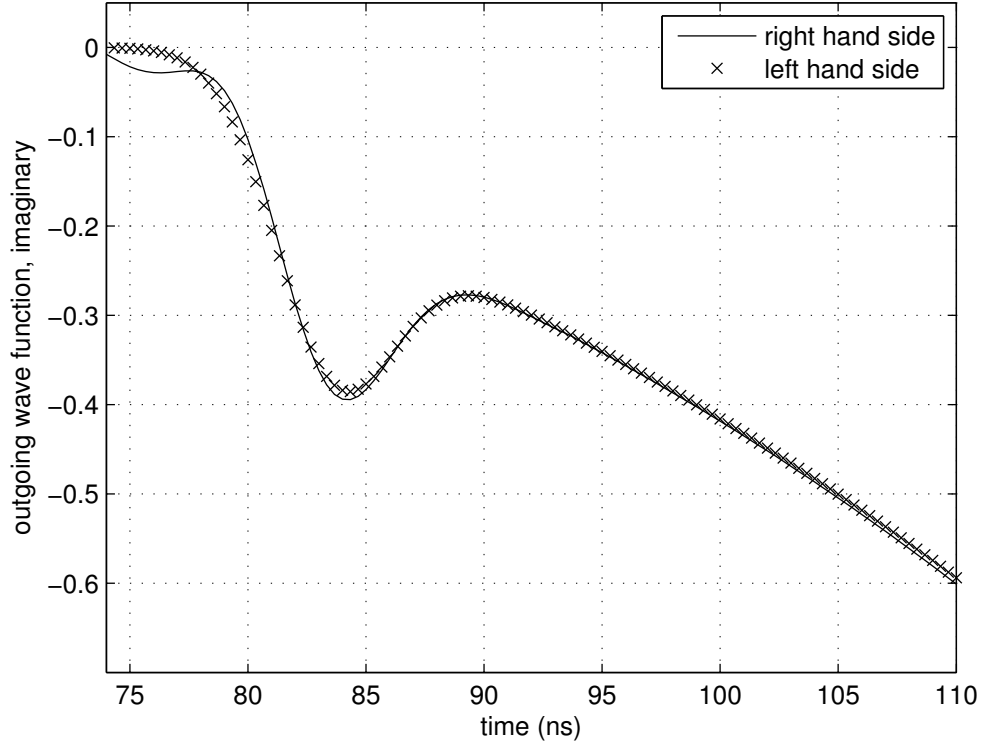
Figure 2.7 Imaginary parts of the outgoing wave function $\Phi_{nm}^{(4)}(\mathbf{R},t)$, left hand side and its expansion, right hand side, in Eq. (2.73) for $n = 4$, $m = 2$, $(R = 25$, $\theta = \pi/2$, $\phi = \pi/6)$, and $(R_0 = 2$, $\theta_0 = \pi/2$, $\phi_0 = \pi/4)$, 5 terms are included in the series expansion.

The numerical error for the expansion of the outgoing wave functions, $\Phi_{nm}^{(4)}(\mathbf{R},t)$, for $n = 4$, $m = 2$, and $(R_0 = 2$, $\theta_0 = \pi/2$, $\phi_0 = \pi/4)$ is depicted in Figure 2.8. $\mathbf{R}$ is taken on the transverse xy plane, and error in dB is plotted by including at most 4 terms in the expansion. $\Phi_{nm}^{(4)}(\mathbf{R},t)$ on the left hand side of Eq. (2.73) is defined outside a circular region at the origin 0 with radius depending on the required accuracy. When the first line of Eq. (2.73) is valid, i.e., $R' \leq R_0$, the outgoing wave functions, $\Phi_{nm}^{(4)}(\mathbf{R},t)$, with reference to the origin 0 is expanded in terms of the incoming wave functions with reference to the origin $0'$; and the error for the expansion is small inside a circular region centered at the origin $0'$ with radius

depending on the number of terms included and the required accuracy (the small dark region around the origin $0'$ in Figure 2.8). When the second line of Eq. (2.73) is valid, i.e., $R' \geq R_0$, the outgoing wave functions, $\Phi_{nm}^{(4)}(\mathbf{R}, t)$, with reference to the origin 0 is expanded in terms of the outgoing wave functions with reference to the origin $0'$, and the error for the expansion is small outside a circular region centered at the origin $0'$ with radius depending on the number of terms included and the required accuracy (the outer dark region in Figure 2.8). This comment on Figure 2.8 is in agreement with the interpretation of the addition theorems, using Figure 2.2, given at the end of Section 2.1. The contour plot of Figure 2.8 does not show perfect circular symmetry around the origins 0 and $0'$, which is theoretically expected, due to the numerical errors depending on the direction and magnitude of the translation.
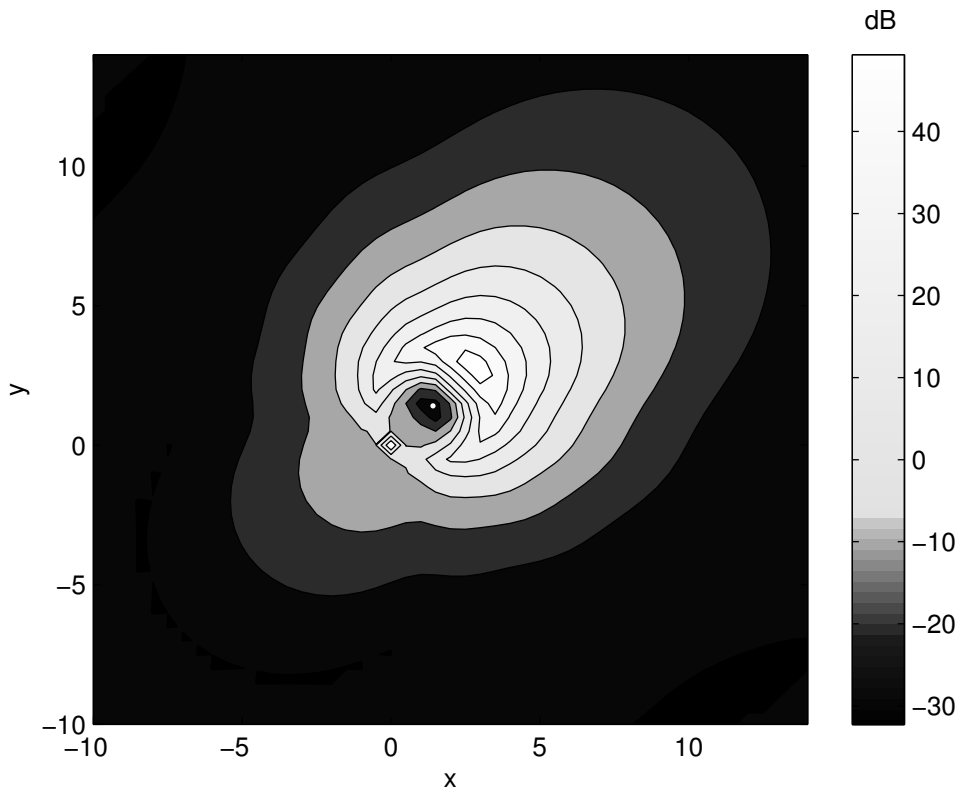
Figure 2.8 Contour plot of error in dB for the expansion of the outgoing wave function, $\Phi_{nm}^{(4)}(\mathbf{R}, t)$, in Eq. (2.73), on the transverse xy plane for $n = 4$, $m = 2$, and $(R_0 = 2, \theta_0 = \pi/2, \phi_0 = \pi/4)$, at most 4 terms are included in the series expansion.

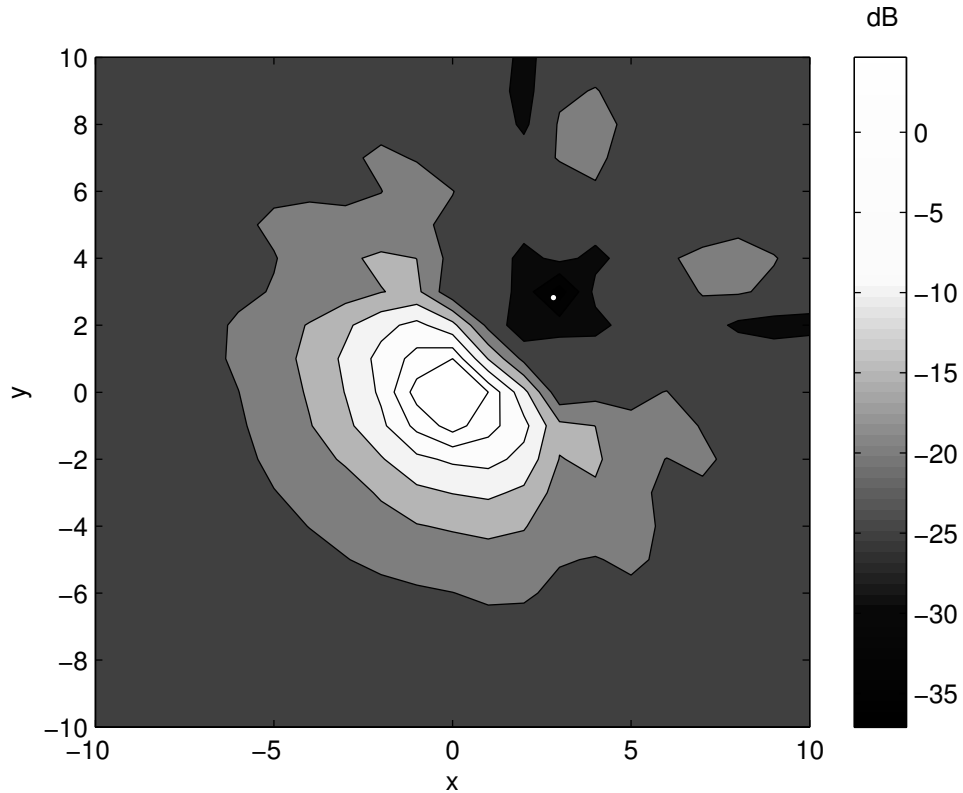Study of many cases showed that; increasing the order and degree of the wave functions, n, m, respectively, tend to increase N, the number of terms that should be included in the series expansion, for a particular numerical accuracy; however, they are not as effective as in the case of the incoming wave functions, Table 2.4.

Table 2.4 Number of terms retained in the wave function expansion of $\Phi_{nm}^{(4)}(\mathbf{R},t)$, N, with respect to n and m for 1 % percent error, for the case $(R=15$, $\theta=\pi/8$, $\phi=\pi/2)$ and $(R_0=1$, $\theta_0=0$, $\phi_0=\pi/4)$.

n	m	N
0	0	3
1	0	3
1	1	3
2	0	3
2	1	3
2	2	3
6	0	4
6	6	4
8	0	3
8	8	5

It is observed that, convergence is mainly determined by $\min\{R',R_o\}$, and R should be chosen large enough with respect to $\min\{R',R_o\}$. Table 2.5 is an example which shows that one has to include more terms in the series expansion, as $\min\{R',R_o\}$ gets larger for fixed n, m and R, and numerical accuracy.

Table 2.5 Number of terms retained in the wave function expansion of $\Phi_{nm}^{(4)}(\mathbf{R},t)$, N, with respect to $\min\{R', R_o\}$ for 1 % percent error, for the case $n = 2$, $m = 2$, $(R = 20$, $\theta = \pi/2$, $\phi = 0)$, and $(\theta_0 = \pi/2$, $\phi_0 = 0)$.

$\min\{R', R_o\}$, m	N
0.1	1
0.5	2
1	3
1.5	5

The effect of the pulse width of the waveform used in smoothing, τ, on N can be seen in Table 2.6. As τ is decreased, N should be increased in order to obtain the same accuracy which is similar to the results of the incoming wave functions.

Table 2.6 Number of terms retained in the wave function expansion of $\Phi_{nm}^{(4)}(\mathbf{R},t)$, N, with respect to τ for 1 % percent error, for the case $n = 2$, $m = 2$, $(R = 20$, $\theta = \pi/2$, $\phi = 0)$, and $(R_0 = 0.75$, $\theta_0 = \pi/2$, $\phi_0 = 0)$.

τ, ns	N
12.75	2
8.5	3
5.7	4

The translational addition theorems for the time domain spherical scalar wave functions are also checked numerically by inverse Fourier transforming the well-known frequency domain expressions.

As a concluding remark, numerical accuracy for the expansions of the incoming and outgoing wave functions in the time domain, i.e., Eq. (2.73), can be interpreted

in a similar way with that in the frequency domain, but there are also additional requirements such as $R \neq 0$, $R_0 \neq 0$, and $R' \neq 0$.

In this chapter, the addition theorems for the spherical scalar wave functions under coordinate translation are described in the frequency domain and derived in the time domain. The derived time domain expressions, which are also checked numerically in this chapter, will be used in solving multiple scattering problems in the following chapters.

CHAPTER 3

TIME DOMAIN SCATTERING OF SCALAR WAVES BY

TWO SPHERES IN FREE-SPACE

In this chapter, first scattering of scalar waves by a single sphere in free-space is reviewed both in the frequency and in the time domain, Section 3.1, then the well-known frequency domain scattering by two spheres is given in Section 3.2. As an application of the time domain translational addition theorems, derived in the previous chapter, formulation and numerical results of the time domain scattering of scalar waves by two spheres in free-space is presented in Section 3.3. The numerical results of the frequency domain scattering are verified with the results given in the literature, Marnevskaya [21], Peterson *et al.* [22], Gaunaurd *et al.* [23] and [24], and Varadan *et al.* [37]. Note that, in those work $e^{-j\omega t}$ time convention is used and the incident plane wave is propagating in the $+z$ direction, which should be paid attention in comparing with the present work. The numerical results of the frequency domain scattering problem are then used in checking the time domain results.

3.1 Scattering of Scalar Waves by a Soft Sphere in Free-Space

Generally, the incident field can be written in the frequency domain as

$$\psi^i(k\mathbf{R}) = \sum_{n=0}^{\infty} \sum_{m=-n}^{n} D_{nm} \, F_{nm}^i \, \varphi_{nm}^{(1)}(k\mathbf{R}) \; , \tag{3.1}$$

where

$$D_{nm} = \frac{-jk(2n+1)(n-m)!}{4\pi(n+m)!}, \tag{3.2}$$

and $\varphi_{nm}^{(1)}(k\mathbf{R})$ is the incoming spherical scalar wave function given in Eq. (2.1). For a known incident field ψ^i, or for a known impressed source, the coefficients $F_{nm}^{\,i}$ are known. Consider the scattering geometry in Figure 3.1,
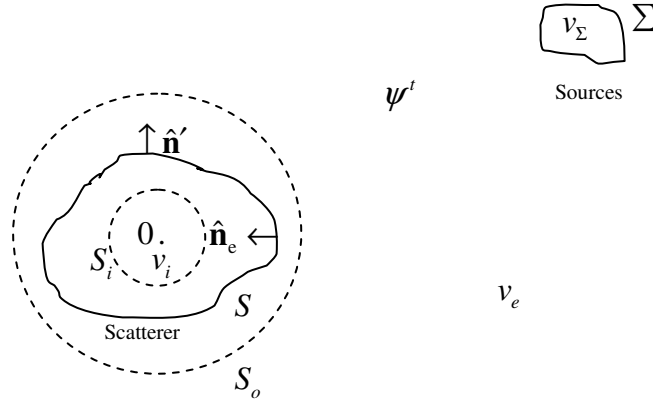
Figure 3.1 A scatterer in the presence of an incident field and surfaces for the T-matrix method.

the total field in the vicinity of the scatterer can be expanded as

$$\psi^t(k\mathbf{R}') = \sum_{\nu=0}^{\infty} \sum_{\mu=-\nu}^{\nu} F_{\nu\mu}^t \, \varphi_{\nu\mu}^{(1)}(k\mathbf{R}') \ , \tag{3.3}$$

and the incident and total field coefficients are related through

$$F_{nm}^i = \sum_{\nu=0}^{\infty} \sum_{\mu=-\nu}^{\nu} Q_{nm,\nu\mu} F_{\nu\mu}^t \ , \tag{3.4}$$

which can be written in matrix form as

$$\mathbf{F}^i = \overline{\mathbf{Q}}\, \mathbf{F}^t \ . \tag{3.5}$$

$\mathbf{F}^i$ and $\mathbf{F}^t$ are column vectors containing F_{nm}^i and $F_{\nu\mu}^t$ in some proper sorting, respectively. $\overline{\mathbf{Q}}$ is a matrix with elements $Q_{nm,\nu\mu}$ which can be shown to be

$$Q_{nm,\nu\mu} = \int_s \varphi_{nm}^{(4)}(k\mathbf{R}')\frac{d}{dn'}\varphi_{\nu\mu}^{(1)}(k\mathbf{R}')\, ds' \ , \tag{3.6}$$

by using the orthonality of Tesseral harmonics and the spherical wave expansion of the scalar free-space Green's function, Eq. (2.40), i.e.,

$$G_0(\mathbf{R},\mathbf{R}';k) = \sum_{n=0}^{\infty}\sum_{m=-n}^{n}\left\{D_{nm}\, j_n(kR_<)h_n^{(2)}(kR_>)\mathrm{Y}_{nm}(\theta_<,\phi_<)\mathrm{Y}_{nm}^*(\theta_>,\phi_>)\right\} \ . \tag{3.7}$$

In Eq. (3.6), $d\,\varphi_{\nu\mu}^{(1)}(k\mathbf{R}')\big/dn'$ corresponds to the directional derivative of $\varphi_{\nu\mu}^{(1)}(k\mathbf{R}')$ along $d\hat{\mathbf{n}}'$, defined in Eq. (C.6), and $\hat{\mathbf{n}}'$ is the unit normal outward from the scatterer as depicted in Figure 3.1.

The scattered field can be written in terms of the outgoing wave functions as

$$\psi^s(k\mathbf{R}) = \sum_{n=0}^{\infty}\sum_{m=-n}^{n}D_{nm}\, F_{nm}^s\, \varphi_{nm}^{(4)}(k\mathbf{R}) \ , \tag{3.8}$$

and the scattered field coefficients can be related to the total field coefficients through

$$F_{nm}^s = \sum_{\nu=0}^{\infty}\sum_{\mu=-\nu}^{\nu}Q_{nm,\nu\mu}^e F_{\nu\mu}^t \ , \tag{3.9}$$

which can be written in matrix form as

$$\mathbf{F}^s = \overline{\mathbf{Q}}^e \, \mathbf{F}^t \ . \tag{3.10}$$

$\mathbf{F}^s$ is a column vector containing F_{nm}^s and $\overline{\mathbf{Q}}^e$ is a matrix with elements $Q_{nm,\nu\mu}^e$,

$$Q_{nm,\nu\mu}^e = -\int_s \varphi_{nm}^{(1)}(k\mathbf{R}') \frac{d}{dn'} \varphi_{\nu\mu}^{(1)}(k\mathbf{R}') \, ds' \ . \tag{3.11}$$

The inspection of Eqs.(3.6) and (3.11) shows that

$$\overline{\mathbf{Q}}^e = -\mathrm{Re}\{\overline{\mathbf{Q}}\}, \tag{3.12}$$

where Re implies the "regular part of", in other words, $\mathrm{Re}\{\overline{\mathbf{Q}}\}$ will convert all the Hankel functions in $\overline{\mathbf{Q}}$ into Bessel functions, Chew [2]. The T-matrix can now be defined to relate the scattered field coefficients to the incident field coefficients as

$$\mathbf{F}^s = \overline{\mathbf{T}} \, \mathbf{F}^i \ . \tag{3.13}$$

where

$$\begin{aligned}
\overline{\mathbf{T}} &= \overline{\mathbf{Q}}^e \, \overline{\mathbf{Q}}^{-1} , \\
&= -\mathrm{Re}\{\overline{\mathbf{Q}}\} \, \overline{\mathbf{Q}}^{-1} \ .
\end{aligned} \tag{3.14}$$

Eq. (3.14) indicates that $\overline{\mathbf{Q}}^e$ does not need to be filled separately, i.e., it suffices to fill $\overline{\mathbf{Q}}$ in order to get the T-matrix, $\overline{\mathbf{T}}$. Once the T-matrix is obtained for a given frequency and a scatterer, it can be used for any illumination.

Consider a plane wave incident from the $+z$ axis (from $\theta = 0$), which can be

expanded, using Eq. (2.49), as

$$\psi^i(k\mathbf{R}) = e^{jkz} \,,$$

$$= \sum_{n=0}^{\infty} j^n (2n+1) j_n(kR) P_n(\cos\theta) \,.$$

(3.15)

Let this incident wave insonifies a soft sphere of radius a centered at the origin, the scattered field can be expressed as

$$\psi^s(k\mathbf{R}) = \sum_{n=0}^{\infty} j^n (2n+1) F_n^s \, h_n^{(2)}(kR) P_n(\cos\theta) \,.$$

(3.16)

where the scattered field coefficients, F_n^s, can be found by imposing the Dirichlet boundary condition on the sphere, i.e.,

$$\left(\psi^i + \psi^s\right)\big|_{R=a} = 0 \,,$$

(3.17)

$$F_n^s = -\frac{j_n(ka)}{h_n^{(2)}(ka)} \,.$$

(3.18)

Note that the orthogonality of the wave functions implies that they are linearly independent; and this property enables to interpret Eq. (3.17) as a term-by-term equality, leading to Eq. (3.18). Hence, the T-matrix for the soft sphere centered at the origin is a diagonal matrix given by

$$T_{nm,\nu\mu} = -\frac{j_n(ka)}{h_n^{(2)}(ka)} \delta_{n\nu} \delta_{m\mu} \,.$$

(3.19)

The normalized scattering cross section for a scatterer is defined as

$$\sigma = 4\pi R^2 \frac{\left|\psi^s\right|^2}{\left|\psi^i\right|^2} \frac{1}{\pi a^2} \, , \tag{3.20}$$

and the normalized backscattering cross section is

$$\sigma_b = \sigma(\theta = 0) \, . \tag{3.21}$$

The plot of the normalized backscattering cross section for acoustically soft sphere of radius a with respect to the normalized frequency ka, which is in agreement with Varadan *et al.* [37], is given in Figure (3.2). The observation point in the backscattering direction is chosen in the far field, $(R = 1000, \theta = 0, \phi = 0)$, and at least 30 terms should be retained in the series expansion as ka goes up to 20.
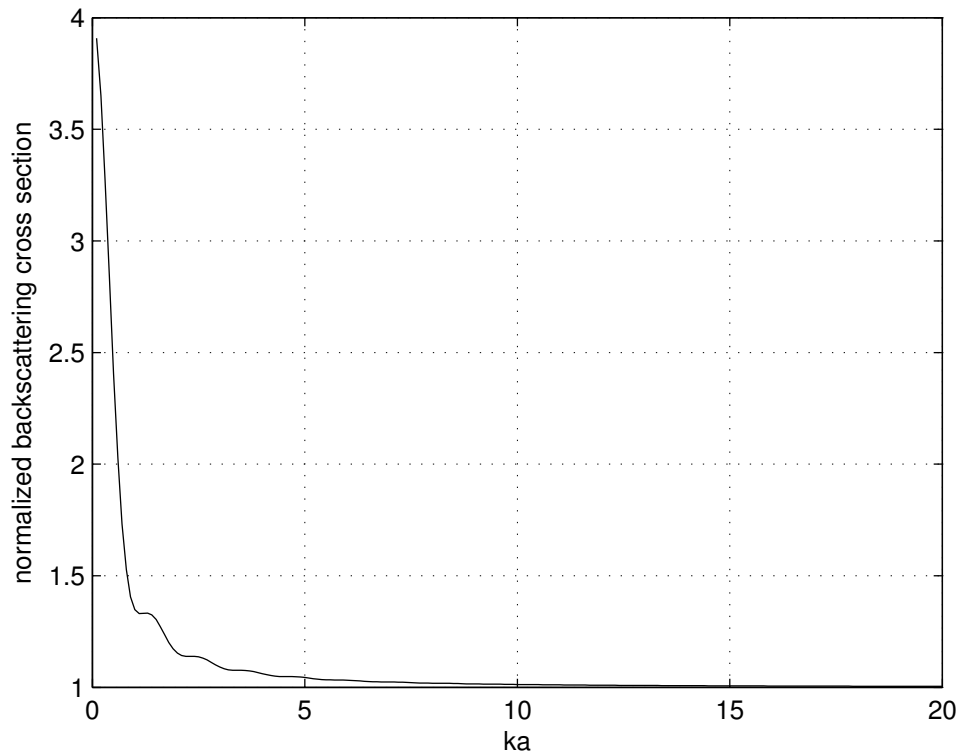
Figure 3.2 Normalized backscattering cross section for acoustically soft sphere of radius a with respect to the normalized frequency ka.

Now, consider the time domain scattering, the time domain T-matrix formulation is given in Appendix A. The specific application of this formulation, which is the scattering by an acoustically soft sphere, is given in Buyukdura *et al.* [13], and can be summarized as follows.

The impulsive plane wave incident from the $+z$ axis (from $\theta = 0$), i.e., $\delta(t+z)$, can be expanded as,

$$\psi^i(\mathbf{R},t) = \frac{1}{2}\sum_{n=0}^{\infty}(-1)^n(2n+1)S_n\left(\frac{R}{c},t\right)P_n(\cos\theta) \ , \tag{3.22}$$

which can be deduced from Eq. (2.48). The scattered field due to this incident field can be written as,

$$\psi^s(\mathbf{R},t) = -\frac{1}{2}\sum_{n=0}^{\infty}(-1)^n(2n+1)c_n(t)\otimes S_n\left(\frac{a}{c},t\right)\otimes O_n\left(\frac{R}{c},t\right)P_n(\cos\theta) \ ,$$
$$\tag{3.23}$$

where the convolving function, $c_n(t)$, can be found by imposing the boundary condition on the sphere which implies

$$c_n(t)\otimes O_n\left(a/c,t\right) = \delta(t) \ . \tag{3.24}$$

Note that, this equation is in the form of Eq. (A.27) and the Q matrix, $\overline{\mathbf{Q}}(t)$, is diagonal with diagonal entries $O_n\left(a/c,t\right)$. The convolving functions, $c_n(t)$, can be found using direct deconvolution. When Eq. (3.23) is expressed according to Eq.(A.21), it is clear that the matrix, $\overline{\mathbf{Q}}^e(t)$, is diagonal with diagonal entries $S_n\left(a/c,t\right)$ and appropriate coefficients. As $\overline{\mathbf{Q}}(t)$ and $\overline{\mathbf{Q}}^e(t)$ is found, the time domain T-matrix for single sphere can be defined as

$$\overline{\mathbf{T}}(t) = -\overline{\mathbf{S}}_a(t)\otimes\overline{\mathbf{\Theta}}_a(t) \ , \tag{3.25}$$

where

$$\overline{\mathbf{\Theta}}_a(t) \otimes \overline{\mathbf{O}}_a(t) = \overline{\mathbf{\delta}}(t) \ , \tag{3.26}$$

and $\overline{\mathbf{\delta}}(t)$ is a diagonal matrix containing $\delta(t)$ in each diagonal entry and $\overline{\mathbf{O}}_a(t)$ and $\overline{\mathbf{S}}_a(t)$ are diagonal matrices containing $O_n(a/c,t)$ and $S_n(a/c,t)$, respectively.

As a numerical example, the plane wave with the Gaussian pulse waveform, defined in Section 2.3, incident from the $+z$ axis on a soft sphere of radius $a = 1\,\mathrm{m}$ is considered. In order to find the scattered field in response to such an incident field, we simply convolve the waveform with Eq. (3.23). Shown in Figure 3.3 are two solutions to the scattered field in the backscatter direction at a distance of $R = 3\,\mathrm{m}$ where the field intensity is plotted versus time. The solid curve is obtained using the present time domain formulation (direct deconvolution is used in finding the scattered field convolving functions), while the cross marks are obtained by inverse Fourier transforming the well-known frequency domain solution. Both solutions are obtained by including 5 terms in the series expansion. An observation made on the time domain solution is that the solution converges rapidly if the dimension of the scatterer is small compared to the wavelength at the highest frequency component of the incident field, which is similar to the case in the solution of problems in the frequency domain.
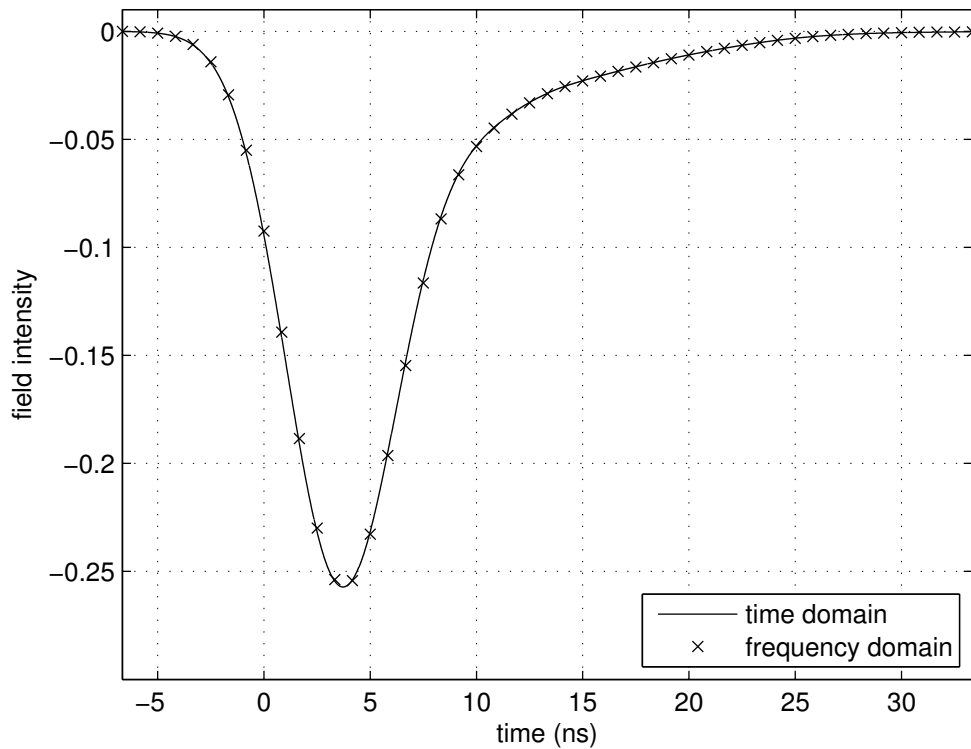
Figure 3.3 Scattered field intensity vs. time at the backscatter direction,
$(R = 3, \theta = 0, \phi = 0)$, due to a Gaussian pulse waveform incident from the $+z$ axis
on a soft sphere of radius $a = 1\,\text{m}$.

3.2 Scattering of Scalar Waves by Two Soft Spheres in Free-Space in the Frequency Domain

The scattering of scalar waves by two spheres is well known in the frequency domain, Marnevskaya [21], Gaunaurd *et al.* [23] and [24]. The present formulation is developed similarly, however more general in the sense that the positions of the spheres are arbitrary, i.e., no simple special case of translation is chosen for the scatterers. Consider the scattering geometry in Figure 3.4.
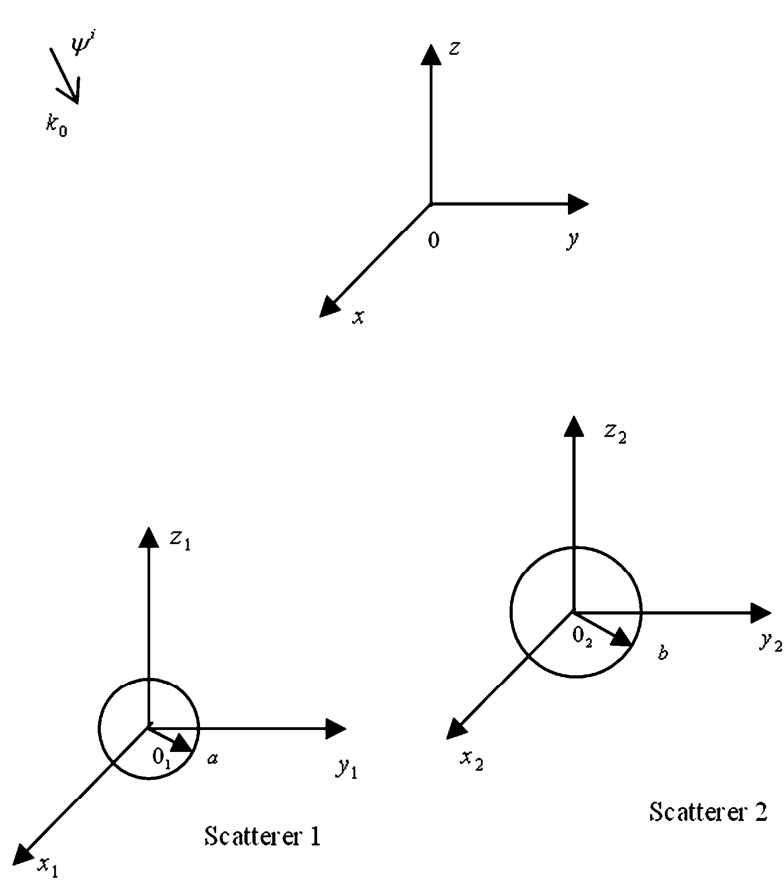
Figure 3.4 Two spheres in the presence of an incident field.

The incident field can be expanded as

$$\psi^i(k\mathbf{R}) = \sum_{n=0}^{\infty} \sum_{m=-n}^{n} F_{nm}^i \, \varphi_{nm}^{(1)}(k\mathbf{R}) \ , \tag{3.27}$$

with reference to the origin 0. The scattered wave from scatterer 1 of radius a can be expanded in terms of the outgoing wave functions expressed in its self-coordinates as

$$\psi^{s1}(k\mathbf{R}_1) = \sum_{n=0}^{\infty} \sum_{m=-n}^{n} F_{nm}^{s1} \, \varphi_{nm}^{(4)}(k\mathbf{R}_1) \ , \tag{3.28}$$

The scattered wave from scatterer 2 of radius b can be expanded similarly in its self-coordinates as

$$\psi^{s2}(k\mathbf{R}_2) = \sum_{n=0}^{\infty} \sum_{m=-n}^{n} F_{nm}^{s2} \, \varphi_{nm}^{(4)}(k\mathbf{R}_2) \ . \tag{3.29}$$

The total scattered field is then,

$$\psi^{s}(k\mathbf{R}) = \psi^{s1}(k\mathbf{R}_1) + \psi^{s2}(k\mathbf{R}_2) \ , \tag{3.30}$$

where the coefficients F_{nm}^{s1} and F_{nm}^{s2} are, as yet, unknown and can be found by imposing the boundary conditions on the surfaces of both spheres. Using the translational addition theorems given in Section 2.1, i.e., Eqs. (2.24) - (2.27), the total field on the surface of the scatterer 1 can be expressed in the coordinate system 1 as

$$\psi^{t}(k\mathbf{R}_1) = \sum_{n=0}^{\infty} \sum_{m=-n}^{n} \left\{ F_{nm}^{i} \sum_{\nu=0}^{\infty} \sum_{\mu=-\nu}^{\nu} \left\{ \beta_{10}(m,n|\mu,\nu;k)\varphi_{\nu\mu}^{(1)}(k\mathbf{R}_1) \right\} \right.$$

$$\left. + F_{nm}^{s1} \, \varphi_{nm}^{(4)}(k\mathbf{R}_1) + F_{nm}^{s2} \sum_{\nu=0}^{\infty} \sum_{\mu=-\nu}^{\nu} \left\{ \alpha_{12}(m,n|\mu,\nu;k)\varphi_{\nu\mu}^{(1)}(k\mathbf{R}_1) \right\} \right\} \ , \tag{3.31}$$

where

$$\beta_{10}(m,n\,|\,\mu,\nu;k) = (-1)^{\mu}(j)^{\nu-n}(2\nu+1)$$

$$\sum_{\rho} \left\{ (j)^{\rho} \, a(m,n\,|\,-\mu,\nu\,|\,\rho)\, \varphi_{\rho,(m-\mu)}^{(1)}(k\mathbf{R}_{o,10}) \right\}, \tag{3.32}$$

and

$$\alpha_{12}\left(m,n\left|\mu,\nu;k\right.\right)=(-1)^{\mu}(j)^{\nu-n}(2\nu+1)$$

$$\sum_{\rho}\left\{(j)^{\rho}\ a\left(m,n\left|-\mu,\nu\left|\rho\right.\right.\right)\varphi_{\rho,(m-\mu)}^{(4)}(k\mathbf{R}_{o,12})\right\}.$$

(3.33)

Also, note that $\mathbf{R}_{o,10}$ represents the translation from origin 0 to 0_1 and $\mathbf{R}_{o,12}$ the translation from origin 0_2 to 0_1, i.e.,

$$\mathbf{R}=\mathbf{R}_{o,10}+\mathbf{R}_1\ ,$$

(3.34)

$$\mathbf{R}_2=\mathbf{R}_{o,12}+\mathbf{R}_1\ .$$

(3.35)

In Eq. (3.31), first term is the incident field written in the coordinate system 1, second term is the scattered field from the scatterer 1 in its self coordinates, and the third term is the scattered field from the scatterer 2 written in the coordinate system 1. The first and the third terms can be viewed as the incident field impinging on the scatterer 1.

Similarly, the total field on the surface of the scatterer 2 can be expressed in the coordinate system 2 as

$$\psi^t(k\mathbf{R}_2)=\sum_{n=0}^{\infty}\sum_{m=-n}^{n}\left\{F_{nm}^i\sum_{\nu=0}^{\infty}\sum_{\mu=-\nu}^{\nu}\left\{\beta_{20}\left(m,n\left|\mu,\nu;k\right.\right)\varphi_{\nu\mu}^{(1)}(k\mathbf{R}_2)\right\}\right.$$

$$\left.+F_{nm}^{s1}\sum_{\nu=0}^{\infty}\sum_{\mu=-\nu}^{\nu}\left\{\alpha_{21}\left(m,n\left|\mu,\nu;k\right.\right)\varphi_{\nu\mu}^{(1)}(k\mathbf{R}_2)\right\}+F_{nm}^{s2}\ \varphi_{nm}^{(4)}(k\mathbf{R}_2)\right\}\ ,$$

(3.36)

where

$$\beta_{20}\left(m,n \left| \mu,\nu;k\right.\right)=(-1)^{\mu}(j)^{\nu-n}(2\nu+1)$$

$$\sum_{\rho}\left\{(j)^{\rho}\ a\!\left(m,n \left| -\mu,\nu \right| \rho\right)\varphi_{\rho,(m-\mu)}^{(1)}(k\mathbf{R}_{o,20})\right\},$$

(3.37)

and

$$\alpha_{21}\left(m,n \left| \mu,\nu;k\right.\right)=(-1)^{\mu}(j)^{\nu-n}(2\nu+1)$$

$$\sum_{\rho}\left\{(j)^{\rho}\ a\!\left(m,n \left| -\mu,\nu \right| \rho\right)\varphi_{\rho,(m-\mu)}^{(4)}(k\mathbf{R}_{o,21})\right\}.$$

(3.38)

Note that $\mathbf{R}_{o,20}$ represents the translation from origin 0 to 0_2 and $\mathbf{R}_{o,21}$ the translation from origin 0_1 to 0_2, i.e.,

$$\mathbf{R}=\mathbf{R}_{o,20}+\mathbf{R}_2 \ ,$$

(3.39)

$$\mathbf{R}_1=\mathbf{R}_{o,21}+\mathbf{R}_2 \ .$$

(3.40)

For the case of soft spheres, imposing the Dirichlet boundary conditions on the surface of each sphere, $\left.\psi^t\right|_{R_1=a}=0$, and $\left.\psi^t\right|_{R_2=b}=0$, and using the orthogonality of the Tesseral harmonics over a spherical surface, the following two coupled equations for the coefficients are obtained,

$$-F_{n'm'}^{s1}\,h_{n'}^{(2)}(ka)=j_{n'}(ka)\sum_{n=0}^{\infty}\sum_{m=-n}^{n}F_{nm}^{i}\,\beta_{10}\left(m,n\left|m',n';k\right.\right)$$

$$+j_{n'}(ka)\sum_{n=0}^{\infty}\sum_{m=-n}^{n}F_{nm}^{s2}\,\alpha_{12}\left(m,n\left|m',n';k\right.\right)\ ,$$

(3.41)

and

$$-F_{n'm'}^{s2}\, h_{n'}^{(2)}(kb) = j_{n'}(kb) \sum_{n=0}^{\infty} \sum_{m=-n}^{n} F_{nm}^{i}\, \beta_{20}\big(m,n\big|m',n';k\big)$$

$$+ j_{n'}(kb) \sum_{n=0}^{\infty} \sum_{m=-n}^{n} F_{nm}^{s1}\, \alpha_{21}\big(m,n\big|m',n';k\big) \quad .$$

$$(3.42)$$

It is worth noting that

$$\alpha_{12}\big(m,n\,\big|\mu,\nu;k\big) = (-1)^{n+\nu}\, \alpha_{21}\big(m,n\,\big|\mu,\nu;k\big) , \qquad (3.43)$$

as $\mathbf{R}_{o,21}$ and $\mathbf{R}_{o,12}$ are backwards translations.

The coupled relations, Eqs. (3.41) and (3.42) can be written in matrix notation as

$$\mathbf{F}^{s1} = \overline{\mathbf{T}}_1 \left(\overline{\boldsymbol{\beta}}_{10}\, \mathbf{F}^{i} + \overline{\boldsymbol{\alpha}}_{12}\, \mathbf{F}^{s2} \right) , \qquad (3.44)$$

$$\mathbf{F}^{s2} = \overline{\mathbf{T}}_2 \left(\overline{\boldsymbol{\beta}}_{20}\, \mathbf{F}^{i} + \overline{\boldsymbol{\alpha}}_{21}\, \mathbf{F}^{s1} \right) , \qquad (3.45)$$

where $\overline{\mathbf{T}}_i$ is the isolated-scatterer T-matrix for the i-th scatterer defined in Eq. (3.19), and $\overline{\boldsymbol{\beta}}_{10}$, $\overline{\boldsymbol{\beta}}_{20}$, $\overline{\boldsymbol{\alpha}}_{12}$, and $\overline{\boldsymbol{\alpha}}_{21}$ are matrices containing $\beta_{10}\big(m,n\big|m',n';k\big)$, $\beta_{20}\big(m,n\big|m',n';k\big)$, $\alpha_{12}\big(m,n\big|m',n';k\big)$, and $\alpha_{21}\big(m,n\big|m',n';k\big)$ in some proper sorting, respectively.

The simultaneous solution of the coupled equations, Eqs. (3.44) and (3.45), yield the scattered field coefficients as

$$\mathbf{F}^{s1} = \left(\overline{\mathbf{I}} - \overline{\mathbf{T}}_1\, \overline{\boldsymbol{\alpha}}_{12}\, \overline{\mathbf{T}}_2\, \overline{\boldsymbol{\alpha}}_{21} \right)^{-1} \overline{\mathbf{T}}_1 \left(\overline{\boldsymbol{\beta}}_{10} + \overline{\boldsymbol{\alpha}}_{12}\, \overline{\mathbf{T}}_2\, \overline{\boldsymbol{\beta}}_{20} \right) \mathbf{F}^{i} , \qquad (3.46)$$

$$\mathbf{F}^{s2} = \left(\overline{\mathbf{I}} - \overline{\mathbf{T}}_2\, \overline{\boldsymbol{\alpha}}_{21}\, \overline{\mathbf{T}}_1\, \overline{\boldsymbol{\alpha}}_{12} \right)^{-1} \overline{\mathbf{T}}_2 \left(\overline{\boldsymbol{\beta}}_{20} + \overline{\boldsymbol{\alpha}}_{21}\, \overline{\mathbf{T}}_1\, \overline{\boldsymbol{\beta}}_{10} \right) \mathbf{F}^{i} , \qquad (3.47)$$

which check with Chew [2]. In these equations, $\overline{\mathbf{I}}$ is the identity matrix, and the T-

matrices, $\overline{\mathbf{T}}_i$, are diagonal if the scatterers are spheres. If the incident field is a plane wave, then $\overline{\boldsymbol{\beta}}_{i0}$ is diagonal with entries containing the phase term, $e^{jkR_{o,i0}\cos\theta_{o,i0}}$, with appropriate coefficients, where $\mathbf{R}_{o,i0}$ represents the translation from origin 0 to 0_i. The scattered field coefficients when used in Eqs. (3.28) – (3.30) give the total scattered field in the presence of two scatterers.

In order to check the above formulation, numerical results are compared with some results given in the literature. Consider two soft spheres, oriented as shown in Figure 3.5, illuminated by a plane wave incident from the $+z$ axis, e^{jkz}. The radii of the spheres are chosen as $ka = 1$ and $kb = 1$.
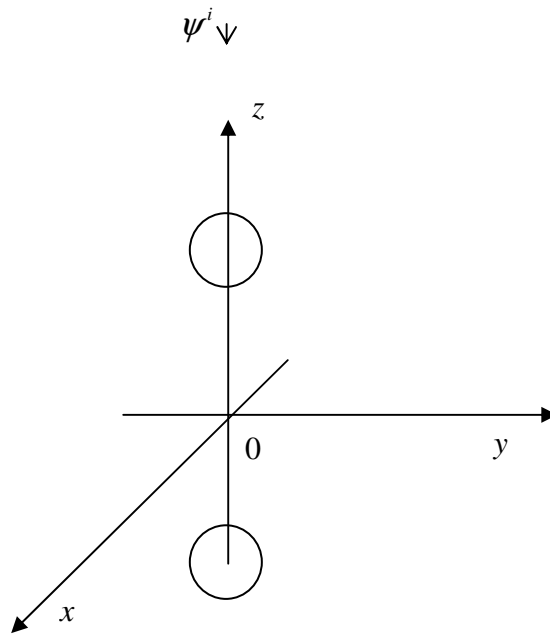
Figure 3.5 Two spheres placed on the z axis, symmetrically with respect to the transverse xy plane, and
illuminated by a plane wave incident from the $+z$ axis, (end-on incidence).

$\left|\psi^s\right|^2$ as a function of θ in the far field with reference to 0 for various values of the separation of the spheres, $kR_{o,21}$ denoted by kd, is illustrated in Figure 3.6, where 10

terms are retained in the series expansion of the scattered field.
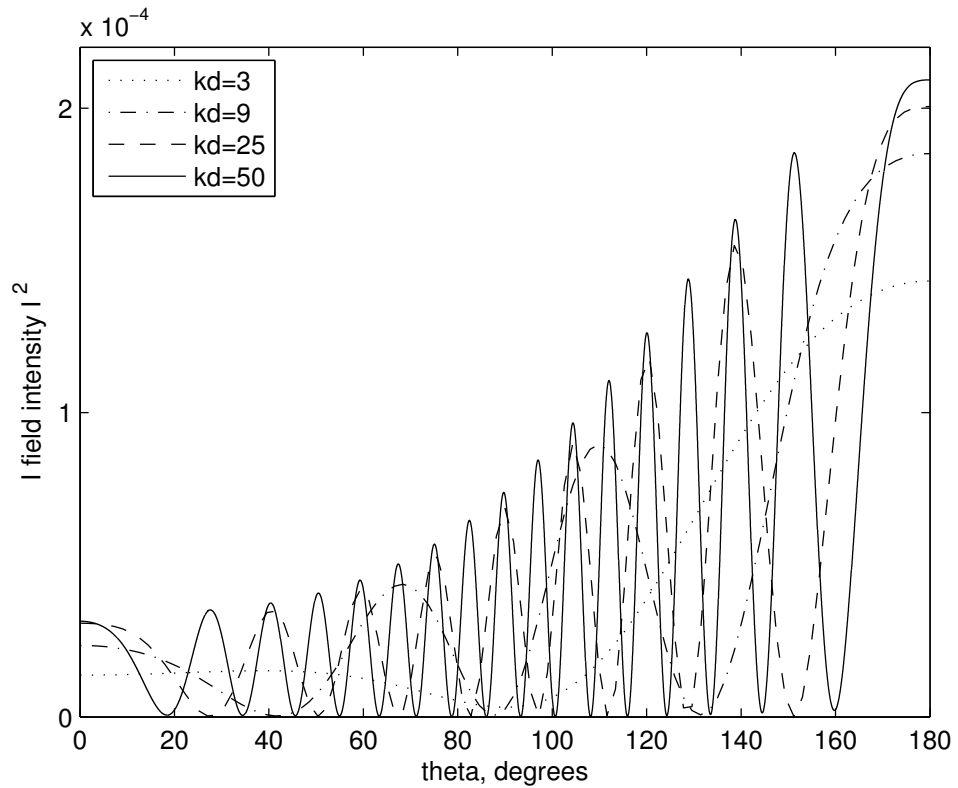
Figure 3.6 $\left| \psi^s \right|^2$ vs. θ in the far field with reference to 0, due to a plane wave incident from the $+z$ axis in the presence of two scatterers ($ka = 1$, $kb = 1$) for various values of the separation of the spheres, $kR_{o,21}$ denoted by kd, scatterers are placed on the z axis, symmetrically with respect to the transverse xy plane.

The plot in Figure 3.6 is in agreement with the plot given in Marnevskaya [21], note that the incident plane wave is propagating in the $+z$ direction in there and this should be taken into account in comparing with the present plot in which the incident wave propagates in the opposite direction. Figure 3.6 illustrates the fact that as the separation of the spheres, $kR_{o,21}$ denoted by kd, increases, $\left| \psi^s \right|^2$ oscillates more and more and it increases on going from the illumination zone to the geometric shadow zone.
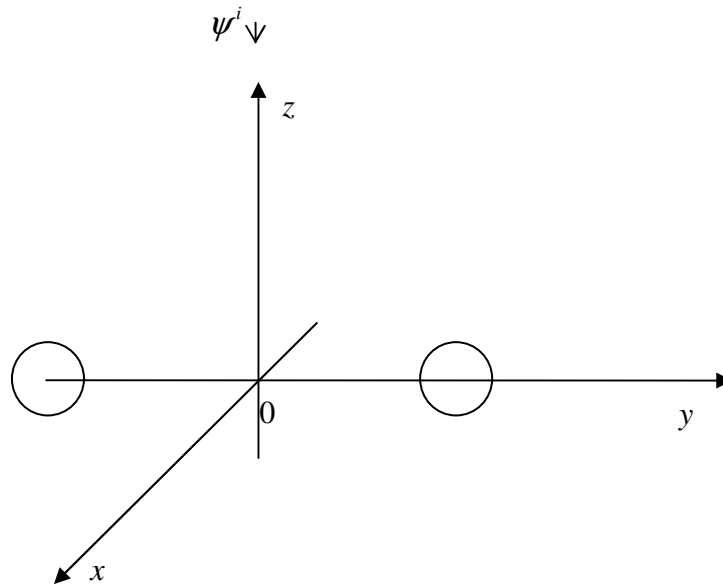
Figure 3.7 Two spheres placed on the y axis, symmetrically with respect to the transverse xz plane, and
illuminated by a plane wave incident from the $+z$ axis, (broadside incidence).

In Figure 3.7, the spheres are placed on the y axis, symmetrically with respect to the transverse xz plane, and $\left| \psi^{s} \right|^{2}$ is plotted as a function of θ in the far field at $\phi = 0$ and $\phi = \pi/2$ with reference to 0, Figures 3.8 and 3.9, respectively. Again the radii of the spheres are chosen as $ka = 1$ and $kb = 1$, and the separation between the spheres is $kR_{o,21} = 100$.
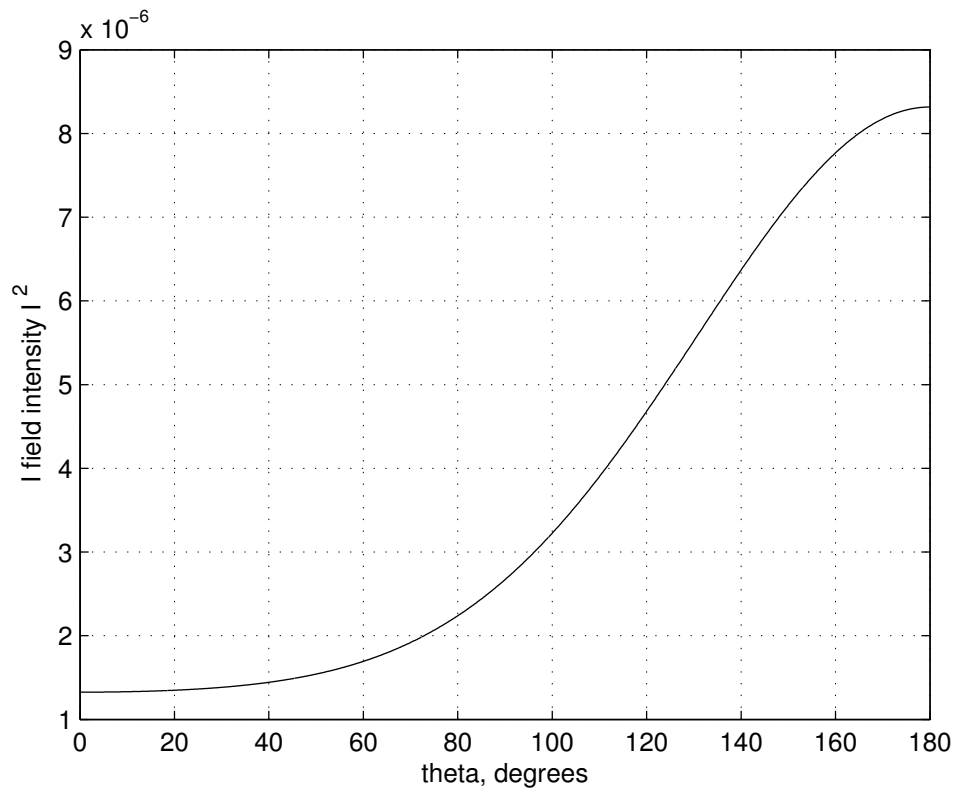
Figure 3.8 $\left| \psi^s \right|^2$ vs. θ in the far field at $\phi = 0$ with reference to 0, due to a plane wave incident from the $+z$ axis in the presence of two scatterers ($ka = 1$, $kb = 1$) for $kR_{o,21} = 100$, scatterers are placed on the y axis, symmetrically with respect to the transverse xz plane.
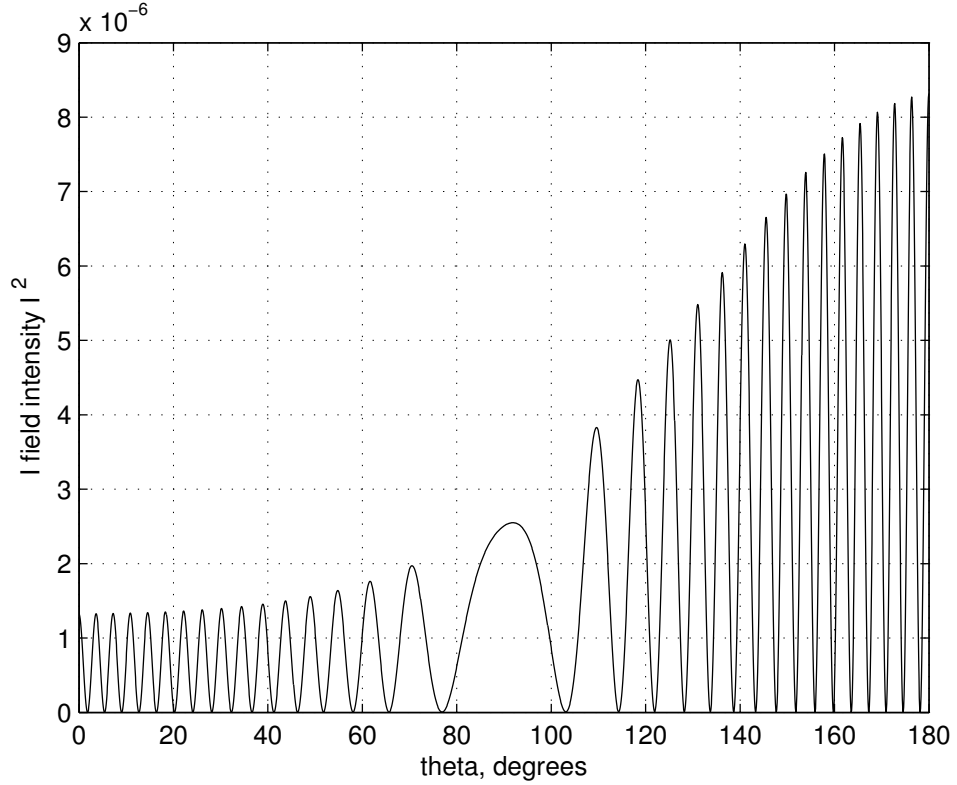
Figure 3.9 $\left|\psi^{s}\right|^{2}$ vs. θ in the far field at $\phi = \pi/2$ with reference to 0, due to a plane wave incident from the $+z$ axis in the presence of two scatterers ($ka = 1$, $kb = 1$) for $kR_{o,21} = 100$, scatterers are placed on the y axis, symmetrically with respect to the transverse xz plane.

The normalized backscattering cross section, Eqs. (3.20) and (3.21), for two soft spheres with radii $ka = 2$ and $kb = 2$ placed on the x axis, symmetrically with respect to the transverse yz plane is plotted as a function of the separation between the scatterers in Figure 3.10. Note that, the scatterers placed on the y axis, symmetrically with respect to the transverse xz plane, Figure 3.7, would yield the same result. The illumination is incident from the $+z$ axis and only 5 terms are retained in the series expansion of the scattered field.
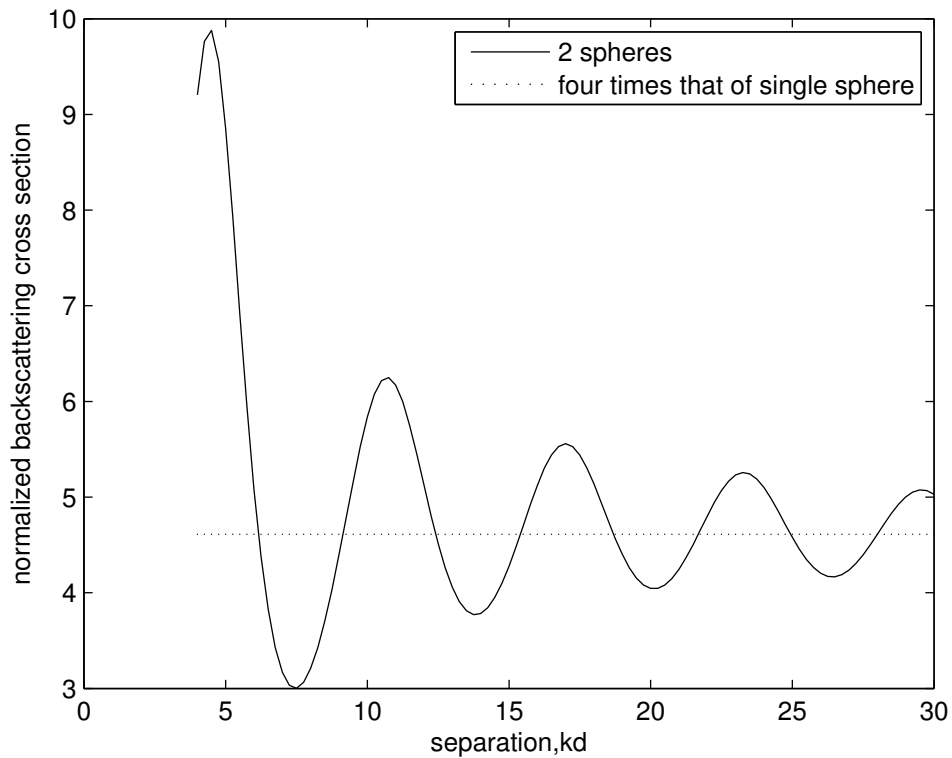
Figure 3.10 Normalized backscattering cross section for two soft spheres vs. the separation between the spheres, $kR_{o,21}$ denoted by kd, the spheres are of radii $ka = 2$, $kb = 2$, and placed on the x axis, symmetrically with respect to the transverse yz plane, the illumination is incident from the $+z$ axis, (broadside incidence).

The normalized backscattering cross section of two soft spheres, Figure 3.10 which checks with the plot of Peterson *et al.* [22], oscillates around four times that of a single soft sphere with $ka = 2$ which is shown with the dashed line.

Consider the scattering geometry in Figure 3.11 where scatterer 1 is of radius $ka = 2$ located at $(2.25/k, \theta_1, 0)$ with reference to 0 and scatterer 2 is of radius $kb = 2$ located at $(2.25/k, \pi - \theta_1, 0)$ with reference to 0, where $\theta_1 = theta * \pi/180$. The illumination is incident from the $+z$ axis.
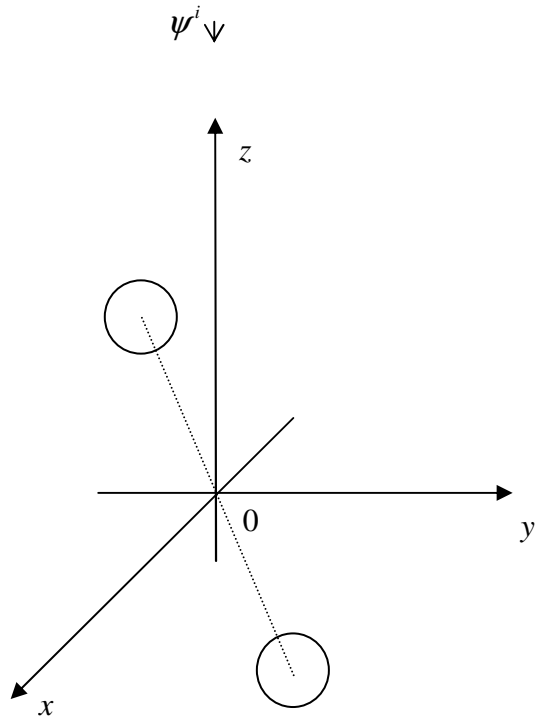
Figure 3.11 Scatterer 1 is of radius $ka = 2$, located at $(2.25/k \,, \theta_1 \,, 0)$ with reference to 0 and scatterer 2 is of radius $kb = 2$, located at $(2.25/k \,, \pi - \theta_1 \,, 0)$ with reference to 0, where $\theta_1 = theta * \pi/180$, the illumination is incident from the $+ z$ axis.

The normalized backscattering cross section is plotted as a function of *theta* in Figure 3.12 and it checks with the plot of Peterson *et al.* [22]. Only 5 terms are retained in the series expansion of the scattered field.
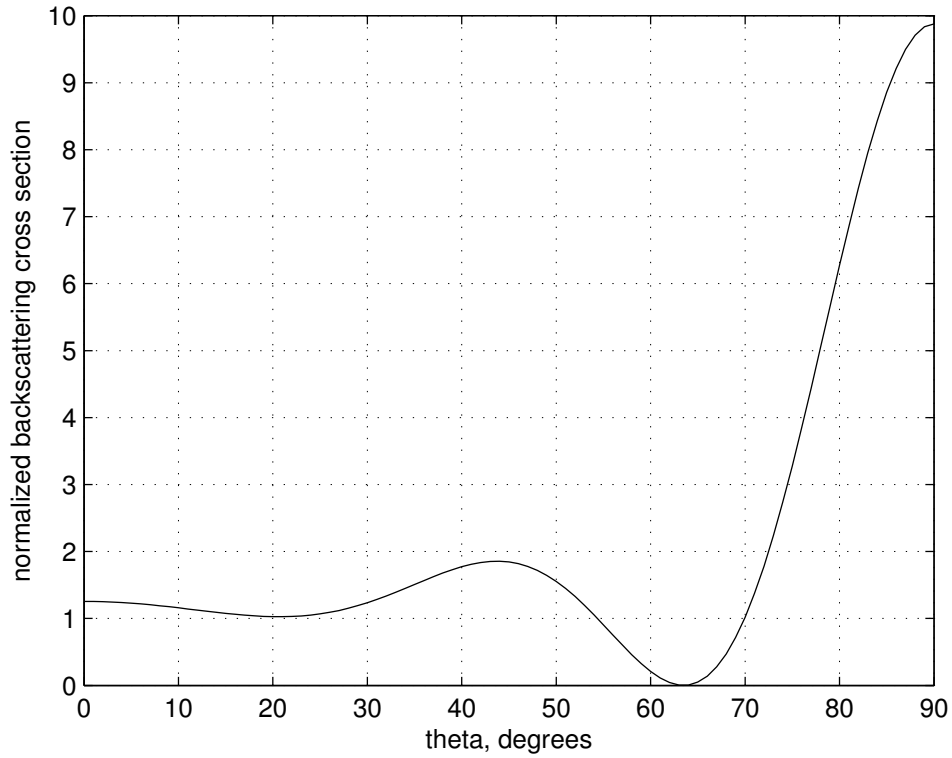
Figure 3.12 Normalized backscattering cross section for two soft spheres vs. *theta*, the spheres are of radii $ka = 2$, $kb = 2$, located at $(2.25/k, \theta_1, 0)$ with reference to 0 and $(2.25/k, \pi - \theta_1, 0)$ with reference to 0, respectively, where $\theta_1 = theta * \pi/180$, the illumination is incident from the $+z$ axis.

The form function is defined as, Gaunaurd *et al.* [23],

$$f_\infty = \frac{2R}{a} \frac{|\psi^s|}{|\psi^i|},$$ (3.48)

and plotted with respect to the normalized frequency ka for end-on incidence (scatterers placed as in Figure 3.5) in Figure 3.13, where the separation between the spheres is $R_{o,21} = 20$, and the observation is in the far field. In the series expansion of the scattered field, again 10 terms are retained.
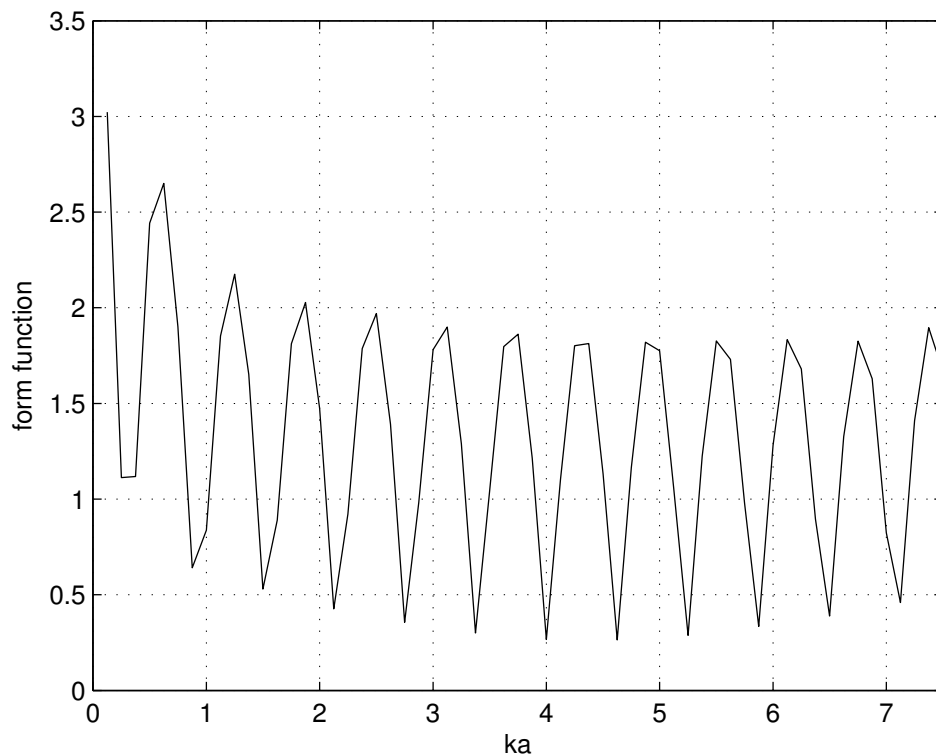
Figure 3.13 Form function for two soft spheres vs. the normalized frequency ka, the spheres are placed on the z axis, symmetrically with respect to the transverse xy plane with separation $R_{o,21} = 20$, the illumination is incident from the $+z$ axis (end-on incidence).

Note that in Figure 3.13, oscillations have approximately unit mean amplitude and peak envelopes around twice the form function value for a single soft sphere at the particular ka value. The form function is plotted with respect to the normalized frequency ka for broadside incidence (scatterers placed as in Figure 3.7) in Figure 3.14, where again the separation between the spheres is $R_{o,21} = 20$, and observation is in the far field. In the series expansion of the scattered field, 10 terms are retained.
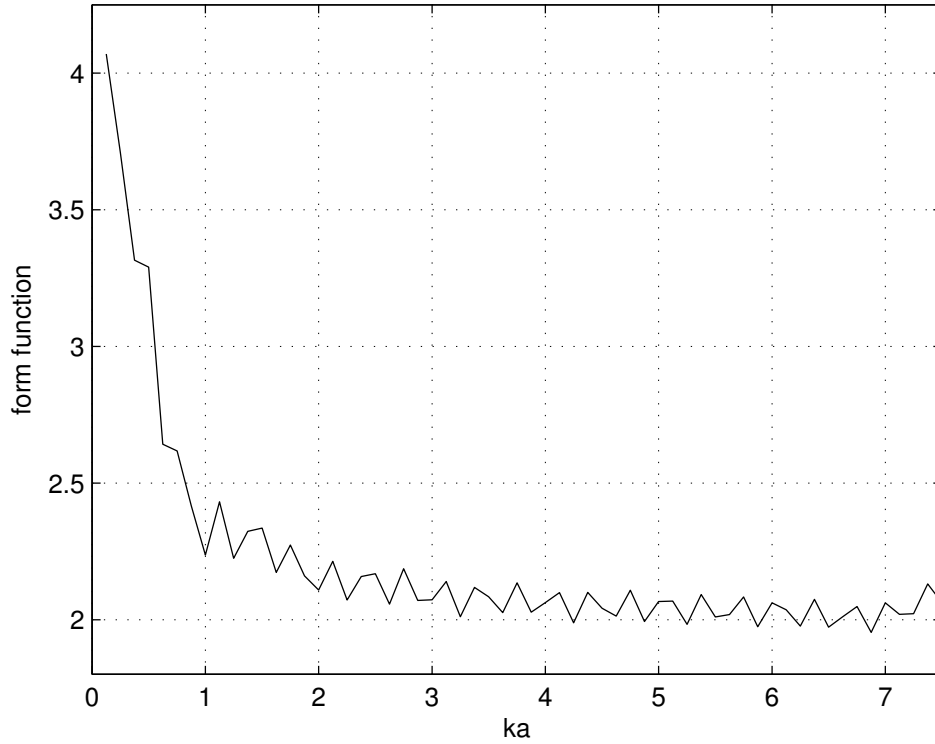
Figure 3.14 Form function for two soft spheres vs. the normalized frequency ka, the spheres are placed on the y axis, symmetrically with respect to the transverse xz plane with separation $R_{o,21} = 20$, the illumination is incident from the $+z$ axis (broadside incidence).

Note that in Figure 3.14, the form function oscillates around twice the form function value for a single soft sphere at the particular ka value. These observations made for the form function of two spheres for the cases of end-on and broadside incidence are similar to Gaunaurd *et al.* [23] and [24], where two rigid spheres, satisfying the Neumann boundary conditions, are worked on.

In order to figure out the effect of coupling between the two spheres on the waveform of the scattered field, scattering of scalar waves by two spheres is solved in the frequency domain using the present formulation and the time domain scattered field is obtained by inverse Fourier transforming the frequency domain solution. Then the result is compared with the results when the effect of coupling is ignored, i.e., two isolated spheres, where $\bar{\boldsymbol{\alpha}}_{12}$ and $\bar{\boldsymbol{\alpha}}_{21}$ are taken to be zero in Eqs. (3.44) and

(3.45). Consider the scattering geometry of Figure 3.7, let scatterer 1 be of radius $a = 0.25\,\text{m}$ and 0_1 has the coordinates $(3\,,\pi/2\,,-\pi/2)$ with reference to 0, and scatterer 2 be of radius $b = 0.25\,\text{m}$ and 0_2 has the coordinates $(3\,,\pi/2\,,\pi/2)$ with reference to 0. In Figure 3.15, two solutions to the scattered field, normalized to the peak of the excitation waveform, observed at $\mathbf{R}$, $(10\,,\pi/2\,,\pi/2)$ with reference to 0, are plotted with respect to time. The solid curve is obtained by inverse Fourier transforming the present frequency domain formulation, while the cross marks are obtained by inverse Fourier transforming the frequency domain solution with coupling ignored. Both solutions are obtained by including only 2 terms in the series expansion.
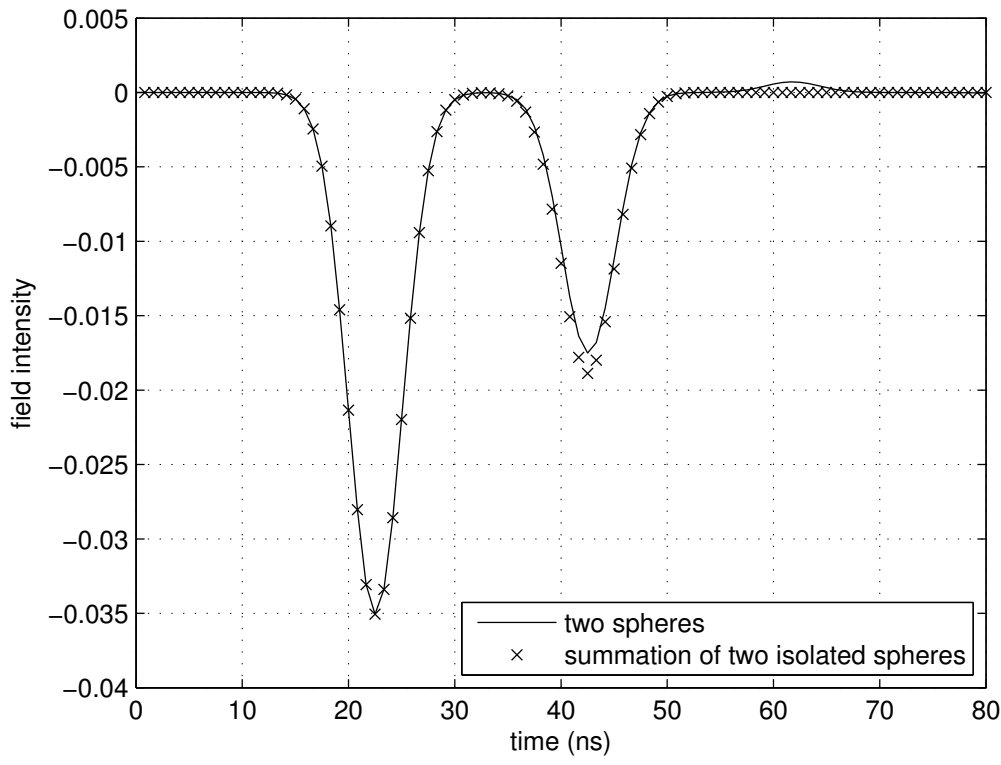
Figure 3.15 The effect of coupling, scattered field intensity vs. time at $(10\,,\pi/2\,,\pi/2)$ with reference to 0 due to a Gaussian pulse waveform incident from the $+z$ axis in the presence of two scatterers, scatterer 1 is of radius $a = 0.25\,\text{m}$, located at $(3\,,\pi/2\,,-\pi/2)$ with reference to 0, and scatterer 2 is of radius $b = 0.25\,\text{m}$, located at $(3\,,\pi/2\,,\pi/2)$ with reference to 0.

3.3 Formulation and Numerical Results for the Time Domain Scattering of Scalar Waves by Two Soft Spheres in Free-Space

Consider scattering by two spheres in free-space as shown in Figure 3.4. The expansion of the incident field in the time domain is given in Eq. (2.38). For a known incident field, or for a known impressed source, $f_{nm}^{i}(t)$ are known. The scattered wave from scatterer 1 of radius a can be expanded in terms of the outgoing wave functions expressed in its self-coordinates as

$$\psi^{s1}(\mathbf{R}_1, t) = \sum_{n=0}^{\infty} \sum_{m=-n}^{n} f_{nm}^{s1}(t) \otimes \Phi_{nm}^{(4)}(\mathbf{R}_1, t) \ , \tag{3.49}$$

and the scattered wave from scatterer 2 of radius b can be expanded similarly in its self-coordinates as

$$\psi^{s2}(\mathbf{R}_2, t) = \sum_{n=0}^{\infty} \sum_{m=-n}^{n} f_{nm}^{s2}(t) \otimes \Phi_{nm}^{(4)}(\mathbf{R}_2, t) \ . \tag{3.50}$$

The total scattered field is then,

$$\psi^{s}(\mathbf{R}, t) = \psi^{s1}(\mathbf{R}_1, t) + \psi^{s2}(\mathbf{R}_2, t) \ , \tag{3.51}$$

where the convolving functions $f_{nm}^{s1}(t)$ and $f_{nm}^{s2}(t)$ are, as yet, unknown and can be found by imposing the boundary conditions on the surfaces of both spheres. Using the translational addition theorems given in Section 2.2, i.e., Eqs. (2.74) - (2.77), the total field on the surface of the scatterer 1 can be expressed in the coordinate system 1 as

$$\psi^t(\mathbf{R}_1,t) = \sum_{n=0}^{\infty} \sum_{m=-n}^{n} \Big\{ \, f_{nm}^i(t) \otimes \sum_{v=0}^{\infty} \sum_{\mu=-v}^{v} \beta_{10}(m,n|\mu,v;t) \otimes \Phi_{v\mu}^{(1)}(\mathbf{R}_1,t)$$

$$+ \, f_{nm}^{s1}(t) \otimes \Phi_{nm}^{(4)}(\mathbf{R}_1,t)$$

$$+ \, f_{nm}^{s2}(t) \otimes \sum_{v=0}^{\infty} \sum_{\mu=-v}^{v} \alpha_{12}(m,n|\mu,v;t) \otimes \Phi_{v\mu}^{(1)}(\mathbf{R}_1,t) \, \Big\} \quad ,$$

$$(3.52)$$

where

$$\beta_{10}(m,n|\mu,v;t) = \frac{1}{2}(-1)^{v-n+\mu}(2v+1)$$

$$\times \sum_{\rho} (-1)^{\rho} a(m,n \mid -\mu,v \mid \rho) \Phi_{\rho,(m-\mu)}^{(1)}(\mathbf{R}_{o,10},t) \quad ,$$

$$(3.53)$$

and

$$\alpha_{12}(m,n|\mu,v;t) = \frac{1}{2}(-1)^{v-n+\mu}(2v+1)$$

$$\times \sum_{\rho} (-1)^{\rho} a(m,n \mid -\mu,v \mid \rho) \Phi_{\rho,(m-\mu)}^{(4)}(\mathbf{R}_{o,12},t) \quad .$$

$$(3.54)$$

Note that, $\mathbf{R}_{o,10}$ and $\mathbf{R}_{o,12}$ are as given in Eqs. (3.34) and (3.35). Similar interpretation with the frequency domain is valid for Eq. (3.52) as, first term is the incident field written in the coordinate system 1, second term is the scattered field from the scatterer 1 in its self coordinates, and the third term is the scattered field from the scatterer 2 written in the coordinate system 1. The first and the third terms can be viewed as the incident field impinging on the scatterer 1.

Similarly, the total field on the surface of the scatterer 2 can be expressed in the coordinate system 2 as

$$\psi^t(\mathbf{R}_2,t) = \sum_{n=0}^{\infty} \sum_{m=-n}^{n} \Big\{ f_{nm}^i(t) \otimes \sum_{v=0}^{\infty} \sum_{\mu=-v}^{v} \beta_{20}(m,n|\mu,v;t) \otimes \Phi_{v\mu}^{(1)}(\mathbf{R}_2,t)$$

$$+ f_{nm}^{s1}(t) \otimes \sum_{v=0}^{\infty} \sum_{\mu=-v}^{v} \alpha_{21}(m,n|\mu,v;t) \otimes \Phi_{v\mu}^{(1)}(\mathbf{R}_2,t)$$

$$+ f_{nm}^{s2}(t) \otimes \Phi_{nm}^{(4)}(\mathbf{R}_2,t) \Big\} \quad ,$$

(3.55)

where

$$\beta_{20}(m,n|\mu,v;t) = \frac{1}{2}(-1)^{v-n+\mu}(2v+1)$$

$$\times \sum_{\rho} (-1)^{\rho} a(m,n\mid -\mu,v\mid \rho)\Phi_{\rho,(m-\mu)}^{(1)}(\mathbf{R}_{o,20},t) \quad ,$$

(3.56)

$$\alpha_{21}(m,n|\mu,v;t) = \frac{1}{2}(-1)^{v-n+\mu}(2v+1)$$

$$\times \sum_{\rho} (-1)^{\rho} a(m,n\mid -\mu,v\mid \rho)\Phi_{\rho,(m-\mu)}^{(4)}(\mathbf{R}_{o,21},t) \quad ,$$

(3.57)

and where $\mathbf{R}_{o,20}$ and $\mathbf{R}_{o,21}$ represent the translations from origin 0 to 0_2, and 0_1 to 0_2, respectively.

Now, as the scatterers are soft spheres, impose the Dirichlet boundary conditions on the surface of each sphere, $\psi^t\big|_{R_1=a} = 0$, and $\psi^t\big|_{R_2=b} = 0$, and use the orthogonality of the Tesseral harmonics over a spherical surface yielding the following two coupled equations for the scattering convolving functions,

$$-f_{n'm'}^{s1}(t) \otimes O_{n'}\left(\frac{a}{c},t\right) = S_{n'}\left(\frac{a}{c},t\right) \otimes \sum_{n=0}^{\infty}\sum_{m=-n}^{n} f_{nm}^{i}(t) \otimes \beta_{10}\left(m,n|m',n';t\right)$$

$$+ S_{n'}\left(\frac{a}{c},t\right) \otimes \sum_{n=0}^{\infty}\sum_{m=-n}^{n} f_{nm}^{s2}(t) \otimes \alpha_{12}\left(m,n|m',n';t\right) \quad,$$

(3.58)

and

$$-f_{n'm'}^{s2}(t) \otimes O_{n'}\left(\frac{b}{c},t\right) = S_{n'}\left(\frac{b}{c},t\right) \otimes \sum_{n=0}^{\infty}\sum_{m=-n}^{n} f_{nm}^{i}(t) \otimes \beta_{20}\left(m,n|m',n';t\right)$$

$$+ S_{n'}\left(\frac{b}{c},t\right) \otimes \sum_{n=0}^{\infty}\sum_{m=-n}^{n} f_{nm}^{s1}(t) \otimes \alpha_{21}\left(m,n|m',n';t\right) \quad.$$

(3.59)

The last two relations, Eqs. (3.58) and (3.59), can be written more compactly using the notation of matrix convolution as

$$-\overline{\mathbf{O}}_{a} \otimes \mathbf{f}^{s1} = \overline{\mathbf{S}}_{a} \otimes \overline{\boldsymbol{\beta}}_{10} \otimes \mathbf{f}^{i} + \overline{\mathbf{S}}_{a} \otimes \overline{\boldsymbol{\alpha}}_{12} \otimes \mathbf{f}^{s2} \quad,$$

(3.60)

$$-\overline{\mathbf{O}}_{b} \otimes \mathbf{f}^{s2} = \overline{\mathbf{S}}_{b} \otimes \overline{\boldsymbol{\beta}}_{20} \otimes \mathbf{f}^{i} + \overline{\mathbf{S}}_{b} \otimes \overline{\boldsymbol{\alpha}}_{21} \otimes \mathbf{f}^{s1} \quad.$$

(3.61)

In Eqs. (3.60) and (3.61), $\overline{\mathbf{O}}_{a}$, $\overline{\mathbf{O}}_{b}$, $\overline{\mathbf{S}}_{a}$, and $\overline{\mathbf{S}}_{b}$ are diagonal matrices containing $O_{n}(a/c,t)$, $O_{n}(b/c,t)$, $S_{n}(a/c,t)$, and $S_{n}(b/c,t)$, respectively; $\mathbf{f}^{i}$, $\mathbf{f}^{s1}$, and $\mathbf{f}^{s2}$ are column vectors containing $f_{nm}^{i}(t)$, $f_{nm}^{s1}(t)$, and $f_{nm}^{s2}(t)$, respectively; and $\overline{\boldsymbol{\beta}}_{10}$, $\overline{\boldsymbol{\beta}}_{20}$, $\overline{\boldsymbol{\alpha}}_{12}$, and $\overline{\boldsymbol{\alpha}}_{21}$ are matrices containing $\beta_{10}\left(m,n|m',n';t\right)$, $\beta_{20}\left(m,n|m',n';t\right)$, $\alpha_{12}\left(m,n|m',n';t\right)$, and $\alpha_{21}\left(m,n|m',n';t\right)$, in some proper sorting, respectively. In order to solve for $\mathbf{f}^{s1}$ and $\mathbf{f}^{s2}$, as in Eqs. (3.26) and (A.27), let

$$\overline{\boldsymbol{\Theta}}_{a} \otimes \overline{\mathbf{O}}_{a} = \overline{\boldsymbol{\delta}} \quad,$$

(3.62)

$$\overline{\mathbf{\Theta}}_b \otimes \overline{\mathbf{O}}_b = \overline{\mathbf{\delta}} \ , \tag{3.63}$$

where $\overline{\mathbf{\delta}}$ is a diagonal matrix containing $\delta(t)$ in each diagonal entry. The definition of the time domain isolated-scatterer T-matrix, Eq. (3.25), is used for each sphere to write

$$\overline{\mathbf{T}}_1 = -\overline{\mathbf{S}}_a \otimes \overline{\mathbf{\Theta}}_a \ , \tag{3.64}$$

$$\overline{\mathbf{T}}_2 = -\overline{\mathbf{S}}_b \otimes \overline{\mathbf{\Theta}}_b \ . \tag{3.65}$$

Convolving Eqs. (3.60) and (3.61) with $\overline{\mathbf{\Theta}}_a$ and $\overline{\mathbf{\Theta}}_b$, respectively, from the left; and using Eqs. (3.64) and (3.65), the coupled equations, Eqs. (3.60) and (3.61), can be rewritten as

$$\mathbf{f}^{s1} = \overline{\mathbf{T}}_1 \otimes \left(\overline{\mathbf{\beta}}_{10} \otimes \mathbf{f}^i + \overline{\mathbf{\alpha}}_{12} \otimes \mathbf{f}^{s2} \right) \ , \tag{3.66}$$

$$\mathbf{f}^{s2} = \overline{\mathbf{T}}_2 \otimes \left(\overline{\mathbf{\beta}}_{20} \otimes \mathbf{f}^i + \overline{\mathbf{\alpha}}_{21} \otimes \mathbf{f}^{s1} \right) \ . \tag{3.67}$$

Solving Eqs. (3.66) and (3.67) simultaneously yield the final expressions,

$$\left(\overline{\mathbf{\delta}} - \overline{\mathbf{T}}_1 \otimes \overline{\mathbf{\alpha}}_{12} \otimes \overline{\mathbf{T}}_2 \otimes \overline{\mathbf{\alpha}}_{21} \right) \otimes \mathbf{f}^{s1} = \overline{\mathbf{T}}_1 \otimes \left(\overline{\mathbf{\beta}}_{10} + \overline{\mathbf{\alpha}}_{12} \otimes \overline{\mathbf{T}}_2 \otimes \overline{\mathbf{\beta}}_{20} \right) \otimes \mathbf{f}^i \ , \tag{3.68}$$

$$\left(\overline{\mathbf{\delta}} - \overline{\mathbf{T}}_2 \otimes \overline{\mathbf{\alpha}}_{21} \otimes \overline{\mathbf{T}}_1 \otimes \overline{\mathbf{\alpha}}_{12} \right) \otimes \mathbf{f}^{s2} = \overline{\mathbf{T}}_2 \otimes \left(\overline{\mathbf{\beta}}_{20} + \overline{\mathbf{\alpha}}_{21} \otimes \overline{\mathbf{T}}_1 \otimes \overline{\mathbf{\beta}}_{10} \right) \otimes \mathbf{f}^i \ . \tag{3.69}$$

Expressions in Eqs. (3.66) – (3.69) are in similar form with the frequency domain relations, Eqs. (3.44) – (3.47). Using direct matrix deconvolution given in the Appendix B, find the diagonal matrices $\overline{\mathbf{\Theta}}_a$ and $\overline{\mathbf{\Theta}}_b$ from Eqs. (3.62) and (3.63), respectively; and then using Eqs. (3.64) and (3.65) determine the T-matrices, $\overline{\mathbf{T}}_1$ and $\overline{\mathbf{T}}_2$, and finally, solve the matrix equations Eqs. (3.68) and (3.69) for $\mathbf{f}^{s1}$ and $\mathbf{f}^{s2}$,

again using direct matrix deconvolution. These scattered field convolving functions when used in Eqs. (3.49) – (3.51) give the total scattered field in the presence of two scatterers. The time domain T-matrices, $\overline{\mathbf{T}}_i$, are diagonal if the scatterers are spheres. If the incident field is a plane wave, then $\overline{\boldsymbol{\beta}}_{i0}$ is diagonal with entries containing the delay (or advance) term, $\delta\left(t + R_{o,i0}\cos\theta_{o,i0}/c\right)$, with appropriate coefficients, where $\mathbf{R}_{o,i0}$ represents the translation from origin 0 to 0_i.

The scattered wave from scatterer 1 and scatterer 2 expressed in its self-coordinates could also have been expanded in the form of Eq. (3.23), instead of Eqs. (3.49) and (3.50), as

$$\psi^{s1}(\mathbf{R}_1,t) = \sum_{n=0}^{\infty}\sum_{m=-n}^{n} g_{nm}^{s1}(t) \otimes S_n\left(\frac{a}{c},t\right) \otimes \Phi_{nm}^{(4)}(\mathbf{R}_1,t) \ , \tag{3.70}$$

$$\psi^{s2}(\mathbf{R}_2,t) = \sum_{n=0}^{\infty}\sum_{m=-n}^{n} g_{nm}^{s2}(t) \otimes S_n\left(\frac{b}{c},t\right) \otimes \Phi_{nm}^{(4)}(\mathbf{R}_2,t). \tag{3.71}$$

Then, the coupled equations would be

$$\left(-\overline{\mathbf{O}}_a + \overline{\boldsymbol{\alpha}}_{12} \otimes \overline{\mathbf{S}}_b \otimes \overline{\boldsymbol{\Theta}}_b \otimes \overline{\boldsymbol{\alpha}}_{21} \otimes \overline{\mathbf{S}}_a\right) \otimes \mathbf{g}^{s1} = \overline{\boldsymbol{\beta}}_{10} \otimes \mathbf{f}^i - \overline{\boldsymbol{\alpha}}_{12} \otimes \overline{\mathbf{S}}_b \otimes \overline{\boldsymbol{\Theta}}_b \otimes \overline{\boldsymbol{\beta}}_{20} \otimes \mathbf{f}^i \ , \tag{3.72}$$

$$\left(-\overline{\mathbf{O}}_b + \overline{\boldsymbol{\alpha}}_{21} \otimes \overline{\mathbf{S}}_a \otimes \overline{\boldsymbol{\Theta}}_a \otimes \overline{\boldsymbol{\alpha}}_{12} \otimes \overline{\mathbf{S}}_b\right) \otimes \mathbf{g}^{s2} = \overline{\boldsymbol{\beta}}_{20} \otimes \mathbf{f}^i - \overline{\boldsymbol{\alpha}}_{21} \otimes \overline{\mathbf{S}}_a \otimes \overline{\boldsymbol{\Theta}}_a \otimes \overline{\boldsymbol{\beta}}_{10} \otimes \mathbf{f}^i \ . \tag{3.73}$$

The column vectors $\mathbf{g}^{s1}$ and $\mathbf{g}^{s2}$ which contain $g_{nm}^{s1}(t)$ and $g_{nm}^{s2}(t)$, respectively, can be solved by deconvolution and used in Eqs. (3.70) and (3.71) in order to get the same scattered field which is obtained through Eqs. (3.68), (3.69), (3.49), and (3.50). The coupled equations, Eqs. (3.68) and (3.69), are more general in the sense that they can be used for any scatterers once the T-matrices for the scatterers are known, while Eqs. (3.72) and (3.73) are valid only for soft spheres.

As a multiple scattering example, the scattering by two soft spheres in free-space in response to a plane wave incident from the $+z$ axis (from $\theta = 0$) is given. The incident field is of the Gaussian waveform, $e^{-5.65t^2/\tau^2}$, and the convolving function in Eq. (2.38) for this particular incident field is

$$f_{n0}^i(t) = \frac{1}{2}(-1)^n(2n+1)\,e^{-5.65t^2/\tau^2}\,. \tag{3.74}$$

Note that $m = 0$ and the field is independent of ϕ. In order to find the scattered field in response to such an incident field, the formulation given above is used. Consider the geometry in Figure 3.7. Let scatterer 1 be of radius $a = 0.25\,\text{m}$ and 0_1 has the coordinates $(3, \pi/2, -\pi/2)$ with reference to 0, and scatterer 2 be of radius $b = 0.25\,\text{m}$ and 0_2 has the coordinates $(3, \pi/2, \pi/2)$ with reference to 0. In Figure 3.16, two solutions to the scattered field, normalized to the peak of the excitation waveform, observed at $\mathbf{R}$, $(10, \pi/2, \pi/2)$ with reference to 0, are plotted with respect to time and good agreement is observed. The solid curve is obtained using the present time domain formulation, while the cross marks are obtained by inverse Fourier transforming the well-known frequency domain solution. Both solutions are obtained by including only 2 terms in the series expansion.
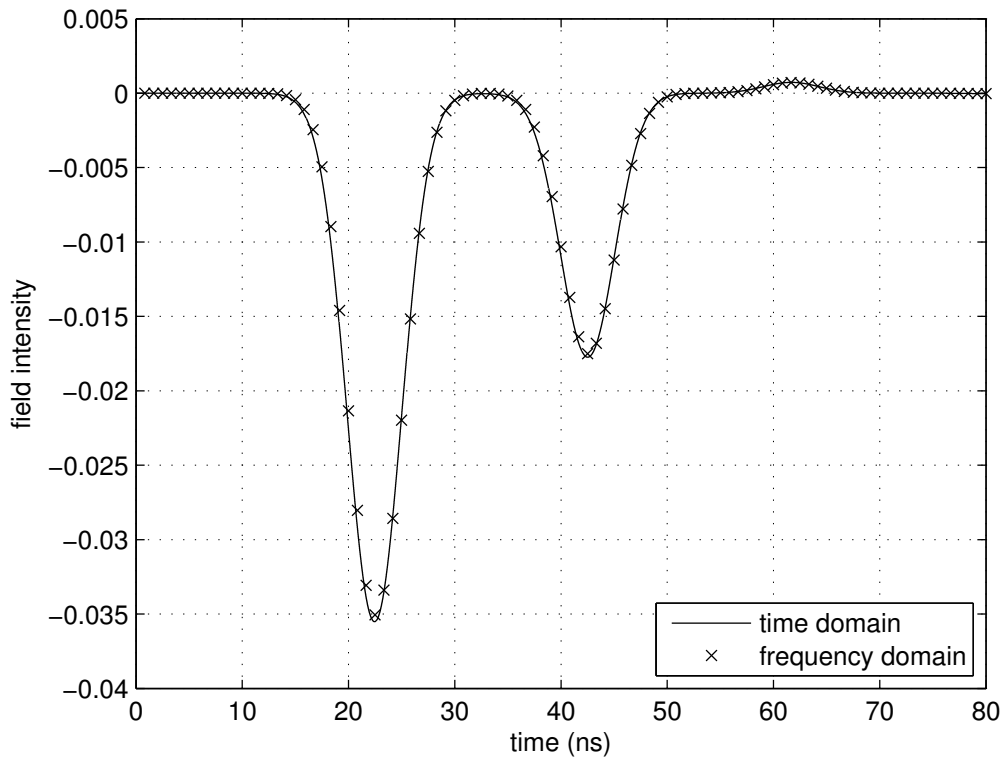
Figure 3.16 Scattered field intensity vs. time at $(10\,,\pi/2\,,\pi/2)$ with reference to 0 due to a Gaussian pulse waveform incident from the $+z$ axis in the presence of two scatterers, scatterer 1 is of radius $a = 0.25\,\mathrm{m}$, located at $(3\,,\pi/2\,,-\pi/2)$ with reference to 0, and scatterer 2 is of radius $b = 0.25\,\mathrm{m}$, located at $(3\,,\pi/2\,,\pi/2)$ with reference to 0.

As a second example consider the geometry in Figure 3.17.
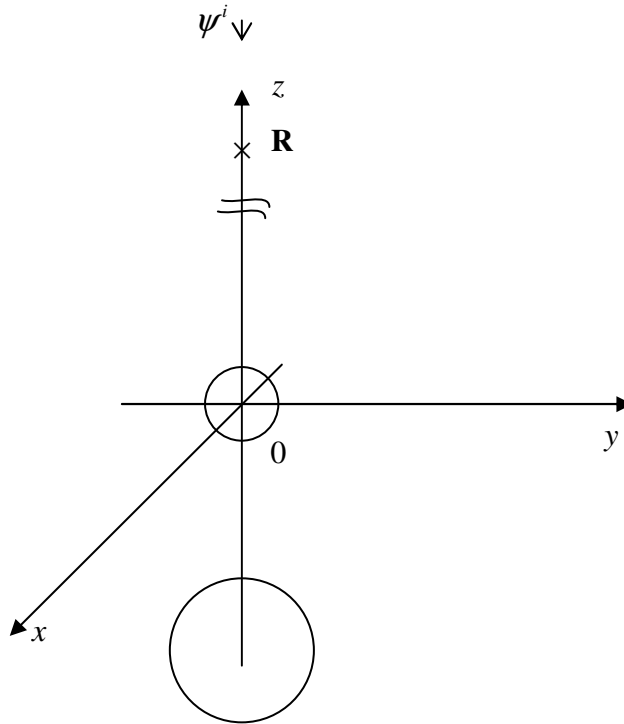
Figure 3.17 Scattering geometry for two spheres, scatterer 1 of radius $a = 0.25$ is at the origin 0 with and scatterer 2 of radius $b = 0.75$ is at 0_2 which has the coordinates $(3, \pi, 0)$ with reference to 0, the observation point, denoted by $\mathbf{R}$, is at $(10, 0, 0)$ with reference to 0.

Let scatterer 1 be of radius $a = 0.25\,\text{m}$ and 0_1 has the coordinates $(0, 0, 0)$ with reference to 0 coinciding with the origin 0, and scatterer 2 be of radius $b = 0.75\,\text{m}$ and 0_2 has the coordinates $(3, \pi, 0)$ with reference to 0. In Figure 3.18, two solutions to the scattered field, normalized to the peak of the excitation waveform, observed at the backscatterer direction $\mathbf{R}$, $(10, 0, 0)$ with reference to 0, are plotted with respect to time. The solid curve is obtained using the present time domain formulation, while the cross marks are obtained by inverse Fourier transforming the well-known frequency domain solution. Both solutions are obtained by including 3 terms in the series expansion.

Figure 3.18 Scattered field intensity vs. time at $(10, 0, 0)$ with reference to 0 due to a Gaussian pulse waveform incident from the $+z$ axis in the presence of two scatterers, scatterer 1 is of radius $a = 0.25\,\text{m}$, located at the origin 0, and scatterer 2 is of radius $b = 0.75\,\text{m}$, located at $(3, \pi, 0)$ with reference to 0.

In the computation of the numerical examples, Eqs. (3.62) and (3.63) are solved by treating the $\delta(t)$ terms separately, Azizoglu [17], Koc *et al.* [18], and Appendix B; however, in solving the scattered field convolving functions, Eqs. (3.72) and (3.73), this approach becomes very complicated, so an easier way, which is convolving both sides of the equations by the Gaussian waveform (with narrower pulse width compared to the waveform of the incident field), in order to smoothen the $\delta(t)$ terms before the deconvolution, is chosen. In this approach, the waveform should be truncated in order to make the first sample nonzero in the deconvolution algorithm, and this introduces some error, the error in the time domain solutions of

the above examples at the falling edges of the pulses. Figure 3.19 illustrates this fact where the solid line is the solution for $f(t)$ in

$$g(t - 0.65) \otimes f(t) = g(t - 3) \otimes h(t - 3) , \qquad (3.75)$$

using the direct deconvolution where

$$g(t) = e^{-5.65t^2/\tau_1^2} , \qquad (3.76)$$

$$h(t) = e^{-5.65t^2/\tau_2^2} . \qquad (3.77)$$

The pulse width of the test function $g(t)$ is chosen as $\tau_1 = \tau_2/2$, i.e., $g(t)$ with wider bandwith than $h(t)$ in order to avoid the filtering. The rising edge of the Gaussian, $g(t - 0.65)$, on the left hand side is truncated at $t = 0$ in the direct deconvolution algorithm, and the exact solution, which is $f(t) = h(t - 5.35)$, is plotted using cross marks. Note that the error encountered is similar to the error in the scattering examples, Figures 3.16 and 3.18. The error in the peak of the waveform can be corrected by brute force, or it can be decreased by truncating the test function less, however this makes the deconvolution algorighm unstable due to the numerical errors caused by matrix inversion and the recursion. The error due to the recursive nature of the algorithm becomes dominant as time increases.
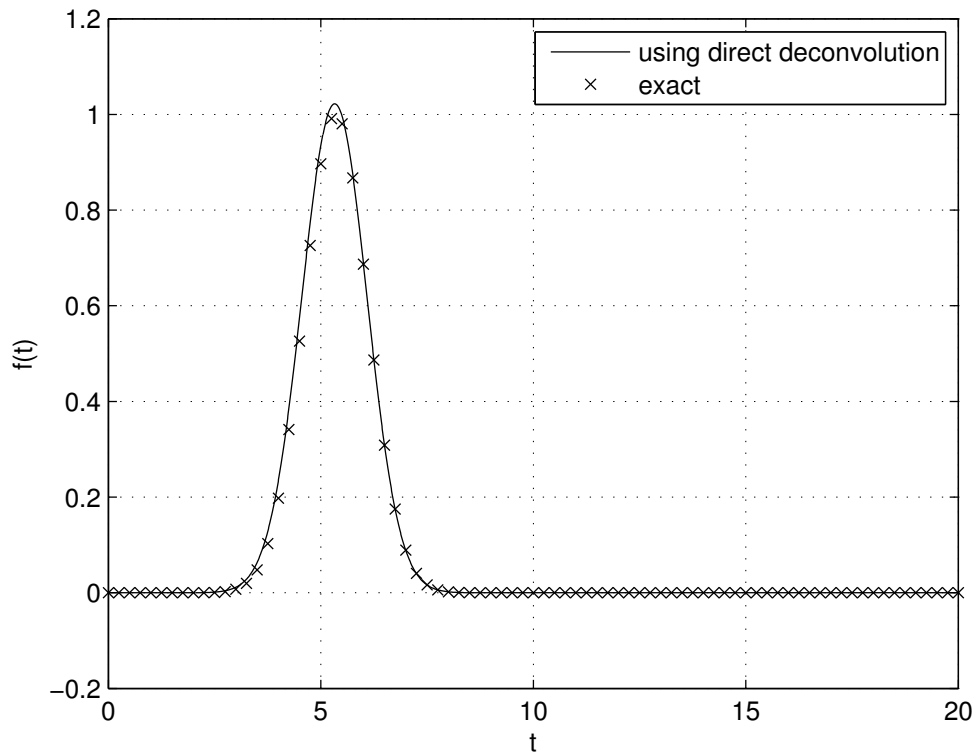
Figure 3.19 Illustration of the error encountered in direct deconvolution.

Alternative methods to the direct deconvolution, such as using system identification techniques, Goodwin *et al.* [44], can be used to solve the deconvolution problem more accurately.

In addition to the direct deconvolution algorithm, the plenty of convolution operations and the numerical properties of the addition theorems described in Chapter 2 are the possible causes of error in the numerical computation of the time domain solution. If the number of terms retained in the series expansion, i.e. the matrix dimensions in Eqs. (3.68), (3.69), (3.72), and (3.73), are increased, then the time step in the numerical computation should be decreased, and this increases the simulation time.

In order to illustrate the physical phenomenon of multiple scattering more clearly, consider again the geometry in Figure 3.7. Let scatterer 1 be of radius $a = 0.5\,\text{m}$ and 0_1 has the coordinates $(3, \pi/2, -\pi/2)$ with reference to 0, and scatterer 2 be of

radius $b = 0.5\,\text{m}$ and 0_2 has the coordinates $(3\,,\pi/2\,,\pi/2)$ with reference to 0. The scattered field is observed at $\mathbf{R}$, $(2\,,\pi/2\,,\pi/2)$ with reference to 0, which is in between the scatterers. In Figure 3.20, the solid curve is obtained using the present time domain formulation, the cross marks are obtained by inverse Fourier transforming the well-known frequency domain solution, and the dotted line indicate the summation of two isolated spheres (where coupling between the spheres are ignored). The solutions are obtained by including only 2 terms in the series expansion.
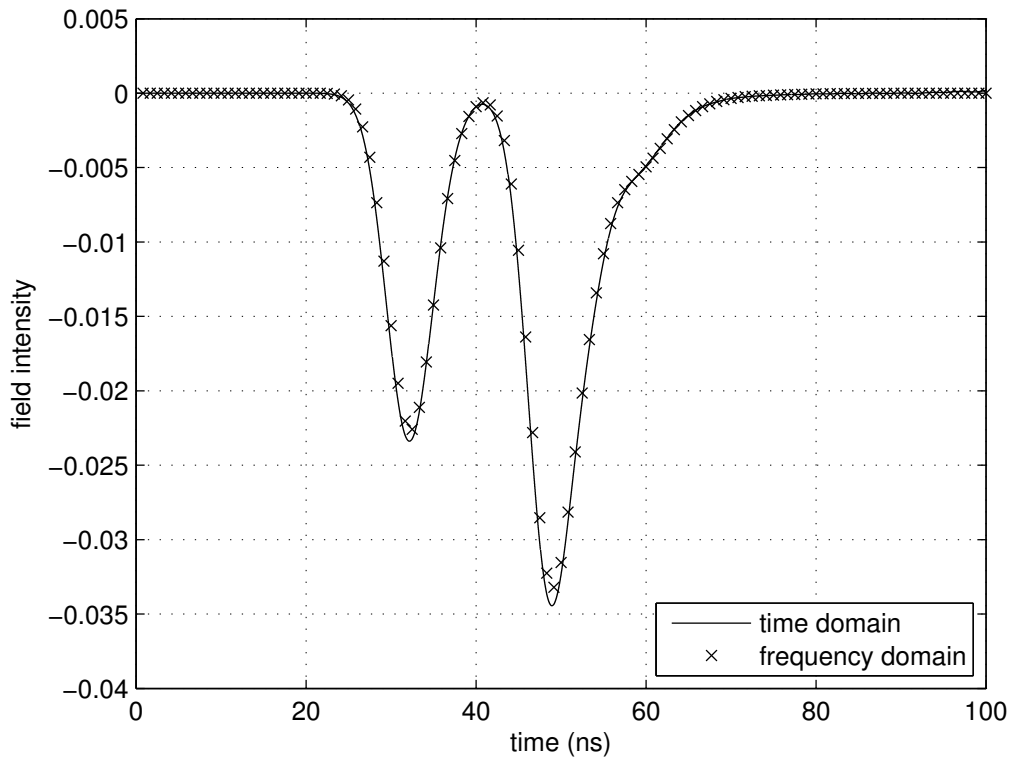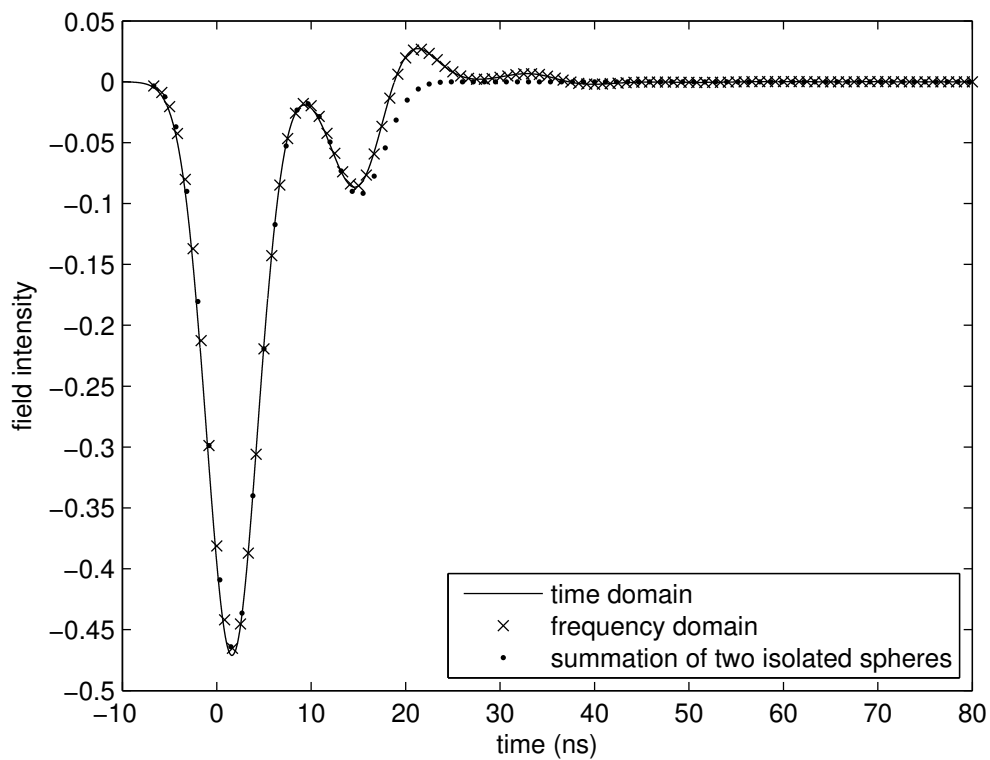

Figure 3.20 Scattered field intensity vs. time at $(2\,,\pi/2\,,\pi/2)$ with reference to 0 due to a Gaussian pulse waveform incident from the $+z$ axis in the presence of two scatterers, scatterer 1 is of radius $a = 0.5\,\text{m}$, located at $(3\,,\pi/2\,,-\pi/2)$ with reference to 0, and scatterer 2 is of radius $b = 0.5\,\text{m}$, located at $(3\,,\pi/2\,,\pi/2)$ with reference to 0.

The first pulse which is approximately centered at $t = 1.6$ ns may be viewed as the wave scattered from scatterer 2, while the second pulse which is approximately centered at $t = 14.5$ ns may be viewed as the wave scattered from scatterer 1. In order to depict the second and higher order scattering, Figure 3.20 is zoomed for $t > 18$ ns in Figure 3.21.
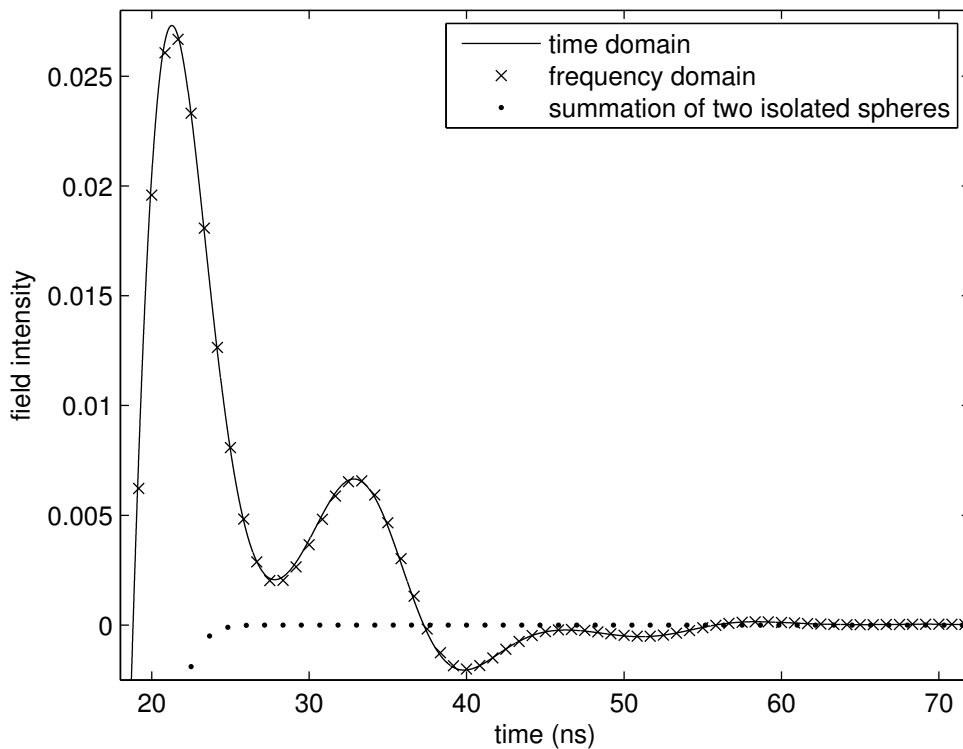
Figure 3.21 Zoomed view of Figure 3.20 in order to depict the second and higher order scattering.

The pulse which is approximately centered at $t = 21.3$ ns may be viewed as the second order scattering, the wave scattered by scatterer 1, then by scatterer 2. Similarly, the pulse which is approximately centered at $t = 32.9$ ns may be viewed as the second order scattering, the wave scattered by scatterer 2, then by scatterer 1. The third order scattering is also clear in Figure 3.21, the pulses approximately centered

at $t = 40\,\text{ns}$ and $t = 51.7\,\text{ns}$. The time of arrivals for the pulses due to first, second, third, and higher orders scattering are as expected from the geometry of the scatterers and the observation point.

An observation made on the time domain solution is that the solution converges rapidly if the dimensions and the separation of the scatterers are small compared to the wavelength at the highest frequency component of the incident field, which is similar to the case in the solution of problems in the frequency domain.

The time domain multiple scattering formulation given in this chapter can also be used for scatterers of arbitrary shape in which the T-matrices are not necessarily diagonal, and this will be illustrated in the next chapter. Once the time domain isolated-scatterer T-matrices are known for each of the two scatterers of arbitrary shape, the scattered field convolving functions can be solved using Eqs. (3.68) and (3.69) by direct deconvolution, and then can be used in Eqs. (3.49) – (3.51), in order to obtain the total scattered field.

CHAPTER 4

TIME DOMAIN SCATTERING OF SCALAR WAVES BY

TWO OBJECTS IN FREE-SPACE

The time domain scattering of scalar waves by an object in free-space using the T-matrix method, Koc *et al.* [29], is reviewed using the formulations of Appendices A, B, and C and then, time domain scattering by two objects is presented using the time domain isolated-scatterer T-matrix of the single object and the time domain multiple scattering formulation of the previous chapter, Eqs. (3.49) – (3.51) and Eqs. (3.68) and (3.69). In order to simulate a non-spherical surface, for which the T-matrix is not diagonal, a shifted sphere whose center is displaced from the coordinate origin is used and the surface integrals necessary to find the matrix entries are evaluated numerically.

4.1 Time Domain Scattering of Scalar Waves by an Object in Free-Space

The time domain T-matrix formulation given in Appendix A can be used to find the scattered field from a scatterer of arbitrary shape. The shifted sphere whose center is displaced from the coordinate origin, Figure 3.1, can simulate the non–spherical surface as its T-matrix defined with respect to the coordinate origin (not the center of the sphere) is not diagonal.

In order to find the scattered field, first the matrix $\overline{\mathbf{Q}}(t)$ is filled by Eq. (A.19), where surface integrals are evaluated numerically. The formulation necessary for the evaluation of the surface integrals is given in Appendix C. Then, $\mathbf{f}^t(t)$ can be found by direct deconvolution in Eq. (A.20) where $\mathbf{f}^i(t)$ is known. After filling the matrix $\overline{\mathbf{Q}}^e(t)$ again by the numerical evaluation of the surface integrals, Eq. (A.23), the

scattered field convolving functions $\mathbf{f}^s(t)$ can be found using Eq. (A.24). Once $\mathbf{f}^s(t)$ is known, the scattered field can be found by Eq. (A.21).
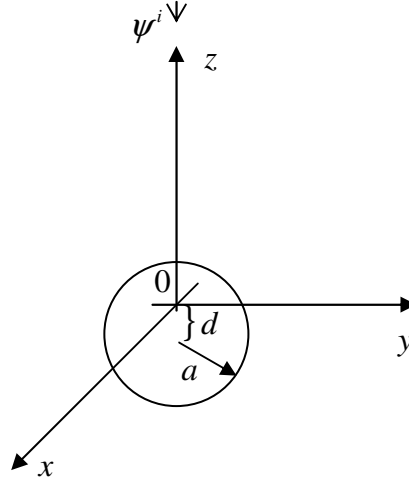
Figure 4.1 A sphere displaced from the coordinate origin.

Equivalent to the procedure described above, without finding $\mathbf{f}^t(t)$, the T-matrix can be found using Eqs. (A.26) and (A.27) after filling the matrices $\overline{\mathbf{Q}}(t)$ and $\overline{\mathbf{Q}}^e(t)$, and then it can be used in Eq. (A.25) yielding $\mathbf{f}^s(t)$, which gives the scattered field by Eq. (A.21). In the direct deconvolution problem, algorithm given in Eqs. (B.7) through (B.13) is used.

As a numerical example, the plane wave with the Gaussian pulse waveform, defined in Section 2.3, incident from the $+z$ axis on a soft sphere of radius $a = 0.5\,\mathrm{m}$ displaced by $(-a/4)$ on the $+z$ axis is considered. Shown in Figure 4.2 are two solutions to the scattered field in the backscatter direction at a distance of $R = 3\,\mathrm{m}$ where the field intensity is plotted versus time. The solid curve is obtained using the present time domain T-matrix formulation, while the cross marks are obtained by the exact solution. The exact solution can either be obtained by inverse Fourier transforming the frequency domain solution or directly by the time solution.

In the exact solution, the translational addition theorems given in Chapter 2 can be used in conjunction with the formulation and numerical simulation for the centered sphere given in Section 3.1; or simply by intuition, the scattered field in the presence of the centered (with respect to the coordinate origin) sphere can be observed at $R = (3 + a/4)\,\text{m}$ and an extra time delay of $(a/(4c))\,\text{m/s}$ can be introduced.
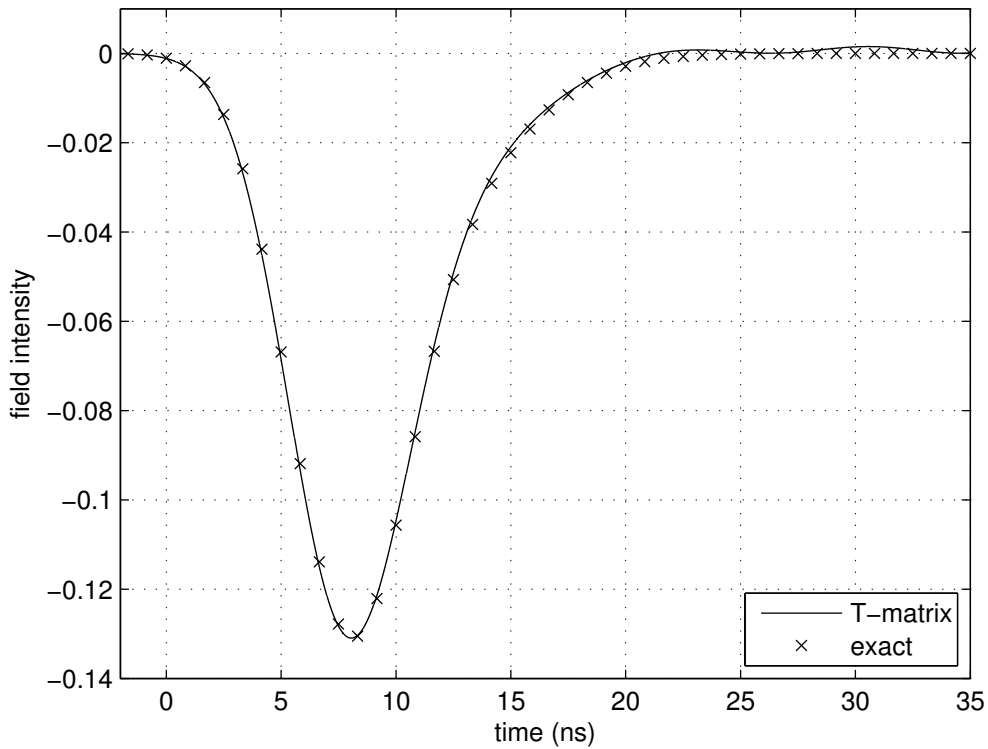
Figure 4.2 Scattered field intensity vs. time at the backscatter direction, $(R = 3\,,\ \theta = 0\,,\ \phi = 0)$, due to a Gaussian pulse waveform incident from the $+z$ axis on a soft sphere of radius $a = 0.5\,\text{m}$ displaced by $(-a/4)$ on the $+z$ axis.

Both solutions are obtained by including 4 terms in the series expansion, and good agreement is worth noting. It is observed that the solution converges rapidly if the dimension of the scatterer is small compared to the wavelength at the highest frequency component of the incident field, and the displacement of the sphere, d,

should be kept around $a/4$, i.e., d cannot approach 0 or exceed a because of the numerical errors encountered in the evaluation of the surface integrals.

The T-matrix for a scatterer is symmetric in the frequency domain, Chew [2], and this must also be true in the time domain, however, it is observed that the time domain T-matrix is not exactly equal to its transpose in the above example because of the numerical errors encountered.

4.2 Solution for the Time Domain Scattering of Scalar Waves by Two Objects in Free-Space

Once the time domain isolated-scatterer T-matrices are known for each of the two scatterers of arbitrary shape, the total scattered field can be found with the aid of the translational addition theorems. Hence, the coupled equations in terms of the T-matrices, Eqs. (3.66) and (3.67), developed for the scattering by two spheres in Chapter 3, can be used for scatterers of arbitrary shape. The scattered field convolving functions can be solved using Eqs. (3.68) and (3.69) by direct deconvolution, and then used in Eqs. (3.49) – (3.51), in order to obtain the total scattered field.

The time domain isolated-scatterer T-matrix for an object can be found using the formulation given in Appendix A. First fill the matrix, $\overline{\mathbf{Q}}(t)$, by evaluating the surface integrals, Eq. (A.19), and then solve for $\overline{\Theta}$ in Eq. (A.27) using direct matrix deconvolution. Matrix convolution of $\overline{\mathbf{Q}}^e(t)$, which is again filled by evaluating the surface integrals by Eq. (A.23), with $\overline{\Theta}$ yields the time domain isolated-scatterer T-matrix, Eq. (A.26). After obtaining the T-matrices for each of the scatterers, solve the matrix equations Eqs. (3.68) and (3.69) for the scattered field convolving functions, $\mathbf{f}^{s1}$ and $\mathbf{f}^{s2}$, again using direct matrix deconvolution. The scattered field convolving functions when used in Eqs. (3.49) – (3.51) give the total scattered field in the presence of two scatterers.

As a multiple scattering example, scattering by two objects (two soft spheres, each displaced from its self-coordinate origin) in free-space in response to a plane

wave incident from the $+z$ axis (from $\theta = 0$) is given. The incident field is of the Gaussian waveform, $e^{-5.65t^2/\tau^2}$, and the convolving function for this particular incident field is given in Eq. (3.74). In order to find the scattered field in response to such an incident field, the formulation described above is used. Consider the geometry in Figure 3.7, but now with spheres replaced by scatterers of arbitrary shape, i.e., shifted spheres. Let scatterer 1 be of radius $a = 0.25\,\text{m}$ displaced by $(-a/4)$ on the $+z$ axis and 0_1 has the coordinates $(3, \pi/2, -\pi/2)$ with reference to 0, and scatterer 2 be of radius $b = 0.25\,\text{m}$ displaced by $(-b/4)$ on the $+z$ axis and 0_2 has the coordinates $(3, \pi/2, \pi/2)$ with reference to 0. In Figure 4.3, two solutions to the scattered field, normalized to the peak of the excitation waveform, observed at $\mathbf{R}$, $(10, \pi/2, \pi/2)$ with reference to 0, are plotted with respect to time. The solid curve is obtained using the present time domain formulation, while the cross marks are obtained by inverse Fourier transforming the frequency domain solution in which the scatterers are spheres placed at their coordinate origins (the coordinate origins of the scatterers are translated such that they coincide the centers of the spheres, $\mathbf{R}_{o,10}$ and $\mathbf{R}_{o,12}$ are changed compared to the former solution, and the fields are expanded with respect to the new coordinate origins). The former is the time domain solution evaluated by the T-matrix method, while the latter is the exact solution obtained by inverse Fourier transforming the frequency domain solution of two spheres. Both solutions are obtained by including only 2 terms in the series expansion.
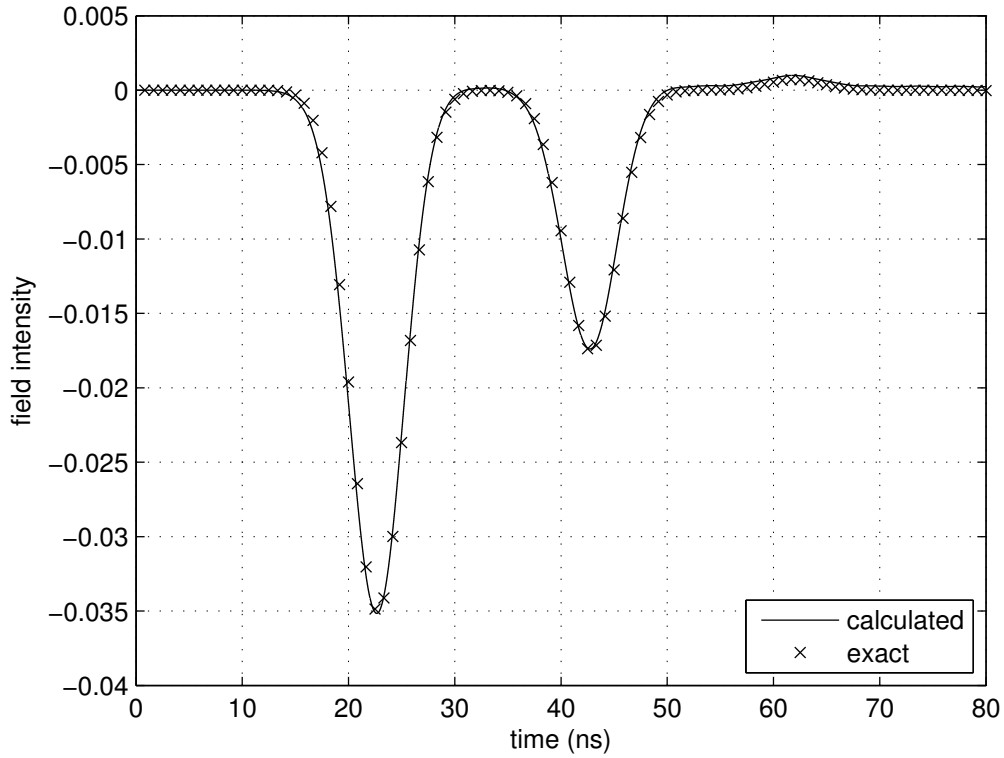
Figure 4.3 Scattered field intensity vs. time at $(10\,,\pi/2\,,\pi/2)$ with reference to 0 due to a Gaussian pulse waveform incident from the $+z$ axis in the presence of two scatterers, scatterer 1 is of radius $a=0.25\,\text{m}$ displaced by $(-a/4)$ on the $+z_1$ axis, located at $(3\,,\pi/2\,,-\pi/2)$ with reference to 0, and scatterer 2 is of radius $b=0.25\,\text{m}$ displaced by $(-b/4)$ on the $+z_2$ axis, located at $(3\,,\pi/2\,,\pi/2)$ with reference to 0.

It is observed that the solution converges rapidly if the dimensions and separation of the scatterers are small compared to the wavelength at the highest frequency component of the incident field. The formulation for scattering by two objects uses the same formulation for scattering by two spheres, but now the T-matrices of the scatterers are the T-matrices for scatterers of arbitrary shape and are not diagonal, so the numerical errors in the solution of the scattering by two spheres, and the solution of the scattering by an object are all encountered in this solution. Hence, the radii and the displacements of the spheres are chosen small (compared to the wavelength at the highest frequency component of the incident field) in order to keep the number of

terms retained in the series expansion for the desired accuracy, small, avoiding the numerical errors caused by large matrix sizes.

CHAPTER 5

CONCLUSION

The time domain spherical scalar wave functions, which are useful for the solution of time domain scattering, are introduced. The translational addition theorems for these wave functions are derived and numerically checked, the convergence properties are discussed. It is observed that, numerical accuracy for the the translational addition theorems in the time domain can be interpreted in a similar way with that in the frequency domain, but with some additional requirements, depending on the required accuracy, such as the observation point should not be in the vicinity of the coordinate origins, the first coordinate origin and the second which is translated from the first one, and the translation of the coordinate origins with respect to each other should not approach zero.

The translational addition theorems derived for the time domain spherical scalar wave functions are applied to multiple scattering problems and time domain scattering of scalar waves by two scatterers in free-space is formulated. As an application of the formulation, scattering by two soft spheres and scattering by two objects (scatterers of arbitrary shape whose T-matrices are not diagonal) in free-space are solved entirely in the time domain, and the utility of the formulation is demonstrated.

It is observed that the solutions converge rapidly if the dimensions and the separation of the scatterers are small compared to the wavelength at the highest frequency component of the incident field. Numerical results are found to be in agreement with those obtained by inverse Fourier transforming the well-established frequency domain solutions. The possible causes of the numerical errors encountered in the time domain solution are the direct deconvolution algorithm used, the plenty of convolution operations, and the numerical properties of the addition theorems. If the number of terms retained in the series expansion of the field is kept small (small

matrix dimensions in the governing equations), which is possible for electrically small scatterers, then adequate results can be obtained within reasonable simulation time. For electrically large scatterers in which the number of terms retained in the series expansion has to be increased, one must use accurate and efficient time domain numerical algorithms, also, alternative methods to the direct deconvolution such as using system identification techniques can be used in the deconvolution problem, and the convolution integrals can be evaluated by Gaussian integration in order to obtain more accurate results.

The time domain approach of the present work is not proposed as an alternative to the frequency domain approach; however, there are cases where the time domain is indispensable, such as the modeling of the field in the presence of moving sources and targets. Therefore, the significance of this work is the contribution of the time domain formulation of multiple scattering to the literature. It is believed that, the present time domain formulation also provides physical insight into the wave propagation and scattering mechanism, and is suitable for time domain applications such as time gating and time domain modeling.

Finally, it is foreseen that the time domain T-matrix formulation given here can be generalized for n-scatterers and, as well as that, the present work can be extended to vector electromagnetic scattering problems.

REFERENCES

[1] C. L. Bennett and G. F. Ross, "Time-domain electromagnetics and its applications," *Proc. IEEE,* vol. 66, pp. 299-318, March 1978.

[2] W. C. Chew, *Waves and Fields in Inhomgeneous Media.* New York: IEEE Press, 1995.

[3] D. S. Jones, *Acoustic and Electromagnetic Waves.* New York: Oxford U. P., 1986.

[4] R. F. Harrington, *Time-Harmonic Electromagnetic Fields.* New York: McGraw-Hill, 1961.

[5] J. D. Jackson, *Classical Electrodynamics.* New York: Wiley , 1962.

[6] J. J. Bowman, T. B. A. Senior and P. L. E. Uslenghi, *Electromagnetic and Acoustic Scattering by Simple Shapes.* Amsterdam: North Holland, 1969.

[7] L. B. Felsen, "Alternative field representations in regions bounded by spheres, cones, and planes," *IRE Trans. Antennas Propagat.,* vol. AP-5, pp. 109-121, Jan. 1957.

[8] W. C. Davidon, "Time-dependent multipole analysis," *J. Phys. A: Math., Nucl. Gen.,* vol. 6, pp. 1635-1646, Nov. 1973.

[9] E. Heyman and A. J. Devaney, "Time-dependent multipoles and their application for radiation from volume source distributions," *J. Math. Phys.,* vol. 37, pp. 682-692, Feb. 1996.

[10] E. A. Marengo and A. J. Devaney, "Time-dependent plane wave and multipole expansions of the electromagnetic field," *J. Math. Phys.,* vol. 39, pp. 3643-3660, July 1998.

[11] T. B. Hansen, "Spherical expansions of time domain acoustic fields: Application to near-field scanning," *J. Acoust. Soc. Am.,* vol. 98, pp. 1204-1215, Aug. 1995.

[12] T. B. Hansen, "Formulation of spherical near-field scanning for electromagnetic fields in the time domain," *IEEE Trans. Antennas Propagat.,* vol. 45, pp. 620-630, Apr. 1997.

[13] O. M. Buyukdura and S. S. Koc, "Two alternative expressions for the spherical wave expansion of the time domain scalar free-space Green's function and an application: Scattering by a soft sphere," *J. Acoust. Soc. Am.,* vol. 101, pp. 87-91, Jan. 1997.

[14] S. A. Azizoglu, S. S. Koc, and O. M. Buyukdura, "Spherical wave expansion of the time domain free-space dyadic Green's function," *IEEE Trans. Antennas Propagat.,* vol. 52, pp. 677-683, March 2004.

[15] S. A. Azizoglu, S. S. Koc, and O. M. Buyukdura, "Spherical wave expansion of the time domain free-space dyadic Green's function," in *Proc. Ultra-Wideband, Short-Pulse Electromagnetics 5.* New York: Kluwer Academic/Plenum Publishers, 2002, pp. 83-88.

[16] S. A. Azizoğlu, S. S. Koç, O. M. Büyükdura, "Zaman uzamında boşluk diadik Green fonksiyonunun küresel dalga fonksiyonlari ile açılımı için bir ifade," *TMMOB Elektrik Mühendisleri Odası Elektrik-Elektronik Bilgisayar Mühendisliği 8. Ulusal Kongresi,* Gaziantep, Türkiye, 1999, pp. 240-243.

[17] S. A. Azizoglu, "Spherical wave expansion of the time domain free-space dyadic Green's function," M.S. thesis, Dept. Electrical and Electronics Engineering, Middle East Tech. Univ., Ankara, Turkey, 1999.

[18] S. S. Koc, O. A. Civi, and O. M. Buyukdura, "Near-field scanning in the time domain on a spherical surface – a formulation using the free-space Green's function," *J. Acoust. Soc. Am.,* vol. 110, pp. 1778-1782, Oct. 2001.

[19] P. C. Waterman, "New formulation of acoustic scattering," *J. Acoust. Soc. Am.,* vol. 45, number 6, pp. 1417-1429, 1969.

[20] V. Twersky, "Multiple scattering by arbitrary configurations in three dimensions," *J. Math. Phys.,* vol. 3, pp. 83-91, Jan. - Feb. 1962.

[21] L. Marnevskaya, ''Diffraction of a plane scalar wave by two spheres,'' *Sov. Phys. Acoust.,* vol. 14, pp. 356-360, Jan. – March 1969.

[22] B. Peterson and S. Strom, "Matrix formulation of acoustic scattering from an arbitrary number of scatterers," *J. Acoust. Soc. Am.,* vol. 56, pp. 771-780, Sept. 1974.

[23] G. C. Gaunaurd, H. Huang, H. C. Strifors "Acoustic scattering by a pair of spheres," *J. Acoust. Soc. Am.,* vol. 98, pp. 495-507, July 1995.

[24] G. C. Gaunaurd, H. Huang, H. C. Strifors "Acoustic scattering by a pair of spheres: Addenda and corrigenda," *J. Acoust. Soc. Am.,* vol. 101, pp. 2983-2985, May 1997.

[25] V. Twersky, "Multiple scattering of electromagnetic waves by arbitrary configurations," *J. Math. Phys.,* vol. 8, pp. 589-610, March 1967.

[26] C. Liang and Y. T. Lo, "Scattering by two spheres," *Radio Sci.,* vol. 2, pp. 1481-1495, December 1967.

[27] J. H. Bruning and Y. T. Lo, "Multiple scattering of EM waves by spheres - Part I: Multipole expansion and ray-optical solutions," and "Multiple scattering of EM waves by spheres - Part II: Numerical and experimental results," *IEEE Trans. Antennas Propagat.,* vol. 19, pp. 378-390 and-391-400, May 1971.

[28] B. Peterson and S. Strom, "T matrix for electromagnetic scattering from an arbitrary number of scatterers and representation of E(3)," *Phys. Rev. D,* vol. 8, pp. 3661-3678, Nov. 1973.

[29] S. S. Koc, O. A. Civi, and O. M. Buyukdura, "An application of the T-matrix method to time-domain scattering," in *Proc. IEEE Int. Antennas and Propagation Symp. and URSI Radio Science Meeting,* Proc. URSI, Boston, MA, July 8-13, 2001, p. 336.

[30] B. Friedman and J. Russek, "Addition theorems for spherical waves," *Quart. Appl. Math.,* vol. 12, pp. 13-23, 1954.

[31] S. Stein, "Addition theorems for spherical wave functions," *Quart. Appl. Math.,* vol. 19, pp. 15-24, 1961.

[32] O. R. Cruzan, "Translational addition theorems for spherical vector wave functions," *Quart. Appl. Math.,* vol. 20, pp. 33-40, 1962.

[33] M. Danos and L. C. Maximon, "Multipole matrix elements of the translation operator," *J. Math. Phys.,* vol. 6, pp. 766-778, May 1965.

[34] R. C. Wittmann, "Spherical wave operators and the translation formulas," *IEEE Trans. Antennas Propagat.,* vol. 36, pp. 1078-1087, Aug. 1988.

[35] W. C. Chew, "Recurrence relations for three-dimensional scalar addition theorem," *J. Electromag. Waves Appl.,* vol. 6, pp. 133-142, 1992.

[36] W. C. Chew and Y. M. Wang, "Efficient ways to compute the vector addition theorem," *J. Electromag. Waves Appl.,* vol. 7, pp. 651-665, 1993.

[37] V. V. Varadan, A. Lakhtakia and V. K. Varadan, *Field Representations and Introduction to Scattering.* Amsterdam: North Holland, 1991.

[38] S. A. Azizoglu and S. S. Koc, "Translational addition theorems for the time domain spherical scalar wave functions," in *Proc. IEEE Int. Antennas and Propagation Symp.*, Albuquerque, NM, July 9-14, 2006, pp. 943-946.

[39] S. A. Azizoğlu, S. S. Koç, "Zaman uzamı skalar küresel dalga fonksiyonları için öteleme adisyon teoremleri," *12. Elektrik, Elektronik, Bilgisayar, Biyomedikal Mühendisliği Ulusal Kongresi ve Fuarı,* Eskişehir, Türkiye, *2007.*

[40] M. Abramowitz and I. A. Stegun, *Handbook of Mathematical Functions.* New York: Dover, 1972.

[41] E. P. Wigner, *Group Theory and Its Application to the Quantum Mechanics of Atomic Spectra.* New York: Academic Press, 1959.

[42] A. Messiah, *Quantum Mechanics, Vol. 2.* Amsterdam: North Holland, 1962.

[43] J. A. Stratton, *Electromagnetic Theory.* New York: McGraw-Hill, 1941.

[44] G. C. Goodwin and K. S. Sin, *Adaptive Filtering Prediction and Control.* Englewood Cliffs, NJ: Prentice-Hall, 1984.

APPENDIX A

TIME DOMAIN T-MATRIX FORMULATION

The T-matrix method is also known as the extended boundary condition (EBC) method or the null field approach, and it is an alternative to solve the surface integral equation. In this method, the integral equations are imposed not on the surface S, but on some surfaces S_i and S_o away from S as shown in Figure 3.1, in order to simplify the solutions. The frequency domain formulation can be found in Chew [2], and it is developed similarly in the time domain as follows.

Assume that we want to find the scattered field in v_e, the volume outside S, created by a known incident field or by some localized source distribution, $f(\mathbf{R},t)$ enclosed by a closed surface Σ, in the presence of a scatterer. The total field satisfies

$$\left[\nabla^2 - \frac{1}{c^2} \frac{\partial^2}{\partial t^2} \right] \psi(\mathbf{R},t) = f(\mathbf{R},t) \; , \tag{A.1}$$

subject to boundary conditions on S. If the scatterer were not present, the solution would be

$$\psi^i(\mathbf{R},t) = -\int_{v_\Sigma} f(\mathbf{R},t) \otimes g_o(\mathbf{R},\mathbf{R}';t) \, dv' \; , \tag{A.2}$$

where $\psi^i(\mathbf{R},t)$ is the incident field, v_Σ is a volume enclosing all the sources; and $g_0(\mathbf{R},\mathbf{R}';t)$ is the free-space Green's function, i.e.,

$$g_0(\mathbf{R},\mathbf{R}';t) = \frac{1}{c}\sum_{n=0}^{\infty}\sum_{m=-n}^{n}\left\{ d_{nm}\, S_n\!\left(\frac{R_<}{c},t\right)\otimes O_n\!\left(\frac{R_>}{c},t\right) Y_{nm}(\theta_<,\phi_<) Y_{nm}^*(\theta_>,\phi_>)\right\},$$

(A.3)

where

$$d_{nm} = \frac{(-1)^n (2n+1)(n-m)!}{8\pi(n+m)!}\ ,$$

(A.4)

and $Y_{nm}(\theta,\phi)$ are the Tesseral harmonics, given in Eq. (2.12), and $R_>$ stands for the larger of R and R', whereas $R_<$ stands for the smaller. The free-space Green's function satisfies

$$\left[\nabla^2 - \frac{1}{c^2}\frac{\partial^2}{\partial t^2}\right] g_0(\mathbf{R},\mathbf{R}';t) = -\delta(\mathbf{R}-\mathbf{R}')\,\delta(t)\ ,$$

(A.5)

and can also be written in the alternate form using Eq. (2.37) as

$$g_0(\mathbf{R},\mathbf{R}';t) = \frac{(-1)^n c}{R_> R_<}\sum_{n=0}^{\infty}\sum_{m=-n}^{n}\left\{\left[d_{nm}\, P_n\!\left(\frac{R_>^{\,2}+R_<^{\,2}-c^2 t^2}{2R_> R_<}\right) p\!\left(\frac{ct-R_>}{R_<}\right)\right]\right.$$

$$\left.\times Y_{nm}(\theta_<,\phi_<) Y_{nm}^*(\theta_>,\phi_>)\right\}.$$

(A.6)

Convolving Eq. (A.1) by $g_0(\mathbf{R},\mathbf{R}';t)$ and Eq. (A.5) by $-\psi(\mathbf{R},t)$, adding and integrating over v_e yields

$$\int_{v_e} \left[g_o \otimes \nabla^2 \psi - g_o \otimes \frac{1}{c^2} \frac{\partial^2}{\partial t^2} \psi - \psi \otimes \nabla^2 g_o + \psi \otimes \frac{1}{c^2} \frac{\partial^2}{\partial t^2} g_o \right] dv$$

$$= \int_{v_e} \left[g_o \otimes f + \psi \otimes \delta(\mathbf{R} - \mathbf{R}') \, \delta(t) \right] dv \quad .$$

(A.7)

Noting,

$$g_o \otimes \frac{\partial^2 \psi}{\partial t^2} = \frac{\partial^2}{\partial t^2} [g_o \otimes \psi] = \frac{\partial^2 g_o}{\partial t^2} \otimes \psi \quad ,$$

(A.8)

(A.7) simplifies to

$$\int_{v_e} \left[g_0(\mathbf{R}, \mathbf{R}'; t) \otimes \nabla^2 \psi(\mathbf{R}, t) - \psi(\mathbf{R}, t) \otimes \nabla^2 g_o(\mathbf{R}, \mathbf{R}', t) \right] dv$$

$$= -\psi^i(\mathbf{R}', t) + \int_{v_e} \left[\psi(\mathbf{R}, t) \otimes \delta(\mathbf{R} - \mathbf{R}') \right] dv \quad .$$

(A.9)

It can be shown that Green's second identity is valid if multiplication is replaced by convolution, i.e.,

$$\int_{v_e} \left[g_o(\mathbf{R}, \mathbf{R}', t) \otimes \nabla^2 \psi(\mathbf{R}, t) - \psi(\mathbf{R}, t) \otimes \nabla^2 g_o(\mathbf{R}, \mathbf{R}', t) \right] dv$$

$$= \int_s \left[g_o(\mathbf{R}, \mathbf{R}', t) \otimes \frac{\partial}{\partial n_e} \psi(\mathbf{R}, t) - \psi(\mathbf{R}, t) \otimes \frac{\partial}{\partial n_e} g_o(\mathbf{R}, \mathbf{R}', t) \right] ds' \,,$$

(A.10)

since convolution is an operation on the time variable and ∇ operates only on space space variables. Finally, interchanging $\mathbf{R}$ and $\mathbf{R}'$ and using the symmetry property of the Green's function, $g_o(\mathbf{R}, \mathbf{R}', t) = g_o(\mathbf{R}', \mathbf{R}, t)$, yields

$$\int_S \left[\psi(\mathbf{R}',t) \otimes \frac{\partial}{\partial n'} g_o(\mathbf{R},\mathbf{R}',t) - g_o(\mathbf{R},\mathbf{R}',t) \otimes \frac{\partial}{\partial n'} \psi(\mathbf{R}',t) \right] ds'$$

$$= \begin{cases} \psi(\mathbf{R},t) - \psi^i(\mathbf{R},t), & \mathbf{R} \text{ outside } S \\ \\ -\psi^i(\mathbf{R},t), & \mathbf{R} \text{ inside } S. \end{cases}$$

(A.11)

Note that, $\hat{\mathbf{n}}'$ and $\hat{\mathbf{n}}_e$ are the unit normal outward and inward from the scatterer, respectively. Now, assume the Dirichlet boundary condition, $\psi(\mathbf{R},t) = 0$ on S (soft boundary condition), then

$$-\int_S g_o(\mathbf{R},\mathbf{R}',t) \otimes \frac{\partial}{\partial n'} \psi(\mathbf{R}',t) ds' = \begin{cases} \psi^s(\mathbf{R},t), & \mathbf{R} \text{ outside } S \\ \\ -\psi^i(\mathbf{R},t), & \mathbf{R} \text{ inside } S. \end{cases}$$

(A.12)

Let

$$\psi^i(\mathbf{R},t) = \sum_{n=0}^{\infty} \sum_{m=-n}^{n} d_{nm} f_{nm}^i(t) \otimes S_n\left(\frac{R}{c},t\right) Y_{nm}(\theta,\phi).$$

(A.13)

Using the second line of Eq. (A.11), where $R' > R$, yields

$$-\sum_{n=0}^{\infty} \sum_{m=-n}^{n} d_{nm} f_{nm}^i(t) \otimes S_n\left(\frac{R}{c},t\right) Y_{nm}(\theta,\phi) = -\int_S \left\{ \left[\frac{1}{c} \sum_{n=0}^{\infty} \sum_{m=-n}^{n} \left\{ d_{nm} S_n\left(\frac{R}{c},t\right) \right. \right. \right.$$

$$\left. \left. \left. \otimes O_n\left(\frac{R'}{c},t\right) Y_{nm}(\theta,\phi) Y_{nm}^*(\theta',\phi') \right] \otimes \frac{\partial}{\partial n'} \psi(\mathbf{R}',t) \right\} ds'.$$

(A.14)

Changing the order of integration and summation on the right hand side of this equation and using the orthogonality of the expansions, which implies term by term equality, gives

$$f_{nm}^i(t) = \int_S \left[\frac{1}{c} O_n\left(\frac{R'}{c},t\right) \otimes \frac{\partial}{\partial n'} \psi(\mathbf{R}',t) Y_{nm}^*(\theta',\phi') \right] ds' . \qquad (A.15)$$

Now, expand the total field as

$$\psi(\mathbf{R}',t) = \sum_{\nu=0}^{\infty} \sum_{\mu=-\nu}^{\nu} f_{\nu\mu}^t(t) \otimes S_\nu\left(\frac{R'}{c},t\right) Y_{\nu\mu}(\theta',\phi') , \qquad (A.16)$$

and use it in Eq. (A.15) to get

$$f_{nm}^i(t) = \int_S \left\{ \frac{1}{c} O_n\left(\frac{R'}{c},t\right) \otimes \frac{\partial}{\partial n'} \left[\sum_{\nu=0}^{\infty} \sum_{\mu=-\nu}^{\nu} f_{\nu\mu}^t(t) \otimes S_\nu\left(\frac{R'}{c},t\right) Y_{\nu\mu}(\theta',\phi') \right] \right.$$

$$\left. \times Y_{nm}^*(\theta',\phi') \, ds' \right\} . $$

$$\qquad (A.17)$$

In this relation, the order of integration and summation can be changed to get the form,

$$f_{nm}^i(t) = \sum_{\nu=0}^{\infty} \sum_{\mu=-\nu}^{\nu} Q_{nm,\nu\mu}(t) \otimes f_{\nu\mu}^t(t) , \qquad (A.18)$$

where

$$Q_{nm,\nu\mu}(t) = \int_S \left\{ \frac{1}{c} O_n\left(\frac{R'}{c},t\right) Y_{nm}^*(\theta',\phi') \otimes \frac{\partial}{\partial n'} \left[S_\nu\left(\frac{R'}{c},t\right) Y_{\nu\mu}(\theta',\phi') \right] \right\} ds' . $$

$$\qquad (A.19)$$

The relation in Eq. (A.18) can be written in matrix form as

$$\mathbf{f}^i(t) = \overline{\mathbf{Q}}(t) \otimes \mathbf{f}^t(t) \ , \tag{A.20}$$

where $\mathbf{f}^i(t)$ and $\mathbf{f}^t(t)$ are column vectors containing $f_{nm}^i(t)$ and $f_{\nu\mu}^t(t)$ in some proper sorting, respectively. $\overline{\mathbf{Q}}(t)$ is a matrix with elements $Q_{nm,\nu\mu}(t)$ which relates the incident and total field convolving functions. In Eq. (A.20), $\mathbf{f}^i(t)$ and $\overline{\mathbf{Q}}(t)$ are known and $\mathbf{f}^t(t)$ is to be solved. This is a deconvolution problem which can be solved either by direct deconvolution, Appendix B, or by using system identification techniques, Goodwin *et al.* [44].

The scattered field can be written using the first line of Eq. (A.12). Replacing the expansion of the total field given in Eq. (A.16) and the Green's function expansion given in Eq. (A.3) where $R_> = R$ and $R_< = R'$, and also changing the order of integration and summation yields

$$\psi^s(\mathbf{R},t) = \sum_{n=0}^{\infty} \sum_{m=-n}^{n} d_{nm} f_{nm}^s(t) \otimes O_n\left(\frac{R}{c}, t\right) Y_{nm}(\theta, \phi) \ , \tag{A.21}$$

$$f_{nm}^s(t) = \sum_{\nu=0}^{\infty} \sum_{\mu=-\nu}^{\nu} Q_{nm,\nu\mu}^e(t) \otimes f_{\nu\mu}^t(t) \ , \tag{A.22}$$

where

$$Q_{nm,\nu\mu}^e(t) = -\int_S \left\{ \frac{1}{c} S_n\left(\frac{R'}{c}, t\right) Y_{nm}^*(\theta', \phi') \otimes \frac{\partial}{\partial n'}\left[S_\nu\left(\frac{R'}{c}, t\right) Y_{\nu\mu}(\theta', \phi') \right] \right\} ds' . \tag{A.23}$$

Eq.(A.22) can be written in matrix form as

$$\mathbf{f}^s(t) = \overline{\mathbf{Q}}^e(t) \otimes \mathbf{f}^t(t) \ , \tag{A.24}$$

where $\mathbf{f}^s(t)$ is a column vector containing $f_{nm}^s(t)$ and $\overline{\mathbf{Q}}^e(t)$ is a matrix with elements $Q_{nm,\nu\mu}^e(t)$ which relates the scattered and total field convolving functions. In Eq. (A.24), $\mathbf{f}^t(t)$ and $\overline{\mathbf{Q}}^e(t)$ are known and $\mathbf{f}^s(t)$ is to be solved by matrix convolution, which can be achieved similar to matrix multiplication, but now multiplication replaced by convolution as defined in Appendix B. Using Eqs. (A.20) and (A.24), and inspired by the definition of the frequency domain T-matrix, the time domain T-matrix can be defined in order to relate $\mathbf{f}^s(t)$ to $\mathbf{f}^i(t)$ as

$$\mathbf{f}^s(t) = \overline{\mathbf{T}}(t) \otimes \mathbf{f}^i(t) , \tag{A.25}$$

where

$$\overline{\mathbf{T}}(t) = \overline{\mathbf{Q}}^e(t) \otimes \overline{\mathbf{\Theta}}(t) , \tag{A.26}$$

and

$$\overline{\mathbf{\Theta}}(t) \otimes \overline{\mathbf{Q}}(t) = \overline{\mathbf{\delta}}(t) , \tag{A.27}$$

where $\overline{\mathbf{\delta}}(t)$ is a diagonal matrix containing $\delta(t)$ in each diagonal entry. Hence, the scattered field from a scatterer can be found for any illumination by Eq. (A.25) once the T-matrix for that scatterer is known.

APPENDIX B

DIRECT MATRIX DECONVOLUTION

Direct deconvolution algorithm given in Koc *et al.* [18] can be generalized for matrices containing functions of time. The solution for $C_{n'm',\nu\mu}(t)$ is to be found in the equation of the form

$$A_{nm,\nu\mu}(t) = \sum_{n'=0}^{\infty} \sum_{m'=-n'}^{n'} Q_{nm,n'm'}(t) \otimes C_{n'm',\nu\mu}(t) \ , \tag{B.1}$$

where $A_{nm,\nu\mu}(t)$ and $Q_{nm,n'm'}(t)$ are known functions of time. The relation in Eq. (B.1) can be written in matrix form as

$$\overline{\mathbf{A}}(t) = \overline{\mathbf{Q}}(t) \otimes \overline{\mathbf{C}}(t) \ , \tag{B.2}$$

where $\overline{\mathbf{A}}(t)$, $\overline{\mathbf{Q}}(t)$, and $\overline{\mathbf{C}}(t)$ are matrices containing $A_{nm,\nu\mu}(t)$, $Q_{nm,n'm'}(t)$, and $C_{n'm',\nu\mu}(t)$ in some proper sorting, respectively. All the functions that appear in Eq. (B.1) are band limited and the sampling is assumed to be fast enough to determine these functions at any time. If we take samples at T intervals and define $\overline{\mathbf{A}}_i = \overline{\mathbf{A}}(iT)$, $\overline{\mathbf{Q}}_i = \overline{\mathbf{Q}}(iT)$, and $\overline{\mathbf{C}}_i = \overline{\mathbf{C}}(iT)$, the continuous time system may be approximated by a discrete time system as

$$\overline{\mathbf{A}}_i = \overline{\mathbf{Q}}_i \oplus \overline{\mathbf{C}}_i \ , \tag{B.3}$$

where $\oplus$ denotes the convolution sum, i.e.,

$$\overline{\mathbf{A}}_i = \sum_{j=0}^{i} \overline{\mathbf{Q}}_{i-j} \overline{\mathbf{C}}_j \ , \tag{B.4}$$

which is equivalent to evaluating the convolution integral as a Riemann sum. The first few terms of $\overline{\mathbf{A}}_i$ can be written as

$$\overline{\mathbf{A}}_0 = \overline{\mathbf{Q}}_0 \overline{\mathbf{C}}_0 \ ,$$

$$\overline{\mathbf{A}}_1 = \overline{\mathbf{Q}}_0 \overline{\mathbf{C}}_1 + \overline{\mathbf{Q}}_1 \overline{\mathbf{C}}_0 \ ,$$

$$\overline{\mathbf{A}}_2 = \overline{\mathbf{Q}}_0 \overline{\mathbf{C}}_2 + \overline{\mathbf{Q}}_1 \overline{\mathbf{C}}_1 + \overline{\mathbf{Q}}_2 \overline{\mathbf{C}}_0 \ ,$$

$$\vdots$$

$$\overline{\mathbf{A}}_i = \overline{\mathbf{Q}}_0 \overline{\mathbf{C}}_i + \sum_{j=1}^{i} \overline{\mathbf{Q}}_{i-j} \overline{\mathbf{C}}_j \ ,$$

$$\tag{B.5}$$

which shows that at each step one sample of the unknown function can be determined as

$$\overline{\mathbf{C}}_0 = \overline{\mathbf{Q}}_0^{-1} \overline{\mathbf{A}}_0 \ ,$$

$$\overline{\mathbf{C}}_1 = \overline{\mathbf{Q}}_0^{-1} \left(\overline{\mathbf{A}}_1 - \overline{\mathbf{Q}}_1 \overline{\mathbf{C}}_0 \right),$$

$$\overline{\mathbf{C}}_2 = \overline{\mathbf{Q}}_0^{-1} \left(\overline{\mathbf{A}}_2 - \left(\overline{\mathbf{Q}}_1 \overline{\mathbf{C}}_1 + \overline{\mathbf{Q}}_2 \overline{\mathbf{C}}_0 \right) \right),$$

$$\vdots$$

$$\overline{\mathbf{C}}_i = \overline{\mathbf{Q}}_0^{-1} \left(\overline{\mathbf{A}}_i - \sum_{j=1}^{i} \overline{\mathbf{Q}}_j \overline{\mathbf{C}}_{i-j} \right).$$

$$\tag{B.6}$$

Note that only the inverse of $\overline{\mathbf{Q}}_0$ is needed, and since $\overline{\mathbf{Q}}(t)$ can not be identically zero, one can shift the time origin so that the first sample $\overline{\mathbf{Q}}_0$ is non-singular. Unfortunately, the recursive nature of this approach causes numerical problems.

The algorithm explained above can also be used to solve for $\mathbf{c}(t)$ in the equation $\mathbf{a}(t) = \overline{\mathbf{Q}}(t) \otimes \mathbf{c}(t)$, where $\mathbf{a}(t)$ and $\mathbf{c}(t)$ are column vectors containing $a_{nm}(t)$, and $c_{\nu\mu}(t)$ in proper sorting, respectively, and $\overline{\mathbf{Q}}(t)$ is a matrix with elements $Q_{nm,\nu\mu}(t)$.

When the matrices $\overline{\mathbf{A}}(t)$ and $\overline{\mathbf{Q}}(t)$ contain terms proportional to the unit impulse function $\delta(t)$ (and indeed does in the numerical example of the time domain scattering by an object in Chapter 4), i.e., $\overline{\mathbf{A}}(t) = \overline{\mathbf{X}}\,\delta(t)$ and $\overline{\mathbf{Q}}(t) = \overline{\mathbf{Y}}\,\delta(t) + \overline{\mathbf{Z}}(t)$, the solution is in the form of $\overline{\mathbf{C}}(t) = \overline{\mathbf{V}}\,\delta(t) + \overline{\mathbf{W}}(t)$, where Eq. (B2) becomes

$$\overline{\mathbf{X}}\,\delta(t) = \left(\overline{\mathbf{Y}}\,\delta(t) + \overline{\mathbf{Z}}(t)\right) \otimes \left(\overline{\mathbf{V}}\,\delta(t) + \overline{\mathbf{W}}(t)\right), \tag{B.7}$$

and leads to two matrix equations from which the unknown matrix $\overline{\mathbf{C}}(t)$, i.e., $\overline{\mathbf{V}}$ and $\overline{\mathbf{W}}(t)$ can be solved,

$$\overline{\mathbf{X}} = \overline{\mathbf{Y}}\,\overline{\mathbf{V}}, \tag{B.8}$$

$$-\overline{\mathbf{Z}}(t)\,\overline{\mathbf{V}} = \overline{\mathbf{Z}}(t) \otimes \overline{\mathbf{W}}(t) + \overline{\mathbf{Y}}\,\overline{\mathbf{W}}(t). \tag{B.9}$$

The solution to Eq. (B.8),

$$\overline{\mathbf{V}} = \overline{\mathbf{Y}}^{-1}\,\overline{\mathbf{X}}, \tag{B.10}$$

can be used in Eq. (B.9) to solve for $\overline{\mathbf{W}}(t)$. Eq. (B.9) can be written in the form

$$\overline{\mathbf{U}}(t) = \overline{\mathbf{Z}}(t) \otimes \overline{\mathbf{W}}(t) + \overline{\mathbf{Y}}\,\overline{\mathbf{W}}(t), \tag{B.11}$$

where

$$\overline{\mathbf{U}}(t) = -\overline{\mathbf{Z}}(t)\,\overline{\mathbf{V}}.$$

(B.12)

The solution to Eq. (B.11) for $\overline{\mathbf{W}}(t)$ can be found in a similar way to Eq. (B.6) as

$$\overline{\mathbf{W}}_0 = \left(\overline{\mathbf{Z}}_0 + \overline{\mathbf{Y}}\right)^{-1}\overline{\mathbf{U}}_0\,,$$

$$\overline{\mathbf{W}}_1 = \left(\overline{\mathbf{Z}}_0 + \overline{\mathbf{Y}}\right)^{-1}\left(\overline{\mathbf{U}}_1 - \overline{\mathbf{Z}}_1\overline{\mathbf{W}}_0\right),$$

$$\overline{\mathbf{W}}_2 = \left(\overline{\mathbf{Z}}_0 + \overline{\mathbf{Y}}\right)^{-1}\left(\overline{\mathbf{U}}_2 - \left(\overline{\mathbf{Z}}_1\overline{\mathbf{W}}_1 + \overline{\mathbf{Z}}_2\overline{\mathbf{W}}_0\right)\right),$$

$$\vdots$$

$$\overline{\mathbf{W}}_i = \left(\overline{\mathbf{Z}}_0 + \overline{\mathbf{Y}}\right)^{-1}\left(\overline{\mathbf{U}}_i - \sum_{j=1}^{i}\overline{\mathbf{Z}}_j\overline{\mathbf{W}}_{i-j}\right).$$

(B.13)

This approach can be used to solve for $\mathbf{\Theta}(t)$ in the equation $\overline{\mathbf{\Theta}}(t) \otimes \overline{\mathbf{Q}}(t) = \overline{\mathbf{\delta}}(t)$, by handling the $\delta(t)$ terms separately as explained above, where $\overline{\mathbf{\delta}}$ is a diagonal matrix containing $\delta(t)$ in each diagonal entry. Solving for $\mathbf{\Theta}(t)$ in the time domain in such an equation would correspond to matrix inversion if we were in the frequency domain.

FORMULATION FOR THE EVALUATION OF THE SURFACE INTEGRALS IN THE TIME DOMAIN T-MATRIX METHOD

In order to obtain the time domain T-matrix for an object, the matrices, $\overline{\mathbf{Q}}(t)$ and $\overline{\mathbf{Q}}^{e}(t)$, have to be filled by Eqs. (A.19) and (A.23), respectively. The T-matrix is then obtained by Eqs. (A.26) and (A.27). The entries of the matrices, $\overline{\mathbf{Q}}(t)$ and $\overline{\mathbf{Q}}^{e}(t)$, involve surface integrals which have to be evaluated. Below, the formulation necessary for the numerical evaluation of these surface integrals for a shifted sphere, whose center is displaced from the coordinate origin, with the assumption of ϕ symmetry is given.
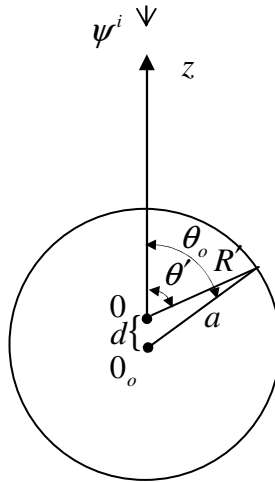

Figure C.1 Geometry for the shifted sphere.

For the particular case of the plane wave incident from the $+z$ axis, which is used in the scattering problems of the present work, $m = 0$ as the field is independent of ϕ variation; and Eq. (A.19) becomes

$$Q_{nv}(t) = 2\pi \int_0^\pi \left\{ \frac{1}{c} O_n\left(\frac{R'}{c}, t\right) P_n(\cos\theta') \right.$$

$$\left. \otimes \frac{\partial}{\partial n'}\left[S_v\left(\frac{R'}{c}, t\right) P_v(\cos\theta') \right] R'^2 \sin\theta' \right\} d\theta' \quad .$$

(C.1)

Consider Figure C.1, for a point on the sphere

$$R' = -d\cos\theta' + \sqrt{a^2 - d^2\sin^2\theta'} \quad , \tag{C.2}$$

where a is the radius of the sphere, R' is the magnitude of the position vector from the origin 0 to a point on the sphere, and 0_o is the center of the sphere. The unit normal outward from the surface of the sphere, $\hat{\mathbf{n}}'$, can be written as

$$\hat{\mathbf{n}}' = \frac{1}{B(\theta')}\left(\hat{\mathbf{R}}' + A(\theta')\hat{\boldsymbol{\theta}}'\right), \tag{C.3}$$

in spherical coordinates where $\hat{\mathbf{R}}'$ and $\hat{\boldsymbol{\theta}}'$ are the unit vectors along the directons of $\mathbf{R}'$ and $\boldsymbol{\theta}'$, respectively, and

$$A(\theta') = \frac{d\sin\theta'}{R'}\left(-1 + \frac{d\cos\theta'}{\sqrt{a^2 - d^2\sin^2\theta'}}\right), \tag{C.4}$$

$$B(\theta') = \sqrt{1 + \frac{d^2\sin^2\theta'}{R'^2}\left(-1 + \frac{d\cos\theta'}{\sqrt{a^2 - d^2\sin^2\theta'}}\right)^2} \quad . \tag{C.5}$$

The directional derivative of a scalar function f along $d\hat{\mathbf{n}}'$ is defined as

$$\frac{df}{dn'} = (\nabla' f).\hat{\mathbf{n}}' \ ,$$

(C.6)

where ∇ denotes the gradient operator. Using Eq. (C.6) for the scalar function defining the surface of the shifted sphere and

$$\nabla'\left[S_v\left(\frac{R'}{c},t\right) P_v\left(\cos\theta'\right)\right] = \frac{d}{dR'}\left[S_v\left(\frac{R'}{c},t\right)\right] P_v\left(\cos\theta'\right) \hat{\mathbf{R}}'$$

$$+ \frac{1}{R'} S_v\left(\frac{R'}{c},t\right) \frac{d}{d\theta'}\left[P_v\left(\cos\theta'\right)\right] \hat{\boldsymbol{\theta}}' \ ,$$

(C.7)

the integrand in Eq. (C.1), which is denoted by Int, can be written as

$$Int = \sin\theta' \, P_n\left(\cos\theta'\right) U_n\left(\frac{R'}{c},t\right) \otimes \left\{ \ C_1(\theta') P_v\left(\cos\theta'\right) \right.$$

$$\times \left[-\frac{c^2 t}{R'^2}\left\{\frac{d}{d\left(ct/R'\right)}\left[P_v\left(\frac{ct}{R'}\right) p\left(\frac{ct}{R'}\right)\right]\right\} - \frac{c}{R'} P_v\left(\frac{ct}{R'}\right) p\left(\frac{ct}{R'}\right)\right]$$

$$\left. - C_2(\theta')\sin\theta'\left[\frac{d}{d(\cos\theta')} P_v\left(\cos\theta'\right)\right] \frac{c}{R'} P_v\left(\frac{ct}{R'}\right) p\left(\frac{ct}{R'}\right)\right\} \ ,$$

(C.8)

where the definition of S_n, Eq. (2.33), and the relation between O_n and U_n, Eq. (2.36), is used along with

$$C_1(\theta') = \frac{1}{B(\theta')},$$

(C.9)

and

$$C_2(\theta') = \frac{A(\theta')}{B(\theta')} \ . \tag{C.10}$$

$U_n(R',t)$ can be represented as the summation of an impulse striking at $t = R'$ and a right-sided signal $s(t,R')$ starting from $t = R'$, Eqs. (2.34) and (2.36), Azizoglu [17], as

$$U_n(R',t) = \delta(t - R') + s(t,R') \ . \tag{C.11}$$

Using

$$\frac{d}{d\left(ct/R'\right)}\left[P_\nu\left(\frac{ct}{R'}\right)p\left(\frac{ct}{R'}\right)\right] = p\left(\frac{ct}{R'}\right)\frac{d}{d\left(ct/R'\right)}\left[P_\nu\left(\frac{ct}{R'}\right)\right]$$

$$+ P_\nu\left(\frac{ct}{R'}\right)[\delta(t + R'/c) - \delta(t - R'/c)] \quad , \tag{C.12}$$

Eq.(C.8) can be rewritten as

$$Int = \sin\theta' P_n(\cos\theta')\Big\{ \ s(t, R'/c)\otimes[h_1(t, R'/c,\theta') + h_2(t, R'/c,\theta')]$$

$$+ h_1(t - R'/c, R'/c,\theta') + h_2(t - R'/c, R'/c,\theta')$$

$$+ \frac{c}{R'}C_1(\theta')P_\nu(\cos\theta')[(-1)^\nu \ s(t + R'/c, R'/c) + s(t - 2R'/c, R'/c)]$$

$$+ \frac{c}{R'}C_1(\theta')P_\nu(\cos\theta')[(-1)^\nu \ \delta(t) + \delta(t - 2R'/c)] \Big\} \quad . \tag{C.13}$$

Note that

$$h_1(t, R', \theta') = C_1(\theta') P_\nu (\cos \theta') \left[-\frac{t}{R'^2} p\left(\frac{t}{R'}\right) \frac{d}{d(t/R')} \left[P_\nu\left(\frac{t}{R'}\right) \right] \right.$$

$$\left. -\frac{1}{R'} P_\nu\left(\frac{t}{R'}\right) p\left(\frac{t}{R'}\right) \right] \quad,$$

(C.14)

$$h_2(t, R', \theta') = -C_2(\theta') \sin \theta' \frac{1}{R'} P_\nu\left(\frac{t}{R'}\right) p\left(\frac{t}{R'}\right) \frac{d}{d(\cos \theta')} P_\nu (\cos \theta') \quad, \qquad (C.15)$$

and

$$P_\nu (1) = 1 \quad, \tag{C.16}$$

$$P_\nu (-1) = (-1)^\nu \quad. \tag{C.17}$$

The integrand Int, given in Eq. (C.13), has to be evaluated numerically in order to fill the matrix $\overline{\mathbf{Q}}(t)$. The last term containing δ terms, can however be exploited more as follows. Integrating it and denoting the result by I_4,

$$I_4 = 2\pi \int_0^\pi \left\{ \frac{c}{R'(\theta')} C_1(\theta') P_n (\cos \theta') P_\nu (\cos \theta') \right.$$

$$\left. \times \left[(-1)^\nu \delta(t) + \delta(t - 2R'(\theta')/c) \right] \sin \theta' \right\} d\theta' \quad,$$

(C.18)

and changing the variables as $u = \cos \theta'$, $du = (-\sin \theta' d\theta')$, Eq. (C.18) becomes

$$I_4 = 2\pi(-1)^v \delta(t) \int_{-1}^{1} \left\{ \frac{c}{R'(u)} C_1(u) P_n(u) P_v(u) \right\} du$$

$$+ 2\pi \int_{-1}^{1} \left\{ \frac{c}{R'(u)} C_1(u) P_n(u) P_v(u) \delta(t - 2R'(u)/c) \right\} du \quad .$$

(C.19)

The first term has to be evaluated numerically, and the second term denoted by I_{4b} can be evaluated analytically, changing the variables in Eq. (C.18) as $u = (t - 2R'(\theta')/c)$, $du = (-2\,dR'/c)$, leads to

$$I_{4b} = 2\pi \int_{t+2(d-a)/c}^{t-2(d+a)/c} \left\{ \frac{c^2}{R'(u)} \frac{C_1(u) P_n(u) P_v(u) \delta(u)}{2d \left[-1 + \dfrac{d\cos\theta'}{\sqrt{a^2 - d^2 \sin^2\theta'}} \right]} \right\} du \quad .$$

(C.20)

As $R'(\theta') = ct/2$, when $u = 0$, and $R'_{\min} = a - d$, $R'_{\max} = a + d$, I_{4b} is nonzero only when $2(a-d)/c < t < 2(a+d)/c$ resulting in

$$I_{4b} = -2\pi \frac{c^2}{R'(\theta')} \frac{C_1(\theta') P_n(\cos\theta') P_v(\cos\theta')}{2d \left[-1 + \dfrac{d\cos\theta'}{\sqrt{a^2 - d^2 \sin^2\theta'}} \right]} \Bigg|_{\theta' = \cos^{-1}\left[\frac{4(a^2 - d^2) - t^2}{4td} \right]} \quad .$$

(C.21)

The entries of the matrix $\overline{\mathbf{Q}}^e(t)$ can be filled similarly. For $m = 0$, Eq. (A.23) becomes

$$Q_{n\nu}^{e}(t) = -2\pi \int_{0}^{\pi} \left\{ \frac{1}{c} S_{n}\left(\frac{R'}{c}, t\right) P_{n} (\cos\theta') \right.$$

$$\left. \otimes \frac{\partial}{\partial n'} \left[S_{\nu}\left(\frac{R'}{c}, t\right) P_{\nu} (\cos\theta') \right] R'^{2} \sin\theta' \right\} d\theta' \quad,$$

(C.22)

and the integrand of Eq. (C.22), which is denoted by Int^{e} and to be evaluated numerically, can be written as

$$Int^{e} = \sin\theta' \, P_{n} (\cos\theta') \left\{ P_{n}\left(\frac{ct}{R'}\right) p\left(\frac{ct}{R'}\right) \otimes \left[h_{1}(t, R'/c, \theta') + h_{2}(t, R'/c, \theta') \right] \right.$$

$$+ \frac{c}{R'} C_{1}(\theta') P_{\nu} (\cos\theta')$$

$$\left. \times \left[(-1)^{\nu} P_{n}\left(\frac{ct}{R'} + 1\right) p\left(\frac{ct}{R'} + 1\right) + P_{n}\left(\frac{ct}{R'} - 1\right) p\left(\frac{ct}{R'} - 1\right) \right] \right\} \quad.$$

(C.23)

CURRICULUM VITAE

PERSONAL INFORMATION

Surname, Name: Azizoğlu, Süha Alp
Nationality: Turkish (TC)
Date and Place of Birth: March 14, 1973, Göynük, Bolu
Marital Status: Single
Phone: +90 533 236 11 63
email: salpazizoglu@hotmail.com

EDUCATION

Degree	Institution	Year of Graduation
MS	METU, EE	1999
BS	METU, EE	1996
High School	TED Ankara College	1991

WORK EXPERIENCE

Year	Place	Enrollment
1997-Present	Aselsan Inc., Comm. Div., Dept. of Electronic Design	Senior RF Design Eng.
1995 July	TRT, Dept. of Eurovision	Intern Eng.ing Student
1994 August	Turkish PTT, Dept. of Radio-Link	Intern Eng.ing Student

FOREIGN LANGUAGES

Advanced English

PUBLICATIONS

1. S. A. Azizoglu, S. S. Koc, and O. M. Buyukdura, "Spherical wave expansion of the time domain free-space dyadic Green's function," *IEEE Trans. Antennas Propagat.,* vol. 52, pp. 677-683, March 2004.

2. S. A. Azizoglu, S. S. Koc, and O. M. Buyukdura, "Spherical wave expansion of the time domain free-space dyadic Green's function," in *Proc. Ultra-Wideband, Short-Pulse Electromagnetics 5.* New York: Kluwer Academic/Plenum Publishers, 2002, pp. 83-88.

3. S. A. Azizoglu, S. S. Koc, "Translational addition theorems for the time domain spherical scalar wave functions," in *Proc. IEEE Int. Antennas and Propagation Symp.*, Albuquerque, NM, July 9-14, 2006, pp. 943-946.

4. S. A. Azizoğlu, S. S. Koç, O. M. Büyükdura, "Zaman uzamında boşluk diadik Green fonksiyonunun küresel dalga fonksiyonlari ile açılımı için bir ifade," *TMMOB Elektrik Mühendisleri Odası Elektrik-Elektronik Bilgisayar Mühendisliği 8. Ulusal Kongresi*, Gaziantep, Türkiye, 1999, pp. 240-243.

5. S. A. Azizoğlu, S. S. Koç, "Zaman uzamı skalar küresel dalga fonksiyonları için öteleme adisyon teoremleri," *Elektrik, Elektronik, Bilgisayar, Biyomedikal Mühendisliği 12. Ulusal Kongre ve Sergisi*, Eskişehir, Türkiye, 2007, pp. 657-660.

6. S. A. Azizoğlu, "Spherical wave expansion of the time domain free-space dyadic Green's function," M.S. thesis, Dept. Electrical and Electronics Engineering, Middle East Tech. Univ., Ankara, Turkey, 1999.